Institute of Thermoelectricity, Academy of Sciences and Ministry of Education and Science of Ukraine

Journal of THERMOELECTRICITY

International Research

Founded in December, 1993

published 4 times a year

No. 3 *2023*

Editorial Board

International Editorial Board

Founders – National Academy of Sciences, Ukraine
Institute of Thermoelectricity of National Academy of Sciences and Ministry of Education and Science of Ukraine

Certificate of state registration № КВ 15496-4068 ПР

Address of editorial office:
Ukraine, 58002, Chernivtsi, General Post Office, P.O. Box 86.
Phone: +(380-372) 90 31 65.
Fax: +(380-3722) 4 19 17.
E-mail: jt@inst.cv.ua
http://www.jt.inst.cv.ua

Signed for publication 24.09.2023. Format 70×108/16. Offset paper №1. Offset printing.
Printer's sheet 11.5. Publisher's signature 9.2. Circulation 400 copies. Order 5.

Printed from the layout original made by “Journal of Thermoelectricity” editorial board
in the printing house of “Bukrek” publishers,
10, Radischev Str., Chernivtsi, 58000, Ukraine

CONTENT

O.M. Manyk, *Cand.Sc (Phys-Math)*[1]
T.O. Manyk, *Cand.Sc. (Phys-Math)*[2]
V.R. Bilynskyi-Slotylo, *Cand.Sc. (Phys-Math)*[1]

[1] Yuriy Fedkovych Chernivtsi National University, 2 Kotsiubynskyi str.,
Chernivtsi, 58012, Ukraine;
e-mail: o.manyk@chnu.edu.ua, slotulo@gmail.com
[2]Military University of Technology Jaroslaw Dombrowski, str. gene Sylwester Kaliskiego, 2,
Warsaw 46, 00-908, Poland
e-mail: tetjana.manyk@wat.edu.pl

THEORETICAL MODELS OF ORDERED ALLOYS OF TERNARY SYSTEMS OF THERMOELECTRIC MATERIALS. 5. CHEMICAL BOND AND STATE DIAGRAMS OF *Cd-Sb-Te*

Theoretical models of ordered alloys of promising thermoelectric materials of ternary systems based on Cd-Sb-Te have been developed. Using inverse triangulation methods, isothermal cross-sections and diagrams of the distribution of phase regions in ternary systems were constructed using binary state diagrams of the initial components (Cd-Sb; Cd-Te; Sb-Te). Calculations of the effective radii of interatomic interaction, electron density redistribution, and dissociation energy of the corresponding chemical bonds forming the Cd-Sb-Te crystal structure depending on the interatomic distances are presented.

Key words: theoretical models, chemical bond, effective radii, dissociation energy, state diagrams, non-equivalent hybrid orbitals (NHO).

Introduction

Ternary systems of tellurides and antimonides are increasingly attracting the attention of specialists in thermoelectricity [1]. This is due to the presence of a number of concentration and structural features in such systems. With a change in the concentration of the initial elements, solid phases of variable composition with a crystalline structure from a densely packed crystal lattice to layered structures are formed. The chemical bond in such systems varies from metallic (in the original components) to covalent (in compounds) and intermediate (in solid solutions). This leads to phase transformations, ordering processes in melts and alloys that shape the physical and chemical properties of the obtained materials [2], [3]. At the same time, all technological issues of the synthesis of new materials based on ternary systems have to be solved experimentally. The reason is that ternary systems are complex, nonlinear, and the well-known developed theoretical approaches for problems of phase transformations of simple systems no longer reveal the conditions for the appearance of ternary properties with the prospect of their change in the desired direction. There is still no consistent theory of phase transformations from the standpoint of chemical bond.

This is why new approaches to solving complex, multifactorial problems are needed to solve technological issues in ternary systems. Their solution is beyond the power of individual disciplines.

Multidimensional understanding of this circumstance requires an unconventional understanding of the theory and the methods of its application in this analysis.

The question of how general principles can be fruitfully used to analyze real systems and to solve specific, multifactorial problems is becoming especially relevant [4], [5].

In this regard, the task set in this work was to develop theoretical models of ordered alloys that would allow generalizing the capabilities of existing models by combining thermodynamic, statistical, and quantum-mechanical approaches, taking into account chemical bond.

The peculiarity of this approach is that a number of considered factors are interconnected and their influence on the properties of the studied materials is revealed indirectly through the parameters of theoretical models. In this case, the considered approach allows solving the inverse problem both at each stage in particular and as a whole. In this case, the initial conditions are chosen as the values of the parameters of physical quantities that the materials should receive, and the result of the research should be the technological parameters of the modes of obtaining these materials. The availability of such information allows us to theoretically describe the processes of melting and crystallization in ternary systems *Cd-Sb-Te* and optimize the synthesis of new materials based on them.

Theoretical models of state diagrams

In constructing the theoretical model of *Cd-Sb-Te*, it was necessary to generalize the results of studies of the physicochemical properties and quantum regularities of the initial components [6 – 8]. The next stage of research is devoted to establishing the dynamics of the formation of a chemical bond by analyzing the interatomic interaction in the initial components, binary systems of the initial components (*Cd-Sb*; *Cd-Te*; *Sb-Te*) and isothermal sections of ternary systems *Cd-Sb-Te* at different temperatures.

The results of theoretical studies of the features of the chemical bond of cadmium are presented in [6]. Analysis of diverse information on the crystal structure, thermodynamic and quantum laws of cadmium made it possible to establish a theoretical model of the chemical bond, determine the force constants of the microscopic theory, characteristic temperatures that must be taken into account when choosing technological solutions for obtaining new thermoelectric materials based on cadmium.

The next constituent element of the *Cd-Sb-Te* ternary system is antimony. This element can be both a constituent component of many binary semiconductor compounds and widely used as an alloying additive. The increased interest in this element is due to the presence of polymorphic transformations in it – its ability to coexist in several structural forms with the same chemical composition. Solving the problem of polymorphic transformations from the standpoint of chemical bond leads to the emergence of new technological approaches to obtaining high-quality materials. In this regard, in [7], research was carried out on the features of the chemical bond and the possibilities of using antimony in the further technological development of new thermoelectric materials. The analysis of the crystal structure given in [7] showed that in antimony compounds the degree of oxidation is – 3, + 3, + 5. Antimony is also known in four metallic allotropic (existing at different pressures) and three amorphous modifications. Under normal conditions, only the crystalline rhombohedral structure is stable. There is also a hexagonal modification of antimony. The physical nature of their occurrence has not yet been determined.

Highly pure single crystals of antimony are plastic at 293 K and brittle at 233 K. Depending on the manufacturing technology, these materials are characterized by different values of physicochemical parameters. Studies of the features of the chemical bond and polymorphic modifications of antimony [7] showed that in the range of 200 – 1000 K, the considered modifications are characterized by the

presence of a fine chemical bond structure with non-equivalent interatomic distances. In this case, the temperature of formation of the first component of the chemical bond of the hexagonal modification $T^{(1)}_{hex}$ and the melting temperature T_m coincide ($T_m = T^{(1)}_{hex} = 903$ K). In the case of the rhombohedral modification, the temperature $T^{(1)}_{rhomb}$ exceeds T_m and the first component of the chemical bond is formed in the liquid phase with overheating. This means that the synthesis of new materials based on antimony must be carried out with regard to the fine structure of the chemical bond.

The examination of the initial components of the studied ternary system is completed by tellurium. Comprehensive studies of tellurium are carried out in [8], where a review of experimental and theoretical works is given, the crystal structure, force and energy parameters of tellurium are considered from the standpoint of chemical bond. It is noted that tellurium is a typical scattered element. It has eight stable and about twenty unstable artificially obtained isotopes. Tellurium is in group VI and period V between selenium and polonium, with which it is similar, although selenium is a metalloid and polonium is a metal. According to the period, tellurium is placed between antimony and iodine, of which antimony is a metal, and iodine is a metalloid.

Tellurium belongs to semiconductor substances and crystallizes in the hexagonal system, forming spiral chains. The tellurium atoms in the chains have a covalent bond, and the chains are bound together by metallic forces. Such a qualitative description of the chemical bond makes it possible to explain some of the physical properties of tellurium. However, in order to obtain materials with the given properties, it is necessary to calculate the technological parameters in terms of chemical bond. Therefore, complex studies of the dynamics of chemical bond formation using the methods of vibration theory, elasticity theory, and molecular models were carried out in [8].

Thus, the studies conducted in [8] showed that tellurium has a complex hexagonal crystal structure, characterized by five different interatomic distances and a consistent structure of melting and crystallization. It was established that the increase in the ratio of the parameters of the hexagonal structure c/a causes a redistribution of the electron density in such a way that d-shells begin to take part in the formation of chemical bonds in the processes of crystallization and melting through the formation of "new" and destruction of "old" chemical bonds of tellurium. In addition, it was established that the selection of specific values of the characteristic frequencies and their corresponding temperatures make it possible not only to control the dynamics of the formation of the tellurium chemical bond, but also the quality of the obtained materials based on tellurium, due to the selection of the composition and structure of the initial components.

The next stage of research is devoted to establishing the dynamics of the formation of chemical bonds of the initial components in going to the structures of binary alloys [9] and heterogeneous equilibria [10] of ternary systems.

To describe the dependence of primary crystallization temperatures on the composition of binary systems, the state diagrams of *Cd-Sb*, *Cd-Te*, *Sb-Te* [9] shown in Fig. 1 were used.

When constructing the distribution diagram of the *Cd-Sb-Te* phase regions, triangulation methods [10] and calculation of chemical bond parameters by quantum-chemical methods [4, 5] were used.

From the analysis of the phase diagrams shown in Fig. 1 it follows that antimony in compounds with cadmium and tellurium behaves similarly, has a double eutectic, and the *Cd-Te* compound melts congruently at 1098 °C and forms degenerate eutectics with its components.

The dependence of the melting temperature on pressure shows that with increasing pressure the melting temperature decreases to 996 °C, and at the triple point the sphalerite structure goes over to the *NaCl* type structure. Subsequently, with increasing pressure, the melting temperature begins to increase [2, 3]. The reason for such behaviour in the *Cd-Te* system has not been established.

Analyzing the phase diagram of *Sb-Te*, it should be noted that there are continuous solid solutions between antimony and Sb_2Te_3 during slow cooling. During rapid cooling of the melt, peritectic reactions with the formation of solid solutions do not have time to occur, and a nonequilibrium eutectic crystallizes from the melt – continuous solid solutions of *Sb*-Sb_2Te_3 are absent.

Of all the components, cadmium antimonide is considered the most studied. The works [2, 3] systematize and summarize publications on the properties of *Cd-Sb*, provide state diagrams, information on phase transformations; physical and chemical interaction of components in liquid and solid states. When studying the properties of *Cd-Sb* near the melting point, in addition to the thermal effect at 456 °C, which corresponds to the melting of *Cd-Sb*, another one was found on the thermograms at 464 °C, accompanied by a sharp increase in electrical conductivity and caused by changes in the short-range order and its transition from a semiconductor to a metallic state. The reason for the appearance of such effects may be the features of the crystalline structure of *Cd-Sb* and the supersaturation of the phase with antimony, which leads to a decrease in the melting temperature. Based on the data on the formation of polymorphic compounds in the *Cd-Sb* system, it was concluded that in the *Cd-Sb* system there is only one stable *Cd-Sb* and two unstable – Cd_4Sb_3 Cd_3Sb_2 compounds, which correspond to one stable and two metastable state diagrams. The short-range order corresponding to *CdSb* molecules exists only up to 500 °C. In liquid alloys of the Cd-Sb system, an irreversible process of rearrangement of the short-range order structure occurs in the sequence $CdSb \rightarrow Cd_4Sb_3 \rightarrow Cd_3Sb_2$, which depends on heat treatment. This information, as well as the data presented above, were obtained experimentally. At the same time, how the initial components in the ternary systems *Cd-Sb-Te* will interact, what will be the regions of extreme points of the dependence of the primary crystallization temperature on the composition, what will be the coordinates of the ternary eutectics of the concentration triangle - there is no answer from the standpoint of chemical bond yet. This work is a continuation of complex studies [3-8] and is devoted to the construction of theoretical models of ordered alloys of ternary systems *Cd-Sb-Te*. A new feature in the study of antimonides and tellurides was the use of a method based on the geometric properties of a triangle [10]. This mathematical approach, the triangulation method, is used in chemistry when studying the state diagrams of ternary systems and allows their distribution into simpler binary systems, taking into account chemical interaction.

In this paper, the inverse problem of triangulation is solved: based on the experimentally established and presented in [9] phase diagrams of binary alloys, taking into account the chemical interaction (solubility; substitution; exchange; formation of compounds; formation of solid solutions and mechanical mixtures) between the elements *Cd*, *Sb*, *Te*, located at the vertices of the triangle, a diagram of the distribution of phase regions for various isothermal sections in the *Cd-Sb-Te* system is constructed, and the parameters of phase transformations are calculated theoretically using quantum chemistry methods [4, 5]. Next, the quantitative ratios of coexisting phases were determined and the limits of phase equilibrium in the liquid-crystal regions were established. The obtained results are shown in Fig. 1 – 4, where the following designations are entered:

α – solid phase based on *Cd*;
β – solid phase based on *Te*;
γ – solid phase based on *Sb*;
ε – solid phase based on *Cd-Te*;
ρ_1 – solid phase based on $Sb_{0.7}Te_{0.3}$;
ρ_2 – solid phase based on $Sb_{0.4}Te_{0.6}$;
ρ_3 – solid phase based on $Sb_{0.1}Te_{0.9}$;
δ – solid phase based on *Cd-Sb*;

δ_1 – solid phase based on $Cd_{0.9}Sb_{0.1}$;
δ_2 – solid phase based on $Cd_{0.42}Sb_{0.58}$;
σ – solid phase based on intermediate ternary compound *Cd-Sb-Te*;
L – liquid.

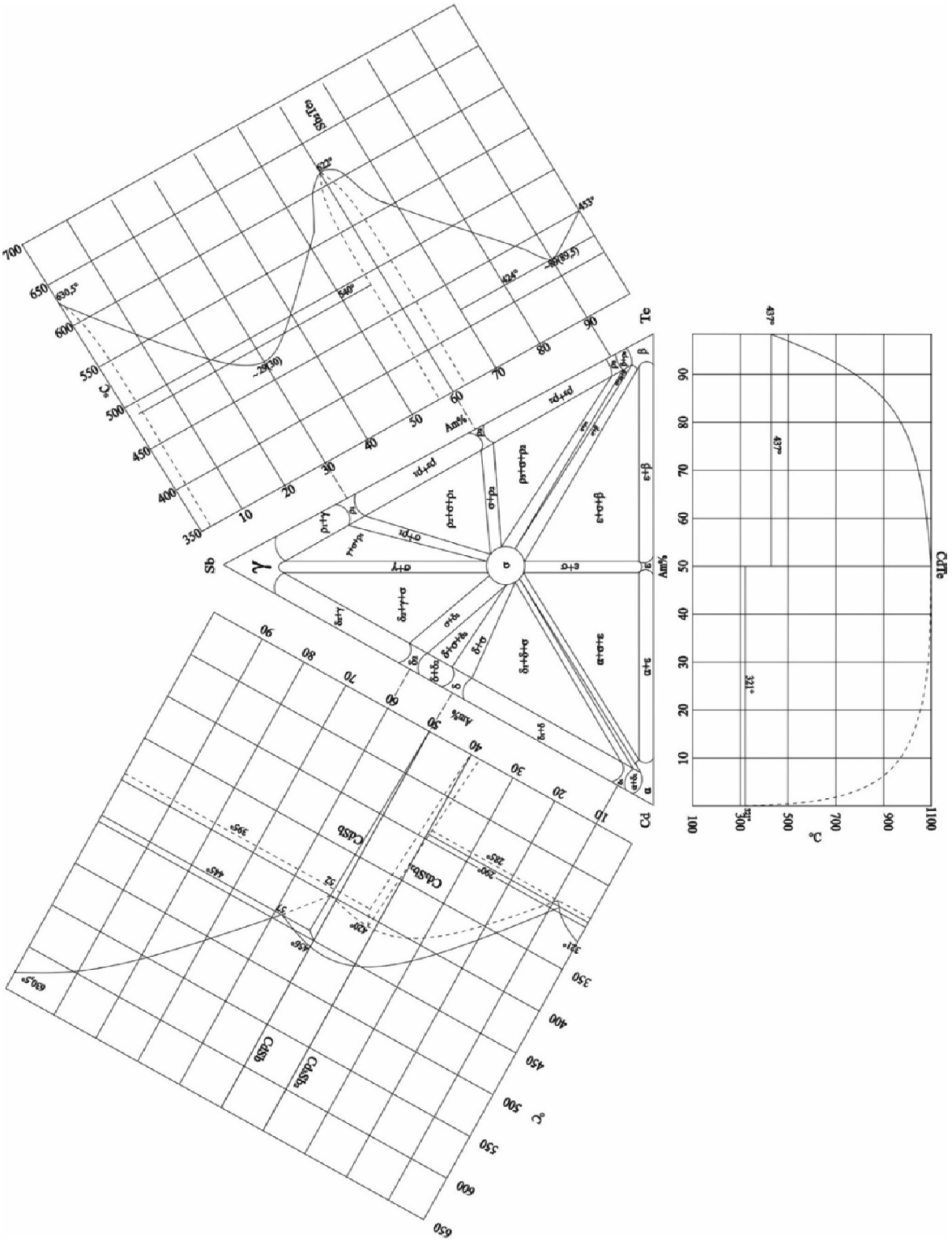

Fig. 1. Diagram of distribution of Cd-Sb-Te phase regions for equilibrium in the solid state.

Fig. 1 shows a diagram of the distribution of *Cd-Sb-Te* phase regions in the solid state. The division of the *Cd-Sb-Te* ternary system into ten ordered ternary subsystems is traced. This makes it possible to consider the issue of interatomic interaction both from the standpoint of stable and metastable phases of state diagrams, as well as chemical bond and temperature.

Fig. 2 shows an isothermal section at a temperature of t = 300 °C, which is lower than the melting point of the components *Cd*, *Sb*, *Te*, and at the same time higher than the temperature of the first eutectic of the *Cd-Sb* system. Unlike the previous case, the section contains conoid triangles with equilibrium phases (L + α + σ) and (L + δ1 + σ), which are realized by primary crystals α, as well as σ and δ1 crystals and liquid.

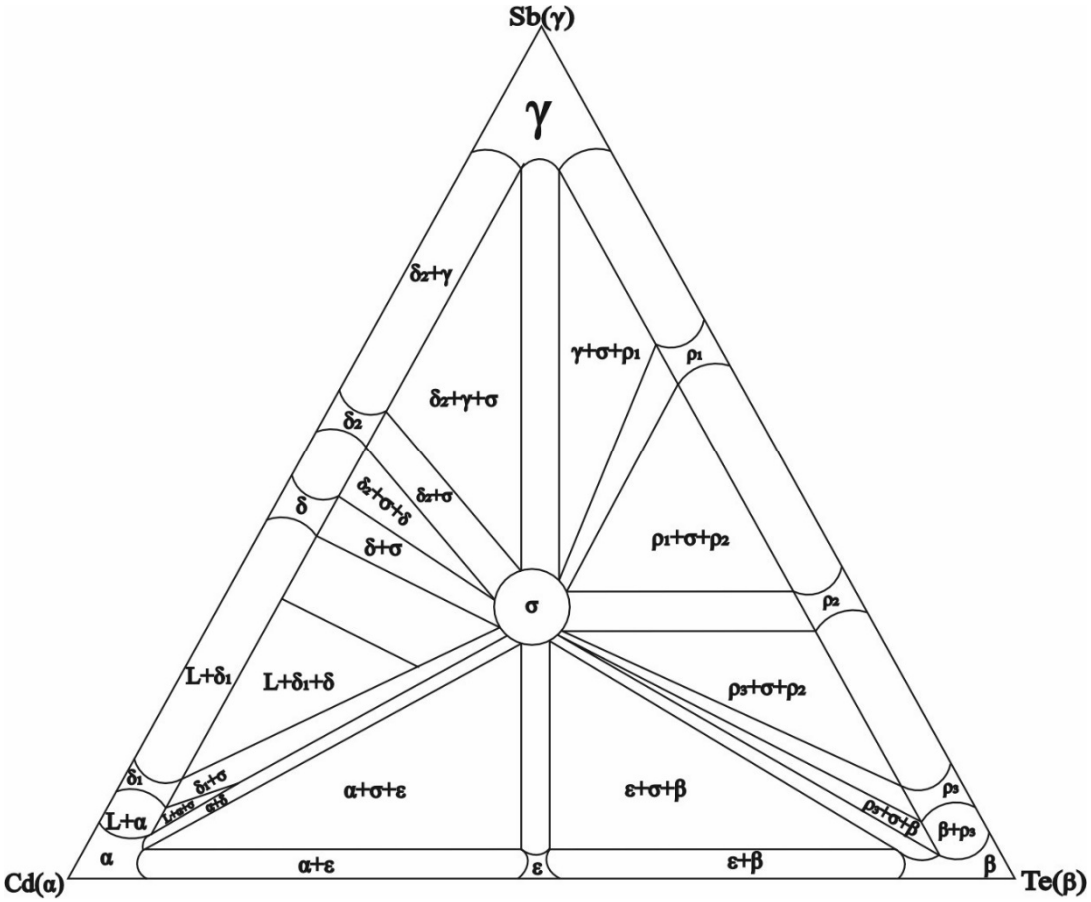

Fig. 2. Cd-Sb-Te isothermal section at t = 300 °C.

This division of ternary systems into separate sectors of binary phase diagrams allows studying the fine structure of cooling and heating of individual elements depending on their environment and the processes of formation of short-range order of chemical bonds.

Fig. 3 shows an isothermal section at a temperature of t = 400 °C, which is higher than the melting point of cadmium, but lower than the melting point of tellurium and antimony. In the *Cd-Sb* diagrams, three-phase equilibria are represented by conoid triangles with phases (L + α + σ), (L + δ1 + σ), and (L + δ + σ). Alloys of the triangle (ε, γ, β) are in the solid state at this temperature.

Fig. 4 shows the isothermal section at t = 600 °C, which is higher than the melting temperature of cadmium and tellurium, but lower than the melting temperature of antimony. Most of the *Cd-Sb* cross-section is occupied by liquid, and on the *Cd-Te, Sb-Te* diagrams, three-phase equilibria are represented

by conoid triangles with phases (L + ρ2 + γ), (L + ρ2 + σ) and (L + σ + ρ3), (L + β + σ), (L + β + ε), (L + α + β), (L + α + ε).

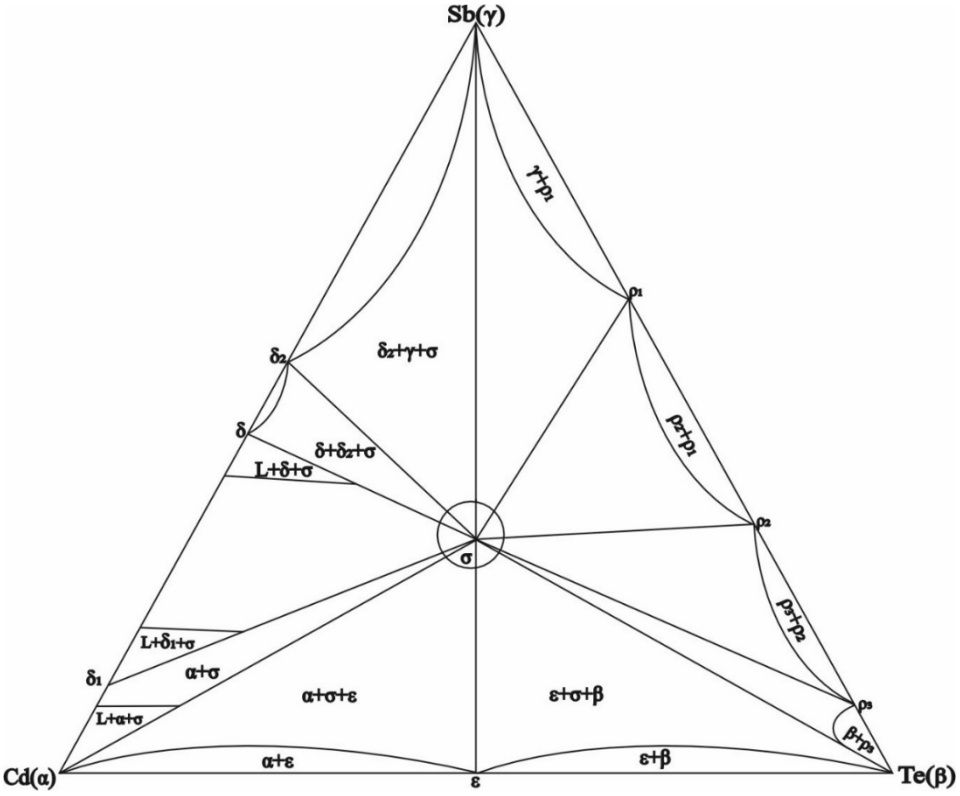

Fig. 3. Cd-Sb-Te isothermal section at t = 400 °C.

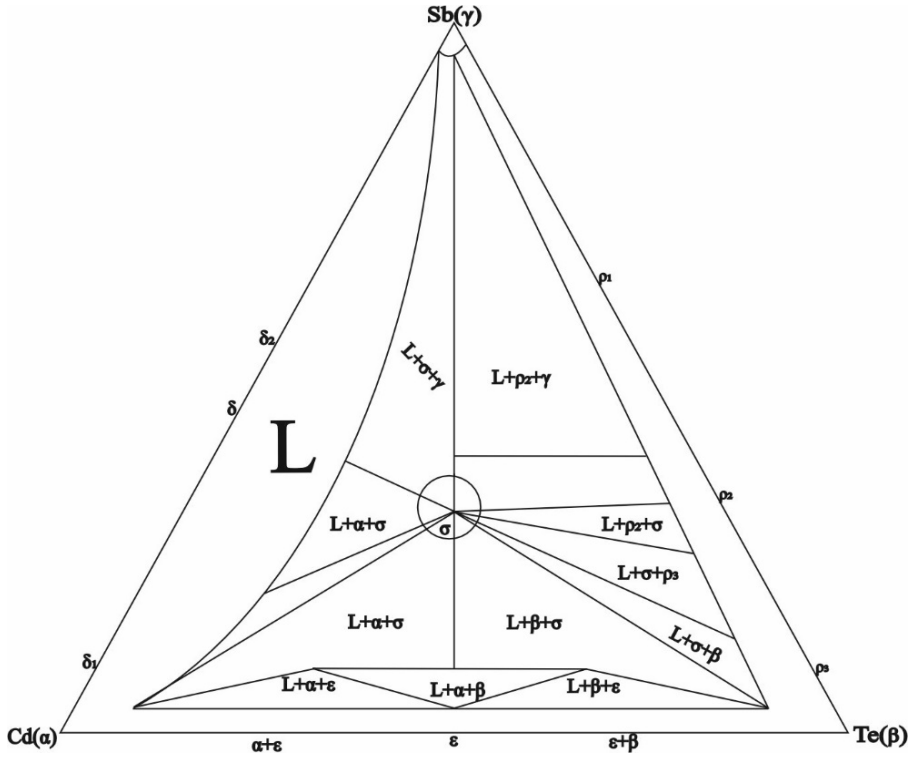

Fig. 4. Cd-Sb-Te isothermal section at t = 600 °C.

Thus, the presented isothermal sections make it possible to separate the limits of phase equilibrium for eutectic and peritectic type diagrams and to optimize the technological modes of obtaining new materials based on *Cd-Sb-Te*.

However, isothermal sections alone do not yet indicate the temperatures of phase transitions of multicomponent systems. Theoretical models are needed that combine generalized experimental data with calculations of the interatomic interaction of components in both phases depending on interatomic distances and increase the role of theoretical calculations in constructing phase diagrams of multicomponent systems.

Theoretical models of chemical bonding of ordered alloys *Cd-Sb-Te*

Theoretical analysis of crystallization processes of thermoelectric materials requires a revision of the fundamentals of the theory of interatomic interaction. The reason for this is that theoretical approaches reflecting the regularities of ordering processes in crystals contradict the formation of a chemical bond, accompanied by the rearrangement of the valence electron shells of interacting atoms and the redistribution of electron density along chemical bonds [5].

On the other hand, taking into account statistical regularities made it possible to obtain the dependence of n electrons on the outer shell of an atom on the Fermi radius r_F, which can be considered the beginning of the quantitative chemical bond theory [11].

Analysis of empirical information about the properties of atoms based on a crystal-chemical approach made it possible to generalize the concept of the Fermi radius to the case of electronic configurations of interacting atoms depending on the length and number of bonds formed by them and to introduce effective ionic radii R_U. The most useful relationship in searching for the connection of R_U with n proved to be the relationship $tg\alpha = \frac{\Delta log R_U}{\Delta n}$ with the properties of atoms in the coordinates $logR_U = f(n)$. Good agreement between the experimental data on the properties of atoms and their ions and the values of R_U and $tg\alpha$ is given by the postulated dependence:

$$logR_{UA}^{x} = logR_{UA}^{0} - xtg\alpha, \tag{1}$$

where R_U^0 is radius of atoms in the unexcited state; x is valence.

The use of the system of ionic radii to describe the chemical bond follows from the principles of quantum mechanics. Since the equation of the system of ionic radii describes the change in R_U of atoms *A* and *B* with a change in the number of electrons in the orbitals of each, then dependence (1) takes the form of a system of equations [11]:

$$logR_{UA}^{+x} = logR_{UA}^{0} - xtg\alpha_A, \tag{2}$$

$$logR_{UB}^{-x} = logR_{UB}^{0} + xtg\alpha_B, \tag{3}$$

$$d_1 = R_{UA}^{+x} + R_{UB}^{-x}, \tag{4}$$

The presence of a minimum interatomic distance d_{min} from the standpoint of the crystal chemical approach is justified by the increase in the internuclear distance with a change in ionicity between the same partners. The disadvantage of this approach is that in many cases the internuclear distances *A-B* in compounds and alloys are less than $d_{min}$and it is impossible to calculate the ion charge using the $Z_{ef} = f(d)$ diagrams. Difficulties can be overcome only by abandoning the attempt to interpret the solution of system (2) – (4) from the standpoint of a crystal-chemical approach. Additional conditions are necessary to translate the crystal chemical system (2) – (4) into the language of quantum chemistry.

It should be taken into account that during the formation of *A*-*B* bonds, the spherical symmetry of the electron density of atoms *A* and *B* is broken and is accompanied by the transition of electrons to other directions of interatomic interaction.

The thus calculated effective charges and effective radii characterize for an arbitrary d_1 the conditions for preservation of continuity of wave function in the zone of interacting atoms. This condition is fulfilled if the extraction $(+\Delta e)$ of electrons or their localization $(-\Delta e)$ change the values of charges that this pair has at $d_1 = d_{min}$, i.e. $Z_{ef}A(B) = Z_{min}A(B) + \left(\frac{\Delta e}{2}\right)$ and are described by the system of equations:

$$d_1 = R_{UA}^{ZA} + R_{UB}^{ZB}, \tag{5}$$

$$logR_{UA}^{ZA} = logR_{UA}^{0} - (Z_{minA} + \left(\frac{\Delta e}{2}\right))tg\alpha_A, \tag{6}$$

$$logR_{UB}^{ZB} = logR_{UB}^{0} - (Z_{minB} + \left(\frac{\Delta e}{2}\right))tg\alpha_B, \tag{7}$$

Replacing x in the system of equations (2) – (4) with $(Z_{min} + \left(\frac{\Delta e}{2}\right))$ in (5) – (7) changes the physical content of these equations. The function $d_1 = f(Z_{ef})$ is calculated from the standpoint of the crystal-chemical approach, $(Z_A = -Z_B)$ is correct from the quantum-molecular point of view only when $d_1 = d_{min}$, but this is sufficient for the system (5) – (7) to be solved for a known d_1 and for the effective radii and redistribution of the electron density to be found. With this approach, system (5) – (7) allows us to agree the theoretical part with the experimental part for all possible values of d_1 in the compounds under consideration. Thus, taking into consideration the quantum interpretation of the empirical material made it possible to obtain

$$D_{A-B}^{(i)} = \left(\frac{C_1(R_{UA}^0 + R_{UB}^0)}{(\text{tg}\,\alpha_A + \text{tg}\,\alpha_B)}\right)\left(\frac{C_2 d_i}{d_i^2 - R_{UA}R_{UB}} - \frac{1}{d_i}\right), \tag{8}$$

where $R_{UA(B)}^0$, $tg\alpha_{A(B)}$ are the coefficients of equations (2) – (4) for atoms *A* and *B*, and R_{UA}, R_{UB} are the effective radii of their ions in *A* – *B* bonds of length d_i, i is the number of non-equivalent interatomic distances in the considered compounds; C_1 is the coefficient reflecting the relationship between dimensional and energy characteristics of interatomic interaction (measured in electron volts); C_2 is a coefficient that depends on the type of crystal structure and chemical bond and is chosen dimensionless.

The above equations were used in the calculations of effective charges, effective radii and dissociation energies of non-equivalent chemical bonds of *Cd-Sb-Te* ternary systems.

The results of calculations of the coefficients of equations (2) – (4) R_U^0 and $tg\alpha$ of the initial components are given in Table 1.

Table 1

Coefficients of equations of the initial components

Z		Element	R_U^0(Å)	$tg\alpha$
48		*Cd*	1.51 Å	0.097
51		*Sb*	1.45 Å	0.074
52		*Te*	1.57 Å	0.076

Effective charges Δq_i, effective radii R_{Ui} and dissociation energies for the nearest neighbours at different interatomic distances $d_i (1 \leq i \leq 6)$ of the structural modifications of cadmium are given in Table 2. The results of calculations for antimony and tellurium are given in Tables 3 and 4.

Table 2

Effective charges Δq_i, effective radii R_{Ui} and dissociation energies D_i of chemical bonds φ_i for the nearest neighbours at different interatomic distances d_i of structural modifications of cadmium

φ_i / Parameters	φ_1	φ_2	φ_3	φ_4	φ_5	φ_6
d_i(Å)	2.8	2.9	3.0	3.1	3.2	3.3
R_{UCd}(Å)	1.4	1.45	1.5	1.55	1.6	1.65
$\Delta q(\varphi_i)$	+ 0.33	+ 0.18	+ 0.025	– 0.05	– 0.27	– 0.4
$D_i(eV)$	1.853	1.789	1.730	1.674	1.622	1.572

Table 3

Effective charges Δq_i, effective radii R_{Ui} and dissociation energies D_i of chemical bonds φ_i for the nearest neighbours at different interatomic distances d_i of structural modifications of antimony

φ_i / Parameters	φ_1	φ_2	φ_3	φ_4	φ_5	φ_6
d_i(Å)	2.8	2.9	3.0	3.1	3.2	3.3
R_{USb}(Å)	1.4	1.45	1.5	1.55	1.6	1.65
$\Delta q(\varphi_i)$	0.2	0	– 0.2	– 0.39	– 0.6	– 0.75
$D_i(eV)$	2.332	2.252	2.177	2.107	2.041	1.98

Table 4

Effective charges Δq_i, effective radii R_{Ui} and dissociation energies D_i of chemical bonds φ_i for the nearest neighbours at different interatomic distances d_i of structural modifications of cadmium

φ_i / Parameters	φ_1	φ_2	φ_3	φ_4	φ_5	φ_6
d_i(Å)	2.8	2.9	3.0	3.1	3.2	3.3
R_{UTe}(Å)	1.4	1.45	1.5	1.55	1.6	1.65
$\Delta q(\varphi_i)$	0.653	0.454	0.26	– 0.0073	– 0.108	– 0.284
$D_i(eV)$	2.46	2.374	2.295	2.221	2.147	2.087

As regards the above parameters for *Cd-Te*, *Sb-Te* and *Cd-Sb* compounds, they are given in Tables 5, 6, 7.

Table 5

Effective charges Δq_i, effective radii R_{Ui} and dissociation energies D_i of chemical bonds φ_i for the nearest neighbours at different interatomic distances d_i of structural modifications of Cd-Te

Parameters \ φ_i	φ_1	φ_2	φ_3	φ_4	φ_5	φ_6
d_i(Å)	2.8	2.9	3.0	3.1	3.2	3.3
R_{UCd}(Å)	1.355	1.41	1.465	1.515	1.576	1.63
R_{UTe}(Å)	1.445	1.49	1.535	1.585	1.624	1.67
$\Delta q(\varphi_i)$	0.497	0.318	0.134	– 0.022	– 0.195	– 0.34
$D_i(eV)$	2.116	2.044	1.977	1.913	1.855	1.798

Table 6

Effective charges Δq_i, effective radii R_{Ui} and dissociation energies D_i of chemical bonds φ_i for the nearest neighbours at different interatomic distances d_i of structural modifications of Sb-Te

Parameters \ φ_i	φ_1	φ_2	φ_3	φ_4	φ_5	φ_6
d_i(Å)	2.8	2.9	3.0	3.1	3.2	3.3
R_{USb}(Å)	1.345	1.444	1.46	1.48	1.53	1.58
R_{UTe}(Å)	1.455	1.456	1.54	1.62	1.67	1.72
$\Delta q(\varphi_i)$	0.43	0.227	0.03	– 0.159	– 0.324	– 0.521
$D_i(eV)$	2.392	2.314	2.235	2.159	2.092	2.029

Table 7

Effective charges Δq_i, effective radii R_{Ui} and dissociation energies D_i of chemical bonds φ_i for the nearest neighbours at different interatomic distances d_i of structural modifications of Cd-Sb

Parameters \ φ_i	φ_1	φ_2	φ_3	φ_4	φ_5	φ_6
d_i(Å)	2.8	2.9	3.0	3.1	3.2	3.3
R_{UCd}(Å)	1.43	1.48	1.53	1.58	1.63	1.68
R_{USb}(Å)	1.37	1.42	1.47	1.52	1.57	1.62
$\Delta q(\varphi_i)$	0.287	0.106	– 0.069	– 0.239	– 0.403	– 0.562
$D_i(eV)$	2.059	1.989	1.922	1.860	1.802	1.748

In the tables, the values of coefficients C_1 and C_2 in the calculations in the first approximation are chosen to be equal to unity.

Discussion of the results and conclusions

As follows from the results obtained in the work, given in Tables 1 – 7 and in Figs. 1 – 4, the application of a complex approach to technological problems made it possible to build theoretical models for the description of ordering processes in alloys of ternary systems based on *Cd-Sb-Te*.

This approach allowed us to describe the processes of formation of interatomic interaction at different technological levels from the standpoint of chemical bond. This is, first of all, the formation of

a crystal structure based on the initial elements (*Cd, Sb, Te*), where information on the physicochemical properties and chemical bond of the initial elements (Tables 1 – 4) was taken into account, binary compounds based on the initial elements (*Cd-Te, Sb-Te, Cd-Sb*) (Tables 5 – 7). What was new was that the paper calculated the dependence of chemical bond parameters on the interatomic distances (effective radii, redistribution of electron density on the corresponding chemical bonds, and dissociation energy of bonds forming the crystal structure).

What was new in the study of ternary *Cd-Sb-Te* systems was that, when constructing the distribution diagram of phase equilibrium regions, the method of inverse triangulation was used using information on the binary compounds of the initial components and their state diagrams. This made it possible to determine quantitative phase ratios and establish the limits of phase equilibrium in the liquid-crystal regions; to separate the boundaries of diagrams of eutectic and peritectic type for solving technological problems of stable and metastable phases, predict cases of congruent and incongruent melting. The obtained results can be used in the development of technological modes of obtaining new materials based on *Cd-Sb-Te*.

References

1. Anatychuk L.I. (2003). *Thermoelectric power converters*. Institute of Thermoelectricity, Kyiv: Naukova Dumka.
2. Belotskij D.P., Manik O.N. (1996). On the relationship between thermoelectric materials melts properties and structures and the state diagrams. 1. Regularities of eleavage manifestation in the state diagrams. *J. Thermoelectricity*, 1, 21 – 47.
3. Belotskij D.P., Manik O.N. (1996). On the relationship of electronic properties and structures of melts to the diagrams of state in the thermoelectric material. 2. Phase changes and electronic properties of melts. *J. Thermoelectricity*, 2, 23 – 57.
4. Manyk O.M., Manyk T.O., Bilynskyi-Slotylo V.R. (2021). Theoretical models of ordered alloys of ternary systems of thermoelectric materials. 1. Chemical bond and state diagrams of *In-Cd-Sb*. *J. Thermoelectricity*. 2, 32 – 42.
5. Manyk O.M., Manyk T.O., Bilynskyi-Slotylo V.R. (2022). Theoretical models of ordered alloys of ternary systems of thermoelectric materials. 2. Chemical bond and state diagrams of *Bi-Pb-Te*. *J. Thermoelectricity*, 1, 5 – 15.
6. Ascheulov A.A., Manyk O.N., Manyk T.O., Marenkin S.F., Bilynskyi-Slotylo V.R. (2011). Peculiarities of chemical bond in cadmium. *Neorganicheskie Materialy – Inorganic Materials*, 47 (9), 1052 – 1056.
7. Ascheulov A.A., Manyk O.N., Manyk T.O., Marenkin S.F., Bilynskyi-Slotylo V.R. (2013). Peculiarities of chemical bond in antimony. *Neorganicheskie Materialy – Inorganic Materials*. 49 (8), 823 – 826.
8. Ascheulov A.A., Manyk O.N., Manyk T.O., Bilynskyi-Slotylo V.R. (2010). Molecular model and chemical bond in tellurium. *Tekhnologiia i Konstruirovaniie v Elektronnoi Apparature – Technology and Design in Electronic Equipment*, 89 (5-6), 46 – 50.
9. Hansen M., Anderko K. (1962). *Struktura dvoinykh splavov [Structure of double alloys]*. Moscow: Metallurgizdat, v. 1, 2 [in Russian].
10. Barchii I.E., Peresh E.Yu., Rizak V.M., Khudolii V.O. (2003). *Heterogenni rivnovahy [Heterogeneous equilibria]*. Uzhhorod, Zakarpattia Publ. [in Ukrainian].
11. Prikhodko E.V. (1973). *Sistema nepolarizovannykh ionnykh radiusov i eio ispolzovaniie dlia analiza*

elektronnogo stroieniia i svoistv veschestv [The system of unpolarized ionic radii and its use for the analysis of the electronic structure and properties of substances]. Kyiv: Naukova Dumka.

Submitted: 21.06.2023.

Маник О.М., *канд. фіз.-мат. наук* [1]
Маник Т.О., *канд. фіз.-мат. наук* [2]
Білинський-Слотило В.Р., *канд. фіз.-мат. наук* [1]

[1] Чернівецький національний університет імені Юрія Федьковича,
вул. Коцюбинського 2, Чернівці, 58012, Україна;
e-mail: o.manyk@chnu.edu.ua, slotulo@gmail.com
[2] Військово-технічний університет ім. Ярослава Домбровського,
вул. ген. Сільвестра Каліського, 2, Варшава 46, 00-908, Польща
e-mail: tetjana.manyk@wat.edu.pl

ТЕОРЕТИЧНІ МОДЕЛІ ВПОРЯДКОВУВАНИХ СПЛАВІВ ПОТРІЙНИХ СИСТЕМ ТЕРМОЕЛЕКТРИЧНИХ МАТЕРІАЛІВ. 5. ХІМІЧНИЙ ЗВ'ЯЗОК ТА ДІАГРАМИ СТАНУ *Cd-Sb-Te*

Розроблено теоретичні моделі впорядковуваних сплавів перспективних термоелектричних матеріалів потрійних систем на основі Cd-Sb-Te. Методами оберненої триангуляції побудовано ізотермічні перерізи та схеми розподілу фазових областей в потрійних системах з використанням бінарних діаграм стану вихідних компонентів (Cd-Sb; Cd-Te; Sb-Te). Представлено розрахунки ефективних радіусів міжатомної взаємодії, перерозподілу електронної густини та енергії дисоціації відповідних хімічних зв'язків, що формують кристалічну структуру Cd-Sb-Te в залежності від міжатомних віддалей.
Ключові слова: теоретичні моделі, хімічний зв'язок, ефективні радіуси, енергія дисоціації, діаграми стану, нееквівалентні гібридні орбіталі (НГО).

Література

1. Anatychuk L.I. (2003). *Thermoelectric power converters*. Institute of Thermoelectricity, Kyiv: Naukova Dumka.
2. Belotskij D.P., Manik O.N. (1996). On the relationship between thermoelectric materials melts properties and structures and the state diagrams. 1. Regularities of eleavage manifestation in the state diagrams. *J. Thermoelectricity*, 1, 21 – 47.
3. Belotskij D.P., Manik O.N. (1996). On the relationship of electronic properties and structures of melts to the diagrams of state in the thermoelectric material. 2. Phase changes and electronic properties of melts. *J. Thermoelectricity*, 2, 23 – 57.
4. Маник О.М., Маник Т.О., Білинський-Слотило В.Р. Теоретичні моделі упорядковуваних сплавів потрійних систем термоелектричних матеріалів. 1. Хімічний зв'язок та діаграми стану *In-Cd-Sb*. // Термоелектрика. – 2021. – №2. – С. 32 – 42.
5. Маник О.М., Маник Т.О., Білинський-Слотило В.Р. Теоретичні моделі упорядковуваних сплавів потрійних систем термоелектричних матеріалів. 2. Хімічний зв'язок та діаграми стану

Bi-Pb-Te // Термоелектрика. – 2022. – №1. – С. 5 – 15.

6. Ascheulov A.A., Manyk O.N., Manyk T.O., Marenkin S.F., Bilynskyi-Slotylo V.R. (2011). Peculiarities of chemical bond in cadmium. *Neorganicheskie Materialy – Inorganic Materials*, 47 (9), 1052 – 1056.
7. Ascheulov A.A., Manyk O.N., Manyk T.O., Marenkin S.F., Bilynskyi-Slotylo V.R. (2013). Peculiarities of chemical bond in antimony. *Neorganicheskie Materialy – Inorganic Materials*. 49 (8), 823 – 826.
8. Ascheulov A.A., Manyk O.N., Manyk T.O., Bilynskyi-Slotylo V.R. (2010). Molecular model and chemical bond in tellurium. *Tekhnologiia i Konstruirovaniie v Elektronnoi Apparature – Technology and Design in Electronic Equipment*, 89 (5-6), 46 – 50.
9. Hansen M., Anderko K. (1962). *Struktura dvoinykh splavov [Structure of double alloys]*. Moscow: Metallurgizdat, v. 1, 2 [in Russian].
10. Барчій І.Є., Переш Є.Ю., Різак В.М., Худолій В.О. Гетерогенні рівноваги // Україна, Ужгород: вид. Закарпаття. – 2003. – 211 с.
11. Prikhodko E.V. (1973). *Sistema nepolarizovannykh ionnykh radiusov i eio ispolzovaniie dlia analiza elektronnogo stroieniia i svoistv veschestv [The system of unpolarized ionic radii and its use for the analysis of the electronic structure and properties of substances]*. Kyiv: Naukova Dumka [in Russian].

Надійшла до редакції: 21.06.2023.

V.V. Lysko

V.V. Lysko, *Cand.Sc (Phys-Math)* [1,2]
O.V. Nitsovich, *Cand.Sc (Phys-Math)* [1,2]

[1]Institute of Thermoelectricity of the NAS
and MES of Ukraine,
1, Nauky str., Chernivtsi, 58029, Ukraine;
[2]Yuriy Fedkovych Chernivtsi National University,
2, Kotsiubynsky str., Chernivtsi, 58012, Ukraine
e-mail: anatych@gmail.com

O.V. Nitsovich

COMPUTER SIMULATION OF THE PROCESS OF MANUFACTURING FLAT INGOTS OF THERMOELECTRIC MATERIALS BASED ON Bi_2Te_3 BY VERTICAL ZONE MELTING METHOD

The results of the development of a computer model for optimizing the process of manufacturing flat ingots of thermoelectric materials based on Bi_2Te_3 using the vertical zone melting method are presented. The created model allows one to study the dependence of the crystallization front shape on various technological parameters – the geometric dimensions of the heater and coolers, their temperatures, speed of movement, etc. This makes it possible to carry out multifactorial optimization of technological modes and equipment design, significantly reducing the material costs and time required for conducting similar experimental studies. Bibl. 19, Figs. 3.
Key words: simulation, vertical zone melting, thermoelectric material, bismuth telluride.

Introduction

The practical use of thermoelectricity today is implemented in three main directions - cooling devices, thermoelectric generators and measuring equipment. For all these areas, the main thermoelectric materials used are alloys based on Bi_2Te_3, since it is solid solutions based on bismuth telluride that have the best thermoelectric properties in the temperature range of 200 – 600°K [1 – 6]. A lot of attention is paid to the improvement of methods of obtaining such materials [7 – 14].

One of the most common industrial methods of growing polycrystalline thermoelectric materials based on *Bi-Te* is the method of vertical zone melting. The quality of the obtained material is affected by various factors, for example: impurity distribution coefficient; length of the molten zone; zone movement speed; degree of mixing of the molten zone; heater temperature, etc. A structurally homogeneous crystal can be obtained only by selecting the optimal growing conditions. The curvature of the crystallization front, which is the main technological characteristic of growth, has a great influence on the quality of the obtained thermoelectric material. The shape of the crystallization front can be convex in the liquid phase, flat or concave in the solid phase. The most favourable for growing single crystals with a low density of defects is a flat crystallization front. The shape of the crystallization front is determined by the radial and axial temperature gradients in the ingot during growth.

Computer simulation of the process of growing thermoelectric materials allows one to study the dependence of the crystallization front shape on various technological parameters, significantly reducing material costs and research time required to ensure the growth of crystals of the required quality.

The papers [15, 16] present the results of computer simulation of the process of vertical zone

melting of thermoelectric material in the form of rods with a round cross-section; in particular, the influence of the temperature and dimensions of the heater, the growth rate and other process parameters on the shape of the crystallization front is investigated. The paper [17] examines the possibility of growing single crystals of thermoelectric materials by the method of vertical zone melting in the presence of electric current passing through the ingot.

An interesting opportunity to improve the structure of the material and reduce technological defects when cutting ingots into thermoelements is the production of ingots in the form of flat rods. The creation of technology for the production of such ingots requires multi-parameter optimization of controlled parameters of the growing process.

Therefore, *the purpose of this work* is to create a computer model of the process of manufacturing flat ingots of thermoelectric materials based on Bi_2Te_3 by the method of vertical zone melting.

1. Physical model of vertical zone melting process

The physical model of growing flat ingots of thermoelectric materials based on Bi_2Te_3 by the method of vertical zone melting is shown in Fig. 1.

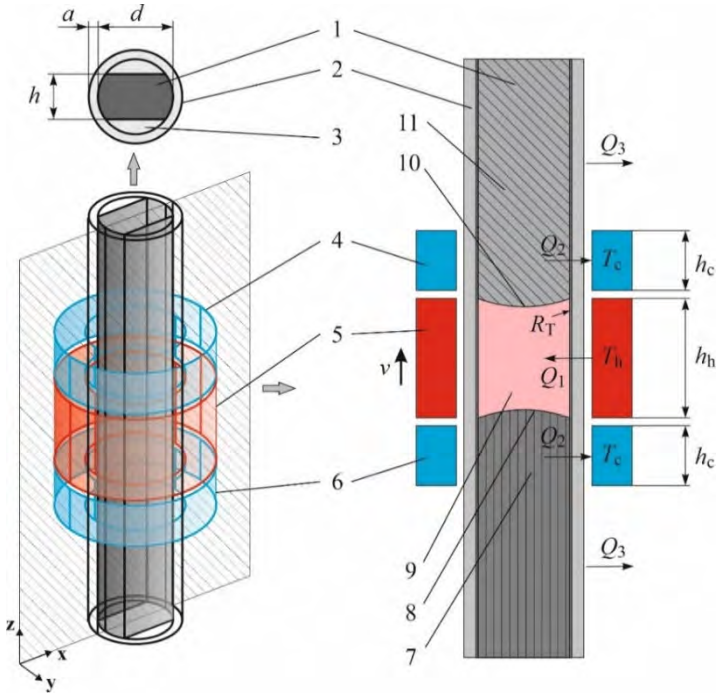

Fig. 1. Physical model of growing thermoelectric materials by vertical zone melting: 1 – thermoelectric material; 2 – container; 3 – quartz inserts; 4, 6 – coolers; 5 – heater; 7 – material in the solid phase (structurally oriented crystal); 8 – crystallization front; 9 – melt zone; 10 – melt front; 11 – material in the solid phase (polycrystal).

The figure shows a fragment of an ingot, which includes polycrystalline material 11, a molten zone 9 and a single crystal 7. The ingot is placed in a container 2. With the help of a heater 5 and a system of coolers 4 and 6, a molten zone 9 is formed, which, moving together with the heater along the ingot, ensures the melting of the polycrystal and the crystallization of the melt below the boundary 8, which is called the crystallization front.

In Fig. 1: T_h is heater temperature; T_c is the temperature of coolers; Q_1 is heat flow transferred from the heater to the container; Q_2 is heat flow transferred from the container to the coolers; Q_3 is heat

flow transferred from the container to the environment; R_T is contact thermal resistance between the walls of the container and the thermoelectric material; *v* is the speed of movement of the thermal unit; *d* is ingot diameter; *a* is the thickness of the container wall. To improve the structure of the material, it is proposed to add special quartz inserts to the container, which will form a flat rod of thermoelectric material with a thickness of *h*.

2. Mathematical and computer models of vertical zone melting process

The COMSOL Multiphysics package of application programs [18] was used for computer simulation of the process of growing the thermoelectric material Bi_2Te_3 [18], which allows simulating almost all physical processes described by algebraic and partial differential equations. For this, it is sufficient to use ready-made modules of the corresponding physical phenomenon. If necessary, the researcher can change the equation built into the COMSOL module, or set his own. The numerical calculation is carried out using the finite element method [19].

The simulation of the movement of the heater and coolers in the COMSOL Multiphysics system was carried out by using the Moving Mesh module, which allows changing the mesh during calculations of non-stationary processes.

The temperature distribution in the studied sample was found from the solution of the differential equation of thermal conductivity, supplemented by the dependences of the physical properties of the studied material, as a function of the phase state at a given point at a given temperature:

$$\rho\, C_p \frac{\partial T}{\partial t} + \rho\, C_p u\, \nabla T + \nabla q = Q, \tag{1}$$

$$q = -\kappa \nabla T, \tag{2}$$

$$\rho = \theta \rho_{phase1} + (1-\theta)\rho_{phase2}, \tag{3}$$

$$C_p = \frac{1}{2}\left(\theta \rho_{phase1}\, C_{p_{phase1}} + (1-\theta)\rho_{phase2}\, C_{p_{phase2}}\right) + L\frac{d\alpha_m}{dT}, \tag{4}$$

$$\alpha_m = \frac{1}{2}\cdot\frac{(1-\theta)\rho_{phase2} - \theta\rho_{phase1}}{\theta\rho_{phase1} + (1-\theta)\rho_{phase2}}, \tag{5}$$

$$\kappa = \theta \kappa_{phase1} + (1-\theta)\kappa_{phase2}, \tag{6}$$

where ρ is the density, C_p is the heat capacity of the material, κ is the thermal conductivity, u is the velocity of the medium which is zero in the problem under study, *T* is the temperature, θ is the phase ratio at a given temperature, α_m is the mass ratio between the phases, *L* is the latent heat of the phase transition, Q is the external heat flow. The $phase1$ and $phase2$ indices indicate which phase the properties belong to, the solid phase or the liquid phase, respectively.

To account for radiation heat transfer, a Surface-to-Surface Radiation boundary condition is added to the Heat Transfer in Solids physics interface in COMSOL Multiphysics by selecting the outer boundaries of the container and thermal unit:

$$-n(-\kappa \nabla T) = \varepsilon \sigma_b (T_{ext}^4 - T^4), \tag{7}$$

where T_{ext} is the wall temperature of the thermal unit; T is the temperature of the container wall, n is

the vector directed along the normal to the surface of the cylinder (container); $\varepsilon = \left(\frac{1}{\varepsilon_1} + \frac{1}{\varepsilon_2} - 1\right)^{-1}$ is the reduced radiation coefficient of the system, ε_1 is the radiation coefficient of the thermal unit, $\varepsilon_2$is the radiation coefficient of the container; σ_b is the Stefan-Boltzmann constant.

Convection and mass transfer of molten Bi_2Te_3 are not taken into account.

To carry out calculations, the geometric dimensions of the system elements, the initial temperatures of the heater and coolers, the liquidus and solidus temperatures of the thermoelectric material based on Bi_2Te_3, as well as the temperature dependence of the properties of the grown material are specified in the created computer model.

3. Results of computer simulation

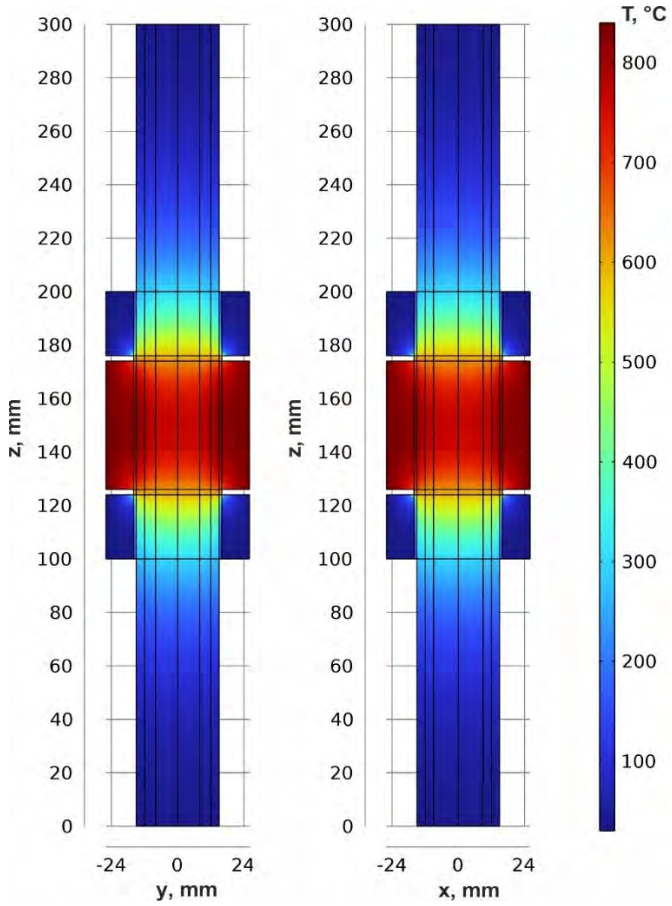

Fig. 2. Typical temperature distribution in a setup for growing thermoelectric materials using the vertical zone melting method. (h = 16 mm; d = 24 mm; a = 3 mm; h_h = 2d; h_c = 1d; T_h = 840°C; T_c = 30°C; v = 0.5 cm/h).

An example of temperature distribution in the sections YZ (x = 0) and XZ (y = 0) for given growing conditions and geometric dimensions (h = 16 mm; d= 24 mm; a = 3 mm; h_h = 2d; h_c = 1d; T_h = 840°C; T_c = 30°C; v = 0.5 cm/h) is given in Fig. 2, an example of crystallization front shape in these sections at different heater temperatures (h = 16 mm; d = 24 mm; a = 3 mm; h_h = 2d; h_c = 1d; T_c = 30°C; v = 0.5 cm/h) – in Fig. 3.

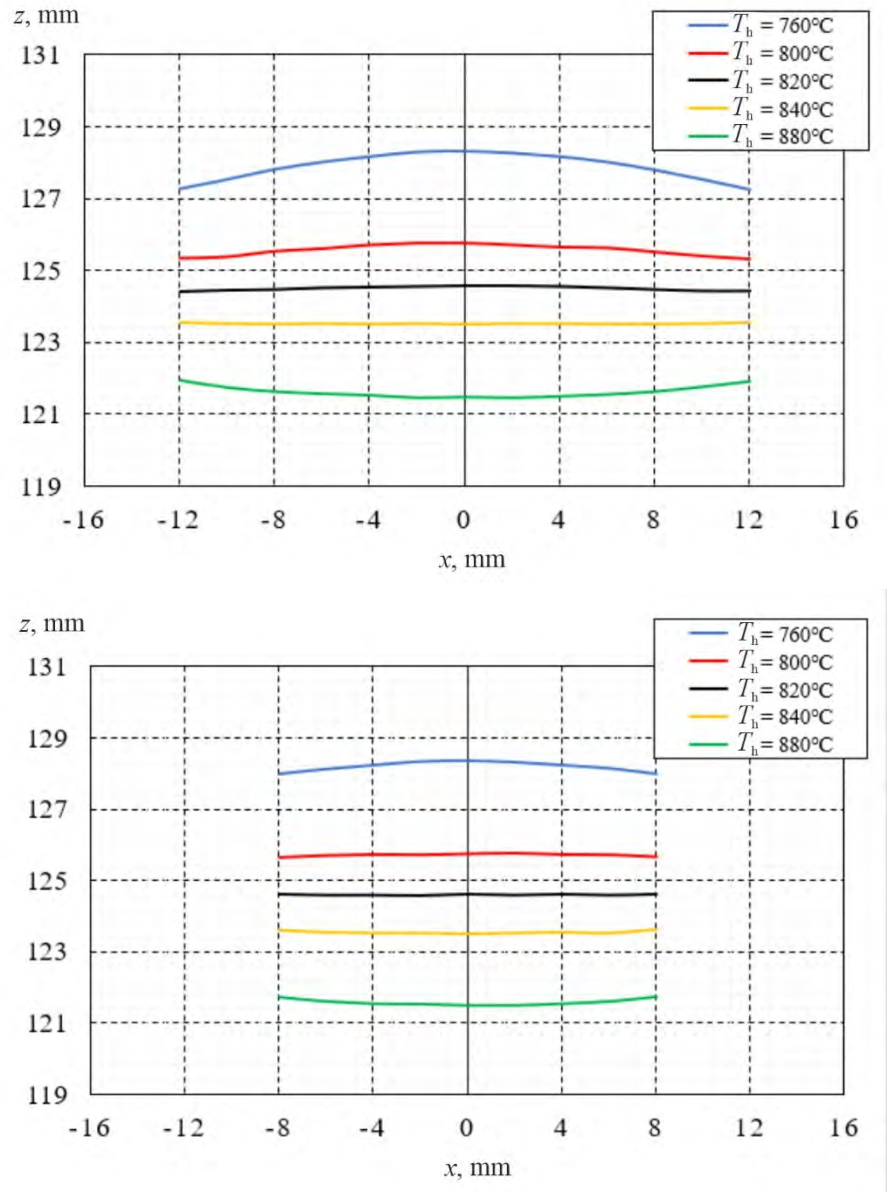

Fig. 3. The shape of the crystallization front in sections XZ (y = 0) and YZ (x = 0) for different temperatures of the heater T_h (h = 16 mm; d = 24 mm; a = 3 mm; h_h = 2d; h_c = 1d; T_c = 30°C; v = 0.5 cm/h).

The created computer model allows one to determine the optimal geometry of the container, the dimensions of the heater and coolers, their temperatures, the speed of movement of the heating unit and other technological parameters and to develop the technology of growing flat ingots of thermoelectric materials based on Bi_2Te_3 without significant costs for the production of a large number of parts of different geometries. and experimental studies.

Conclusions

1. A computer model has been developed to optimize the process of manufacturing flat ingots of thermoelectric materials based on Bi_2Te_3 using the vertical zone melting method.
2. The created computer model allows one to study the dependence of the crystallization front shape on various process parameters (geometric dimensions of the heater and refrigerators, their temperatures, speed of movement, etc.) and thus carry out multifactorial optimization of

technological modes and equipment design, significantly reducing material costs and time, which are necessary for conducting similar experimental studies.

References

1. Cao T., Shi X.L., Li M., Hu B., Chen W., Liu W.Di, W. Lyu, MacLeod J., Chen Z.G. (2023). Advances in bismuth-telluride-based thermoelectric devices: progress and challenges. *EScience*, 3 (3), Article 100122. https://doi.org/0.1016/j.esci.2023.100122.
2. Goldsmid H.J. (2014). Bismuth telluride and its alloys as materials for thermoelectric generation. *Materials*, 7, 2577-2592. https://doi.org/10.3390/ma7042577.
3. Kuo Chia-Hung, Hwang Chii-Shyang, Jeng Ming-Shan, Su Wei-Sheng, Chou Ya-Wen, Ku Jie-Ren (2010). Thermoelectric transport properties of bismuth telluride bulk materials fabricated by ball milling and spark plasma sintering. *Journal of Alloys and Compounds*, 496 (1 – 2), 687 – 690. https://doi.org/10.1016/j.jallcom.2010.02.171.
4. Anatychuk L.I., Hwang Jenn-Dong, Lysko V.V., Prybyla A.V. (2013). Thermoelectric heat recuperators for cement kilns. *J. Thermoelectricity*, 5, 36 – 42.
5. Anatychuk L.I., Lysko V.V., Kravtsov S.O. (2019). Design of thermoelectric generator for transport high-power starting preheater. *J. Thermoelectricity*, 5, 17 – 36.
6. Anatychuk L.I., Lysko V.V. (2021). Computer design of a thermoelectric generator for heat and electricity supply to heavy-duty vehicles. *J. Thermoelectricity*, 2, 79 – 88.
7. Tritt T. (2000). *Recent trends in thermoelectric materials research, Part Two* (Semiconductors and semimetals, Vol. 70). Academic Press, 2000. 320 p. ISBN-13: 978-0127521794.
8. Zhai R.S., Zhu T.J. (2022). Improved thermoelectric properties of zone-melted *p*-type bismuth-telluride-based alloys for power generation. *Rare Met.* 41, 1490 – 1495. https://doi.org/10.1007/s12598-021-01901-2.
9. Saberi Y., Sajjadi S.A. (2022). A comprehensive review on the effects of doping process on the thermoelectric properties of Bi_2Te_3 based alloys. *Journal of Alloys and Compounds*, 904, Article 163918. https://doi.org/10.1016/j.jallcom.2022.163918.
10. Saleemi M., Toprak M.S., Li S., Johnsson M., Muhammed M. (2012). Synthesis, processing, and thermoelectric properties of bulk nanostructured bismuth telluride (Bi_2Te_3). *J. Mater. Chem.* 2, 725 – 730. https://doi.org/10.1039/C1JM13880D.
11. Lysko V.V., Tudoroi P.F. (2019). Computer simulation of extrusion process of Bi_2Te_3 based tape thermoelectric materials. *J. Thermoelectricity*, 2, 58 – 65.
12. Anatychuk L.I., Lysko V.V. (2020). *Thermoelectricity: Vol. 5. Metrology of thermoelectric materials.* Chernivtsi: Bukrek ISBN 978-617-7770-40-3.
13. Anatychuk L.I., Lysko V.V. (2014). On improvement of the accuracy and speed in the process of measuring characteristics of thermoelectric materials. *Journal of Electronic Materials*, 43 (10), 3863–3869. https://doi.org/10.1007/s11664-014-3300-5.
14. Anatychuk L.I., Havrylyuk N.V., Lysko V.V. (2012). Methods and equipment for quality control of thermoelectric materials. *Journal of Electronic Materials*, 41(6), 1680 – 1685. https://doi.org/10.1007/s11664-012-1973-1.
15. Nitsovich O.V. (2018). Research on the conditions of forming a flat crystallization front when growing Bi_2Te_3 based thermoelectric material by vertical zone melting method. *J. Thermoelectricity*. 3, 76 – 82.
16. Anatychuk L.I., Nitsovich O.V. (2018). Simulation of the effect of thermal unit velocity on the

process of growing Bi_2Te_3 based materials by vertical zone melting method. *J. Thermoelectricity,* 3, 76 – 82.
17. Nitsovich O.V. (2018). Computer simulation of Bi_2Te_3 crystallization process in the presence of electrical current. *J. Thermoelectricity*, 5, 12 – 21.
18. COMSOL Multiphysics, v. 6.0. www.comsol.com. COMSOL AB, Stockholm, Sweden. 2021.
19. Reddy J.N. (2006). *An introduction to the finite element method* (Third ed.). McGraw-Hill. ISBN 9780071267618.

Submitted: 14.06.2023.

Лисько В.В., *канд. фіз.-мат. наук* [1,2]
Ніцович О.В., *канд. фіз.-мат. наук* [1]

[1] Інститут термоелектрики НАН та МОН України,
вул. Науки, 1, Чернівці, 58029, Україна;
[2] Чернівецький національний університет імені Юрія Федьковича,
вул. Коцюбинського 2, Чернівці, 58012, Україна
e-mail: anatych@gmail.com

КОМП'ЮТЕРНЕ МОДЕЛЮВАННЯ ПРОЦЕСУ ВИГОТОВЛЕННЯ ПЛОСКИХ ЗЛИТКІВ ТЕРМОЕЛЕКТРИЧНИХ МАТЕРІАЛІВ НА ОСНОВІ Bi_2Te_3 МЕТОДОМ ВЕРТИКАЛЬНОЇ ЗОННОЇ ПЛАВКИ

Представлено результати розробки комп'ютерної моделі для оптимізації процесу виготовлення плоских злитків термоелектричних матеріалів на основі Bi_2Te_3 методом вертикальної зонної плавки. Створена модель дозволяє досліджувати залежності форми фронту кристалізації від різних технологічних параметрів – геометричних розмірів нагрівника та холодильників, їх температур, швидкості руху тощо. Це дає можливість проводити багатофакторну оптимізацію технологічних режимів та конструкції обладнання, суттєво знизивши матеріальні витрати і час, що необхідні для проведення аналогічних експериментальних досліджень. Бібл. 19, рис. 3.

Ключові слова: моделювання, вертикальна зонна плавка, термоелектричний матеріал, телурид вісмуту.

Література

1. Cao T., Shi X.L., Li M., Hu B., Chen W., Liu W.Di, W. Lyu, MacLeod J., Chen Z.G. (2023). Advances in bismuth-telluride-based thermoelectric devices: progress and challenges. *EScience*, 3 (3), Article 100122. https://doi.org/0.1016/j.esci.2023.100122.
2. Goldsmid H.J. (2014). Bismuth telluride and its alloys as materials for thermoelectric generation. *Materials*, 7, 2577-2592. https://doi.org/10.3390/ma7042577.
3. Kuo Chia-Hung, Hwang Chii-Shyang, Jeng Ming-Shan, Su Wei-Sheng, Chou Ya-Wen, Ku Jie-Ren (2010). Thermoelectric transport properties of bismuth telluride bulk materials fabricated by ball milling and spark plasma sintering. *Journal of Alloys and Compounds,* 496 (1 – 2), 687 – 690. https://doi.org/10.1016/j.jallcom.2010.02.171.
4. Anatychuk L.I., Hwang Jenn-Dong, Lysko V.V., Prybyla A.V. (2013). Thermoelectric heat

recuperators for cement kilns. *J. Thermoelectricity*, 5, 36 – 42.
5. Anatychuk L.I., Lysko V.V., Kravtsov S.O. (2019). Design of thermoelectric generator for transport high-power starting preheater. *J. Thermoelectricity*, 5, 17 – 36.
6. Anatychuk L.I., Lysko V.V. (2021). Computer design of a thermoelectric generator for heat and electricity supply to heavy-duty vehicles. *J. Thermoelectricity*, 2, 79 – 88.
7. Tritt T. (2000). *Recent trends in thermoelectric materials research, Part Two* (Semiconductors and semimetals, Vol. 70). Academic Press, 2000. 320 p. ISBN-13: 978-0127521794.
8. Zhai R.S., Zhu T.J. (2022). Improved thermoelectric properties of zone-melted *p*-type bismuth-telluride-based alloys for power generation. *Rare Met.* 41, 1490 – 1495. https://doi.org/10.1007/s12598-021-01901-2.
9. Saberi Y., Sajjadi S.A. (2022). A comprehensive review on the effects of doping process on the thermoelectric properties of Bi_2Te_3 based alloys. *Journal of Alloys and Compounds*,904, Article 163918. https://doi.org/10.1016/j.jallcom.2022.163918.
10. Saleemi M., Toprak M.S., Li S., Johnsson M., Muhammed M. (2012). Synthesis, processing, and thermoelectric properties of bulk nanostructured bismuth telluride (Bi_2Te_3). *J. Mater. Chem.* 2, 725 – 730. https://doi.org/10.1039/C1JM13880D.
11. Lysko V.V., Tudoroi P.F. (2019). Computer simulation of extrusion process of Bi_2Te_3 based tape thermoelectric materials. *J. Thermoelectricity*, 2, 58 – 65.
12. Anatychuk L.I., Lysko V.V. (2020). *Thermoelectricity: Vol. 5. Metrology of thermoelectric materials.* Chernivtsi: Bukrek ISBN 978-617-7770-40-3.
13. Anatychuk L.I., Lysko V.V. (2014). On improvement of the accuracy and speed in the process of measuring characteristics of thermoelectric materials. *Journal of Electronic Materials*, 43 (10), 3863–3869. https://doi.org/10.1007/s11664-014-3300-5.
14. Anatychuk L.I., Havrylyuk N.V., Lysko V.V. (2012). Methods and equipment for quality control of thermoelectric materials. *Journal of Electronic Materials*, 41 (6), 1680 – 1685. https://doi.org/10.1007/s11664-012-1973-1.
15. Nitsovich O.V. (2018). Research on the conditions of forming a flat crystallization front when growing Bi_2Te_3 based thermoelectric material by vertical zone melting method. *J. Thermoelectricity*. 3, 76 – 82.
16. Anatychuk L.I., Nitsovich O.V. (2018). Simulation of the effect of thermal unit velocity on the process of growing Bi_2Te_3 based materials by vertical zone melting method. *J. Thermoelectricity*, 3, 76 – 82.
17. Nitsovich O.V. (2018). Computer simulation of Bi_2Te_3 crystallization process in the presence of electrical current. *J. Thermoelectricity*, 5, 12 – 21.
18. COMSOL Multiphysics, v. 6.0. www.comsol.com. COMSOL AB, Stockholm, Sweden. 2021.
19. Reddy J.N. (2006). *An introduction to the finite element method* (Third ed.). McGraw-Hill. ISBN 9780071267618.

Надійшла до редакції: 14.06.2023.

R.G. Cherkez, *DSc (Phys-Math)* [1,2]
O.M. Porubanyi, *graduate student* [2]
A.S. Zhukova, *student* [2]
M.O. Dubinin, *student* [3]
N.V. Panasiuk, *student* [2]

[1] Institute of Thermoelectricity of the NAS and MES of Ukraine, 1 Nauky str., Chernivtsi, 58029, Ukraine;
[2] Yuriy Fedkovych Chernivtsi National University, 2 Kotsiubynskyi str., Chernivtsi, 58000, Ukraine;
[3] Podilskyi State University, 13 Shevchenko str., Kamianets-Podilskyi, 32316, Ukraine
e-mail: anatych@gmail.com

COMPUTER DESIGN OF PERMEABLE FUNCTIONALLY GRADED MATERIALS FOR THERMOELEMENTS IN ELECTRIC ENERGY GENERATION MODE

Based on the Pontryagin maximum principle of optimal control theory, a methodology for designing optimal functionally graded materials (FGM) for permeable thermoelectric elements is presented. An algorithm and a computer program have been created, which have been tested for finding the optimal FGM for n- and p-type legs based on Bi-Te-Se-Sb. It has been shown that under optimal conditions, 1.3 – 1.7 fold efficiency increase is achieved when using permeable generator thermoelements with FGM compared to traditional thermoelements with homogeneous legs.
Key words: computer design, permeable structures.

Introduction

The possibilities of wide practical application of thermoelectricity for creation of electric energy sources depend primarily on their efficiency. The main ways of increasing the efficiency are considered to be, first of all, improvement of the figure of merit of thermoelectric materials $Z = \alpha^2\sigma/\kappa$ (α – thermoEMF, σ – electrical conductivity, κ – thermal conductivity) and reduction of losses in heat supply and removal systems.

Analysis of the literature. The main methods for increasing the figure of merit of thermoelectric materials were formulated by A.F. Ioffe in the middle of the last century [1]. They come down to optimizing the thermoelectric material by appropriate doping with active impurities to achieve maximum values of $\alpha^2\sigma$ and doping the material with isovalent substitution impurities to reduce thermal conductivity. Such methods were applied to a number of materials, which led to an increase in the figure of merit and, accordingly, contributed to the widespread use of thermoelectricity.

However, in the last decade, despite numerous studies, further growth of the figure of merit of thermoelectric materials has been insignificant. It becomes obvious that the above methods have exhausted themselves. There is a need to find new ways to increase efficiency. Therefore, more and more attention is paid to the study of one-dimensional and filament structures, film materials and quantum well composites. Unfortunately, to date, these methods have not yet yielded significant practical results in thermoelectricity. Thermoelectric materials with programmable functional

inhomogeneity (FGM) are also being studied, which increase the efficiency due to the use of volumetric thermoelectric effects and the correct consideration of the temperature dependence of material properties [2, 3]. Today, this method is considered the most realistic for increasing the efficiency of thermoelectric energy conversion.

The improvement of the heat exchange system consists in the intensification of heat exchange, which can be implemented in the case when heat is supplied or removed not only through the surfaces of the hot and cold junctions, but also by using the volume of thermoelement legs. Such thermoelements are made permeable to heat carriers, due to which they are usually called permeable [6 – 8].

I.V. Zorin in his author's certificates was one of the first to point out the possibility of increasing the efficiency of thermoelectric energy conversion by using permeable thermoelements. A consistent research of the capabilities of thermoelements with permeable legs was pursued in Ukraine. The paper [9] presents a classification of variants of physical models of such thermoelements. Studies of extreme energy characteristics of a generator thermoelement made of permeable legs when passing a heat carrier from the hot to cold junctions confirmed the possibility of a significant efficiency increase [10], where such problems were solved for a homogeneous material of the thermoelement legs without taking into consideration the temperature dependences of its parameters.

Since efficiency increase is achieved both by using thermoelement legs that are permeable to heat carrier and by using inhomogeneous materials, research into the possibilities of the combined influence of these two factors on the efficiency of energy conversion is promising. A new optimization problem arises, which consists in the fact that it is necessary to find such optimal parameters (heat carrier flow rate, electric current density, etc.) that are consistent with the optimal distribution function of the inhomogeneity of the thermoelectric materials of legs (FGM), at which the highest value of the efficiency of the generator thermoelement is achieved.

Model of a permeable FGM thermoelement, mathematical description and method of solving the problem

The physical model of a permeable FGM thermoelement, operating in the electric energy generation mode, is shown in Fig. 1. It contains *n*- and *p*-type legs, the properties of which change with the *x* coordinate due to their dependence on the temperature *T(x)* and the concentration of current carriers $\xi(x)$. The temperature of the heat carrier supplied to the thermoelement is T_m, the temperature of the cold junctions of the thermoelement is T_c. The presence of contact resistances r_0 at the junctions of connecting plates with the thermoelement legs is taken into consideration. The side surfaces of the legs are insulated. The heat carrier is pumped through the thermoelement. Heat from the heat carrier is transferred to the material through heat exchange with the inner surface of the channels of the legs and creates a temperature distribution in the material of the legs. The action of thermoelectric effects leads to the occurrence of thermoEMF.

The stationary distribution of temperatures *T*(*x*) and heat flows *q*(*x*), heat carriers *t*(*x*) in the legs will be found by solving the system of differential equations

$$\left.\begin{aligned} \frac{dT}{d\mathrm{x}} &= -\frac{\alpha\ j}{\kappa}\ T - \frac{j}{\kappa}q, \\ \frac{dq}{d\mathrm{x}} &= \frac{\alpha^2 j}{\kappa}T + \frac{\alpha\ j}{\kappa}q + j\rho + \frac{\alpha_e l}{\left(S - S_K\right) j}\left(t - T\right), \\ \frac{dt}{d\mathrm{x}} &= \frac{\alpha_e}{Gc_P}\left(t - T\right), \end{aligned}\right\}_{n,p} \qquad (1)$$

where $\alpha_{n,p} = \alpha_{n,p}(T(x),\xi_{n,p}(x))$, $\kappa_{n,p} = \kappa_{n,p}(T(x), \xi_{n,p}(x))$, $\rho_{n,p} = \rho_{n,p}(T(x), \xi_{n,p}(x))$ are the Seebeck coefficient, thermal conductivity and electrical resistivity of the material of *n*- and *p*-type legs that depend on the concentration of current carriers $\xi_{n,p}(x)$ and temperature $T(x)$; $x = \frac{x}{l}$ is dimensionless coordinate; $\alpha_e = \alpha_T \Pi_K^1 N_K l$ is effective coefficient of heat transfer, α_T is coefficient of heat transfer of heat carrier in the channels, Π_K^1 is the perimeter of one channel, N_K is the number of channels in the leg, l is the height of thermoelement legs; t is the temperature of heat carrier at point x; T is the temperature of leg at point x; $j = il$; i is current density ($i = \frac{I}{(S - S_K)}$); S – is the cross-sectional area of leg together with the channels; S_K is the cross-sectional area of all channels of the leg; G is mass flow rate of heat carrier; c_p is heat capacity of heat carrier.

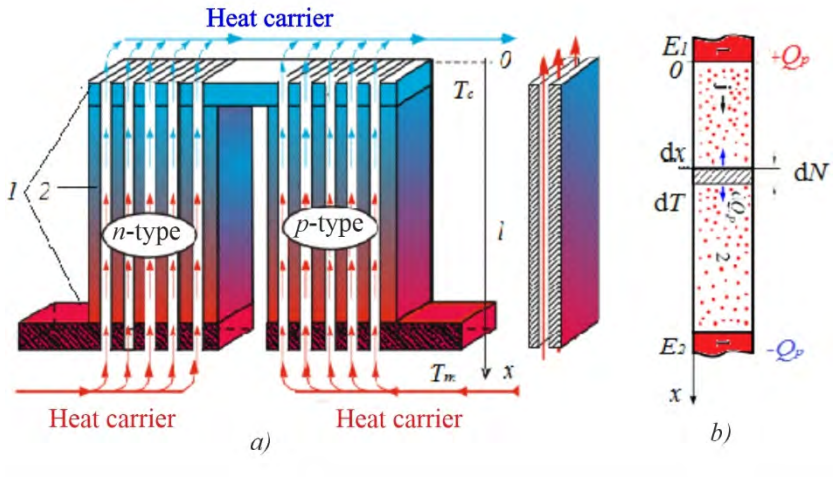

Fig. 1. Model of a permeable generator thermoelement (a): 1 – connecting plates; 2 – legs of n and p conductivity types; (b) – volumetric effects in the legs of an inhomogeneous thermoelement: 1 – electrical contact, 2 – thermoelectric material.

The main task is to find mutually consistent optimal distributions of the current carrier concentrations in the material of the legs $\xi_{n,p}(x)$, the coolant flow rate G and the electric current density j, at which the maximum efficiency is achieved for the given temperatures of the cold junctions T_c, the heat carrier T_m and under the condition of thermal insulation of the hot junctions. Therefore, the boundary conditions for the system of differential equations (1) are as follows:

$$t_{n,p}(1) = T_m, \quad q_n(1) + q_p(1) = 0, \quad T_n(1) = T_p \tag{1}$$

$$T_{n,p}(0) = T_c, \tag{2}$$

The task of achieving maximum efficiency:

$$\eta = \frac{W}{Q_p} \tag{3}$$

where $W = \sum_{n,p}\left\{Gc_P\left(T_m - t(0)\right) + \left(q(0) + j\frac{r_0}{l}\right)\frac{j\left(S - S_K\right)}{l}\right\}$ is electric power generated by thermoelement; $Q_p = \sum_{n,p} Gc_p\left(T_m - T_c\right)$ is thermal energy of the heat carrier; r_0 is contact resistance, can be conveniently reduced to the task of achieving the minimum of functional:

$$J = \ln\left[\sum_{n,p}\left\{G_{C_p}\left(T_m - T_C\right)\right\}\right] - \ln\left[\sum_{n,p}\left\{G_{C_p}\left(T_m - t(0)\right) + \left(q(0) + j\frac{r_0}{l}\right)\frac{jS}{l}\right\}\right] \tag{4}$$

In the language of optimal control theory, the optimization problem is to determine the heat carrier flow rate *G*, the generating current density *j*, and the carrier concentration functions in the leg material $\xi_{n,p}(x)$ (or the concentration value $\xi_{n,p}$, for the case of searching for an optimally homogeneous leg material), which, under the constraints imposed by the system (1), (2), impart to the functional *J* the smallest value.

To solve such an optimization problem, the Pontryagin maximum principle [10] of mathematical optimal control theory is used. For the minimum of *J* the following conditions must be met:

1. Current density must satisfy the equation:

$$-\frac{\partial J}{\partial j} + \sum_{n,p}\int_0^1 \frac{\partial H\ (\psi, T, q, t, j, G)}{\partial j} dx = 0 \tag{5}$$

2. Heat carrier flow rate in the channels must satisfy the equation:

$$-\frac{\partial J}{\partial G} + \sum_{n,p}\int_0^1 \frac{\partial H\ (\psi, T, q, t, j, G)}{\partial G} dx = 0 \tag{6}$$

3. Inhomogeneity functions of legs materials $\xi_{n,p}(x)$ are found from condition:

$$H^*_{n,p}(T(x), q(x), t(x), \psi(x), \xi(x), j, G) = \max_{\xi_{n,p} \in U_\xi} H_{n,p}(T(x), q(x), t(x), \psi(x), \xi, j, G) \tag{7}$$

In the case of searching for optimally homogeneous materials, instead of (7) to find the optimal values of the concentration of current carriers in the legs $\xi_{n,p}$, it is necessary to use the relation

$$\begin{aligned} -\frac{\partial J}{\partial \xi_n} + \int_0^1 \frac{\partial H_n(\psi, T, q, t, j, G)}{\partial \xi_n} dx = 0, \\ -\frac{\partial J}{\partial \xi_p} + \int_0^1 \frac{\partial H_p(\psi, T, q, t, j, G)}{\partial \xi_p} dx = 0. \end{aligned} \tag{8}$$

Here *H* is the Hamilton-Pontryagin function

$$H_{n,p} = \left(\psi_1 f_1 + \psi_2 f_2 + \psi_3 f_3\right)_{n,p}, \tag{9}$$

where $(f_1, f_2, f_3)_{n,p}$ are the right-hand parts of the system of differential equations (1), $\psi = (\psi_1, \psi_2, \psi_3)_{n,p}$ is the momentum vector determined from the solution of the auxiliary system of differential equations canonically conjugate to system (1)

$$\left.\begin{aligned}
\frac{d\psi_1}{d\mathrm{x}} &= \frac{\alpha\ j}{\kappa} R_1 \psi_1 - \left(\frac{\alpha\ j}{\kappa} R_2 - \frac{\alpha_e l}{(S - S_K) j} \right) \psi_2 + \frac{\alpha_e}{G c_P} \psi_3, \\
\frac{d\psi_2}{d\mathrm{x}} &= \frac{j}{\kappa} \psi_1 - \frac{\alpha\ j}{\kappa} \psi_2, \\
\frac{dt}{d\mathrm{x}} &= -\frac{\alpha_e l}{(S - S_K) j} \psi_2 - \frac{\alpha_e}{G c_P} \psi_3,
\end{aligned}\right\}_{n,p} \tag{10}$$

where

$$\left.\begin{aligned}
R_1 &= 1 + \frac{d \ln \alpha}{dT} T - \frac{d \ln \kappa}{dT} \left(T + \frac{q}{\alpha} \right), \\
R_2 &= R_1 + \frac{1}{Z_K} \frac{d \ln \sigma}{dT} + \frac{d \ln \kappa}{dT} \left(T + \frac{q}{\alpha} \right)
\end{aligned}\right\}_{n,p}$$

with the boundary conditions

$$\begin{aligned}
&\psi_1^n(1) + \psi_1^p(1) = 0, \qquad \psi_2^n(1) = \psi_2^p(1), \\
&\psi_2^{n,p}(0) = -\frac{\dfrac{j(S - S_K)}{l}}{\displaystyle\sum_{n,p} \left\{ G c_P (T_m - t(0)) + \left(q(0) + j \frac{r_0}{l} \right) \frac{j(S - S_K)}{l} \right\}}, \\
&\psi_3^{n,p}(0) = \frac{G c_P}{\displaystyle\sum_{n,p} \left\{ G c_P (T_m - t(0)) + \left(q(0) + j \frac{r_0}{l} \right) \frac{j(S - S_K)}{l} \right\}}.
\end{aligned} \tag{11}$$

Based on the system of equations (1), (2), (5) – (11), a computer program has been developed that allows one to determine the optimal distribution of the current carrier concentration $\xi_{n,p}(\mathrm{x})$, the heat carrier flow rate G and the electric current density j, whereby the efficiency (3) of the permeable thermoelement will be maximum.

Calculation results of a permeable thermoelement made of materials based on *Bi-Te-Se-Sb*

Let us consider the application of the described method for calculating a permeable thermoelement with a leg height of 1 cm, a cross-sectional area $S - S_K = 1$ cm^2, the temperature of the cold junctions $T_c = 300$ K; the leg materials are solid solutions $Bi_2(TeSe)_3$ of *n*-type conductivity and $(BiSb)_2Te_3$ for a leg of *p*-type conductivity. Fig. 3 shows the temperature and concentration dependences of such materials obtained by approximating experimental data from the literary sources [10].

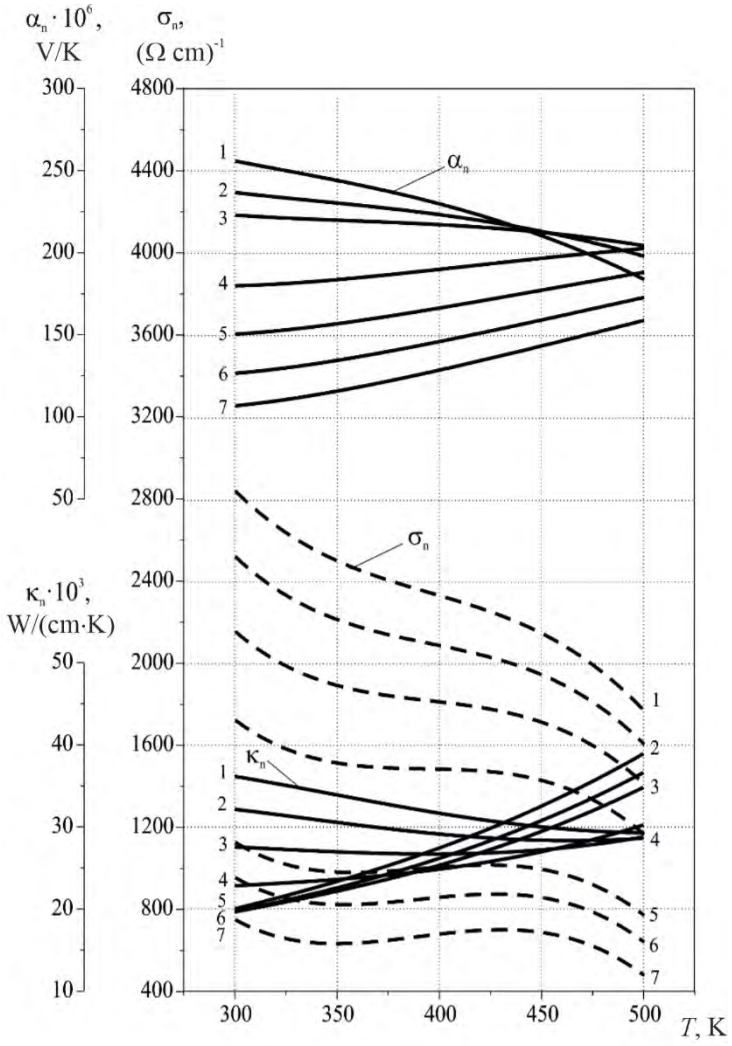

Fig. 2. Temperature dependences of material parameters for different concentrations of current carriers:1 – 6·10^{18} cm^{-3}, 2 – 8·10^{18} cm^{-3}, 3 – 1·10^{19} cm^{-3}, 4 – 2·10^{19} cm^{-3}, 5 – 3·10^{19} cm^{-3}, 6 – 4·10^{19} cm^{-3}, 7 – 5·10^{19} cm^{-3}.

These materials are most widely used to create thermoelectric elements and modules based on them, operating in the temperature range of 300 – 500 K. The given dependences were used as limitations imposed on the properties of the leg materials during computer calculations.

An example of the optimal FGM distribution for the material of *n*- and *p*-type legs is shown in Fig. 4. With this distribution, volumetric thermoelectric effects are realized in the best way, which gives the maximum value of the efficiency of thermal into electrical energy conversion.

Calculations of the efficiency of permeable thermoelements using functionally graded materials were carried out and the results were compared with the efficiency of a permeable thermoelement made of a homogeneous material. The developed computer design methods make it possible to obtain, as a zero approximation, the efficiency value for a permeable thermoelement made of a homogeneous material, taking into account the temperature dependence of the material properties and the choice of such a value of the current carrier concentration for electrons and holes, at which the best efficiency value is achieved in a given temperature range.

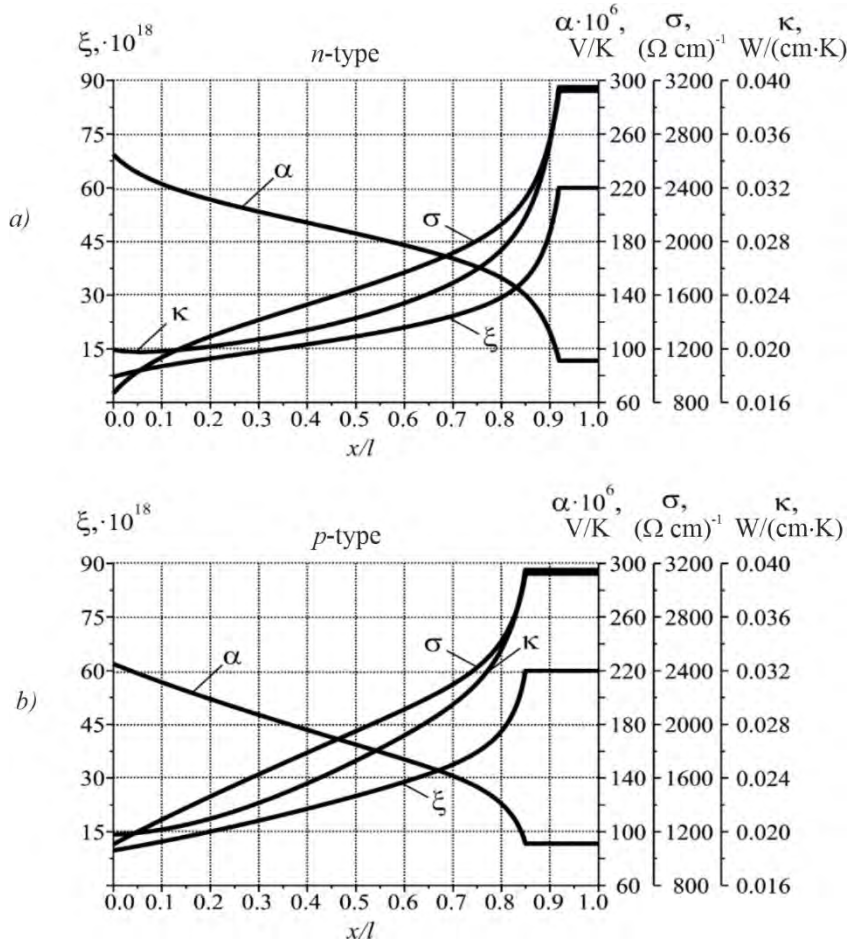

Fig. 3. Optimal distribution of parameters α, σ, κ of a permeable thermoelement along the length of leg l: a) for solid solutions $Bi_2(TeSe)_3$ of n-type conductivity; b) for solid solutions $(BiSb)_2Te_3$ of p-type conductivity; ξ – optimal concentration of current carriers; α, σ, κ – optimal Seebeck coefficient, electrical conductivity and thermal conductivity; heat carrier temperature at the input to thermoelement – 600 K; temperature of thermoelement cold junctions – 300 K; effective heat transfer coefficient – 0.1 W/K.

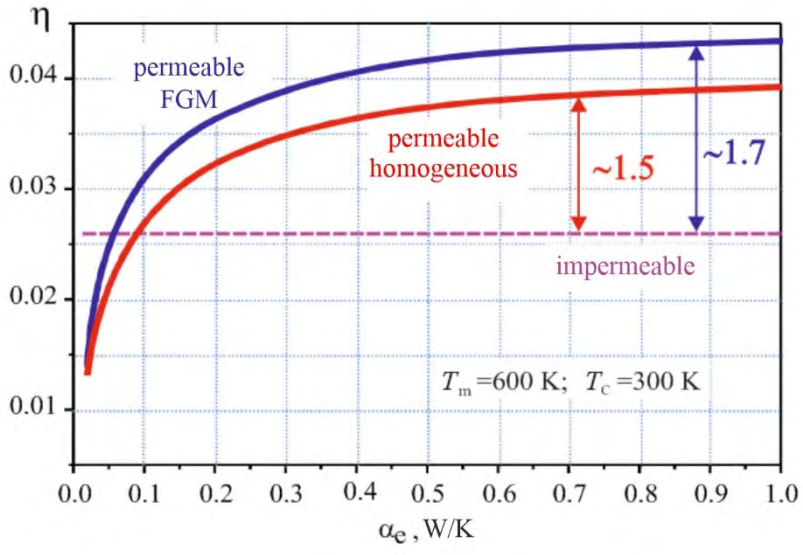

Fig. 4. Dependences of maximum efficiency of a permeable generator thermoelement on the effective coefficient of heat transfer $α_e$.

Computer studies of the maximum values of energy characteristics (efficiency and power) that are realized at optimal FGM, electric current density and heat carrier pumping speed have been carried out. The results of the obtained efficiency values and their comparison are shown in Fig. 4.

It is evident that the efficiency increases by 1.4 times when using permeable homogeneous thermoelements compared to impermeable ones, and by 1.7 times when using permeable thermoelements made of functionally graded materials.

Conclusions

1. Based on the Pontryagin maximum principle of optimal control theory, a method for computer design of optimal functions of thermoelectric material inhomogeneity for permeable thermoelements of maximum efficiency of thermal into electrical energy conversion has been developed.
2. The method was tested on a model of a thermocouple generator thermoelement with permeable legs for materials based on *Bi-Te-Se-Sb*. Computer methods were used to find the optimal distribution functions of the inhomogeneity of electrical conductivity, thermoEMF and thermal conductivity for *n*- and *p*-type materials.
3. It has been shown that permeable thermoelements made of FGM based on *Bi-Te-Se-Sb* at a heat carrier temperature of 600 K provide an increase in efficiency by 1.4 times, and when using permeable thermoelements made of functionally graded materials – by 1.7 times compared to traditional thermoelements.
4. The results obtained indicate the potential of using optimal control theory methods for designing permeable thermoelements made of FGM.

References

1. Anatychuk L.I., Vikhor L.N. (1996). Computer design of thermoelectric functionally graded materials. *Proceedings of the Fourth International Symposium on FGM, Tsukuba, Japan, Oct. 21 – 24, 1996.*
2. Anatychuk L.I., Vikhor L.N., Cherkez R.G. (1997). Computer simulation of functionally graded materials for thermoelectricity. *J. Thermoelectricity*, 3, 43 – 61.
3. *Patent 6673996 B2 USA InCl H 01 L 35/34* Thermoelectric unicouple used for power generation. Caillat T., Zoltan A., Zoltan, L., Snyder J. (USA); California Institute of Technology. N 10/138040; Filed 01.05.2002; Publ. 06.01.2004. – 7 p.
4. *Patent 6673996 B2 USA InCl H 01 L 35/34* Thermoelectric unicouple used for power generation. Caillat T., Zoltan A., Zoltan, L., Snyder J. (USA); California Institute of Technology. N 10/138040; Filed 01.05.2002; Publ. 06.01.2004. – 7 p.
5. Calliat T., Fleurial J.-P., Snyder G.J., Zoltan A., Zoltan D. (1999). *Proc. of the XVIIIth International Conf. on Thermoelectrics (USA, 1999)*, p. 473.
6. El-Genk Mohamed S.and Saber Hamed H. (2003). *Energy Conversion and Management, 44 (7), 1069* (2003); https://doi.org/10.1016/S0196-8904(02)00109-7.
7. Method for improvement of thermoelectric generator efficiency. USSR Certificate of Authorship №162578 / I.V. Zorin, Filed 02.05.1968.
8. Anatychuk L.I., Cherkez R.G. (2003). Permeable thermoelement in generation electric energy mode. *J. Thermoelectricity*, 2, 36.
9. Anatychuk L.I., Luste O.J., Mikhailovsky V.Ya. (2005). Thermoelectric generators for automobiles. *J. Thermoelectricity* 4, 21.

10. Anatychuk L.I., Cherkez R.G. (2010). Permeable segmented thermoelement in generation mode. *J. Thermoelectricity*, 3, 5.
11. Pontryagin L.S., Boltyansky V.G., Gamkrelidze R.V., Mischenko E.F. (1976). *Matematicheskaia Teoriia Optimalnykh Protsessov [Mathematical Theory of Optimal Processes]*. Moscow: Nauka [in Russian].
12. Anatychuk L.I., Vikhor L.N. (2009). *Energy Conversion and Management*, 50 (9), 2366. https://doi.org/10.1016/j.enconman.2009.05.020.

Submitted: 27.06.2023.

Черкез Р.Г, *доктор фіз.-мат. наук* [1,2]
Порубаний О.М., *аспірант* [2]
Жукова А.С., *студент* [2]
Дубінін М.О., *студент* [3]
Панасюк Н.В., *студент* [2]

[1] Інститут термоелектрики НАН та МОН України,
вул. Науки, 1, Чернівці, 58029, Україна;
[2] Чернівецький національний університет імені Юрія Федьковича,
вул. Коцюбинського 2, Чернівці, 58012, Україна;
[3] Подільський державний університет, вул. Шевченка, 13,
Кам'янець-Подільський, 32316, Україна
e-mail: anatych@gmail.com

КОМП'ЮТЕРНЕ ПРОЕКТУВАННЯ ПРОНИКНИХ ФУНКЦІОНАЛЬНО-ГРАДІЄНТНИХ МАТЕРІАЛІВ ДЛЯ ТЕРМОЕЛЕМЕНТІВ В РЕЖИМІ ГЕНЕРАЦІЇ ЕЛЕКТРИЧНОЇ ЕНЕРГІЇ

На основі принципу максимуму Л.С. Понтрягіна теорії оптимального керування представлено методику проектування оптимальних функціонально-градієнтних матеріалів (ФГМ) для проникних термоелектричних елементів. Створено алгоритм та комп'ютерну програму, яку апробовано для знаходження оптимального ФГМ для віток n- та p- типів провідності на основі Bi-Te-Se-Sb. Показано, що в оптимальних умовах, досягається підвищення ККД при використанні проникних генераторних термоелементів із ФГМ у 1.3 – 1.7 раз порівняно з традиційними термоелементами із однорідних віток.
Ключові слова: комп'ютерне проектування, проникні структури.

Література

1. Anatychuk L.I., Vikhor L.N. (1996). Computer design of thermoelectric functionally graded materials. *Proceedings of the Fourth International Symposium on FGM, Tsukuba, Japan, Oct. 21 – 24, 1996.*
2. Anatychuk L.I., Vikhor L.N., Cherkez R.G. (1997). Computer simulation of functionally graded materials for thermoelectricity. *J. Thermoelectricity*, 3, 43 – 61.

3. *Patent 6673996 B2 USA InCl H 01 L 35/34* Thermoelectric unicouple used for power generation. Caillat T., Zoltan A., Zoltan, L., Snyder J. (USA); California Institute of Technology. N 10/138040; Filed 01.05.2002; Publ. 06.01.2004. – 7 p.
4. *Patent 6673996 B2 USA InCl H 01 L 35/34* Thermoelectric unicouple used for power generation. Caillat T., Zoltan A., Zoltan, L., Snyder J. (USA); California Institute of Technology. N 10/138040; Filed 01.05.2002; Publ. 06.01.2004. – 7 p.
5. Calliat T., Fleurial J.-P., Snyder G.J., Zoltan A., Zoltan D. (1999). *Proc. of the XVIIIth International Conf. on Thermoelectrics (USA, 1999),* p. 473.
6. El-Genk Mohamed S.and Saber Hamed H. (2003). *Energy Conversion and Management, 44 (7), 1069* (2003); https://doi.org/10.1016/S0196-8904(02)00109-7.
7. Method for improvement of thermoelectric generator efficiency. USSR Certificate of Authorship №162578 / I.V. Zorin, Filed 02.05.1968.
8. Anatychuk L.I., Cherkez R.G. (2003). Permeable thermoelement in generation electric energy mode. *J. Thermoelectricity*, 2, 36.
9. Anatychuk L.I., Luste O.J., Mikhailovsky V.Ya. (2005). Thermoelectric generators for automobiles. *J. Thermoelectricity* 4, 21.
10. Anatychuk L.I., Cherkez R.G. (2010). Permeable segmented thermoelement in generation mode. *J. Thermoelectricity*, 3, 5.
11. Pontryagin L.S., Boltyansky V.G., Gamkrelidze R.V., Mischenko E.F. (1976). *Matematicheskaia Teoriia Optimalnykh Protsessov [Mathematical Theory of Optimal Processes]*. Moscow: Nauka [in Russian].
12. Anatychuk L.I., Vikhor L.N. (2009). *Energy Conversion and Management*, 50 (9), 2366. https://doi.org/10.1016/j.enconman.2009.05.020.

Надійшла до редакції: 27.06.2023.

Anatychuk L.I., *Acad. NAS Ukraine* [1,2]
Kobylianskyi R.R., *Cand.Sc.(Phys-Math)* [1,2]
Lysko V.V., *Cand. Sc (Phys &Math)*[1,2]
Prybyla A.V., *Cand. Sc (Phys &Math)* [1,2]
Konstantynovych I.A., *Cand. Sc. (Phys and Math)* [1,2]
Kobylianska A.K., *Cand. Sc (Phys &Math)* [1]
Havryliuk M.V. [1,2]
Boychuk V.V. [2]

[1] Institute of Thermoelectricity of the NAS and MES of Ukraine,
1 Nauky str., Chernivtsi, 58029, Ukraine;
[2] Yuriy Fedkovych Chernivtsi National University, 2 Kotsiubynskyi str.,
Chernivtsi, 58000, Ukraine
e-mail: anatych@gmail.com

METHOD OF CALIBRATION OF THERMOELECTRIC SENSORS FOR MEDICAL PURPOSES

This paper presents the results of creating an experimental bench for calibrating thermoelectric heat flux sensors and analyzing their metrological properties. Calibration procedures have been developed for both one and two sensors simultaneously. A new type of thermoelectric sensors capable of simultaneously measuring temperature and heat flux on the surface of the human body has also been created and tested.

Key words: calibration bench, thermoelectric sensor, heat flux, volt-watt sensitivity.

Introduction

The use of thermoelectric sensors is very promising for assessing local thermal radiation on the surface of the human body [1 – 4]. Modern thermoelectric heat flux sensors, created on the basis of high-performance semiconductor materials, are characterized by high sensitivity, fast response, manufacturability, optimal weight-dimensional characteristics, high reliability and low cost [5 – 16]. These sensors are easy to maintain and are capable of continuously monitoring the thermal radiation of the human body [17 – 31], as well as detecting heat losses in remote heating mains.

The issue of calibration of thermoelectric heat flux sensors, which are used in devices for measuring integral heat fluxes of biological objects, losses through building elements, heat-shielding materials and in sections of heating mains, remains relevant. Usually, the calibration of these sensors is performed by the absolute method, which includes the use of a blocking heater and differential thermocouples as indicators of zero temperature difference [32, 33]. However, such calibration requires an increase in the accuracy of measurements, since these sensors are measuring instruments. Increasing the accuracy is possible by using an additional highly sensitive thermoelectric heat flux sensor [34 – 40].

Therefore, *the main purpose of the work* is to create an experimental bench for calibrating thermoelectric heat flux sensors using an improved method, as well as to analyze their metrological properties.

1. Design of the experimental bench for calibrating thermoelectric heat flux sensors (HFS)

To analyze metrological parameters and calibrate thermoelectric heat flux sensors (HFS) in the temperature range from – 30 °C to + 130 °C, a bench design was created, shown in Fig. 1.

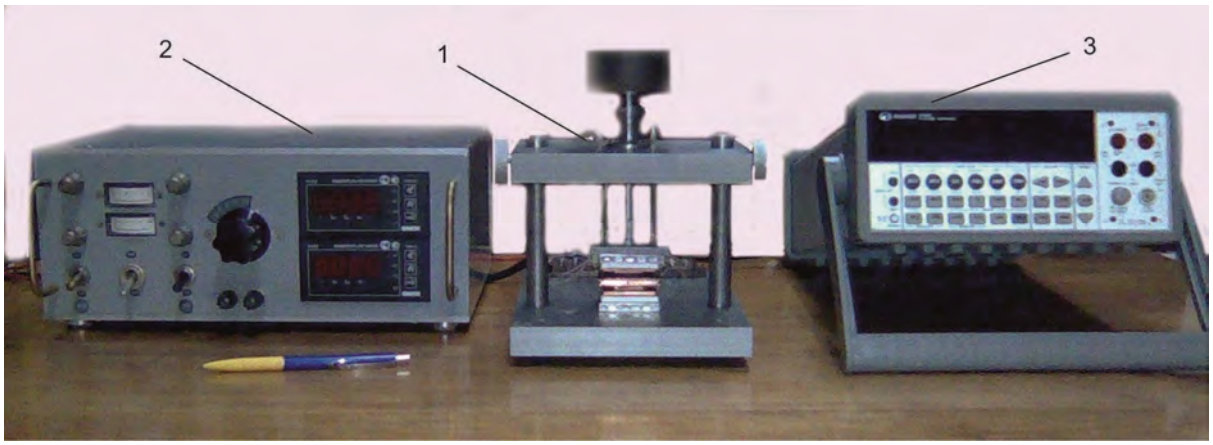

Fig. 1. Visual inspection of the bench for analysis of metrological properties and calibration of thermoelectric heat flux sensors (HFS).

The bench includes a measuring unit 1, a control unit 2 and a measuring instrument 3 (high-precision digital multimeter). The measuring unit 1 is equipped with an aluminum platform on which liquid heat exchangers, a clamping device and a switchboard are installed. One or two HFS under study can be placed between the hot and cold heat exchangers.

Measuring unit 1 is schematically shown in Fig. 2.

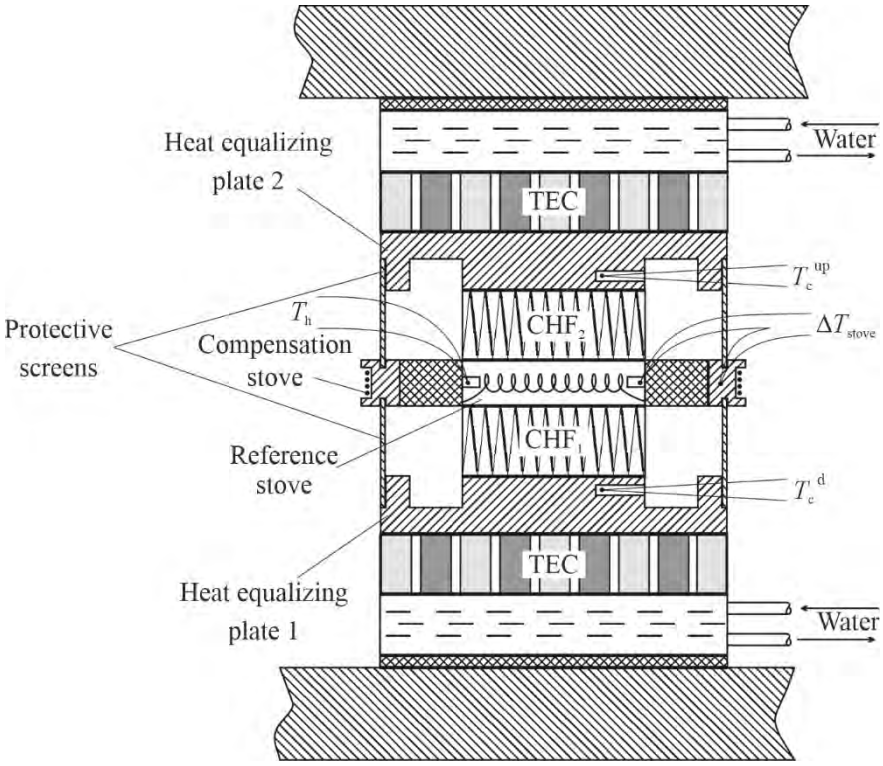

Fig. 2. Schematic representation of the measuring unit of the bench for calibrating thermoelectric heat flux sensors (HFS).

As can be seen in Figs. 1 and 2, two identical heat exchange modules designed for heat removal – cold heat exchangers – are installed on the lower base of the aluminum platform and on the suspension of the upper base of the measuring unit 1. These heat exchangers are reversible, as they are based on thermoelectric coolers (TECs) with liquid heat removal, and can operate in both cooling and heating modes depending on the direction of electric current flow. On the working side of the TEC, copper plates are fixed for heat equalization with built-in temperature sensors – platinum resistance thermometers. These plates have a highly polished flat surface – the working platform, on which the studied HFS is placed. The opposite side of the HFS is in contact with a hot heat exchanger – a flat heater, which has two polished working surfaces (upper and lower). The flat heater is made thin enough to minimize the area of its side surface and ensure uniform heating throughout the volume. The body of this heater also has a temperature sensor – a platinum resistance thermometer. The use of platinum temperature sensors allows one to accurately measure and control the temperature of the working areas of heat exchangers using thermostats with an accuracy of ± 0.1°C in the temperature range from – 30 to + 130 °C.

Since the side surface of the hot heat exchanger is not included in the heat exchange processes with the HFS and can be a source of heat loss, an annular protective heater was installed to minimize these losses. The main task of this heater is to maintain a temperature that corresponds to the temperature of the hot heat exchanger. The temperature is controlled by a differential thermocouple connected to the free channel of the thermostat. The thermostat is configured so that the appropriate adjustment of the supply voltage to the heater of the annular protective furnace provides a zero thermocouple signal, which contributes to the adiabatic insulation of the side surface of the hot heat exchanger.

The annular protective heater also plays an important role in transferring its temperature to the protective screen located opposite the side surface of the investigated HFS. On the lower and upper surfaces of the annular protective heater, there are pre-milled grooves into which the "hot" ends of the protective screens are inserted. The "cold" ends of these screens are in thermal contact with the working surfaces of the cold heat exchangers. This creates a temperature gradient on the surfaces of the protective screens in the vertical direction, which corresponds to the temperature on the side surface of the vehicle, thus ensuring that heat is not dissipated into the environment during the vehicle calibration.

The bench uses two cold heat exchangers, which allows for the simultaneous comparative calibration of two HFSs. When only one HFS is calibrated, the second cold heat exchanger functions as an additional protective heater. It is set to a temperature similar to that of the hot heat exchanger using a thermostat, which provides adiabatic protection against heat loss from the unused surface of the hot heat exchanger. The thermostating process of all heat exchangers is controlled by control unit 2, which includes adjustable power supplies for TEC and heaters, two dual-channel microprocessor temperature controllers RE-202, switching elements and control terminals for measurements.

All electrical connections from the measuring unit 1 are assembled on a terminal block and connected to the control unit 2 via a cable. A measuring device is also connected to this unit – a high-precision digital multimeter M3500, which has the ability to transfer measurement results to a personal computer in real time. This configuration of the bench allows for effective calibration of thermoelectric HFSs and investigation of their metrological characteristics in dynamics.

2. Procedure for calibrating one thermoelectric heat flux sensor (HFS)

- Using the specialized bench shown in Fig. 1, calibration of one thermoelectric heat flux sensor (HFS) is performed according to the following procedure:
- Connect measuring unit 1 to control unit 2;

- Connect input cable of measuring device 3 to the corresponding terminals on the control unit 2;
- Connect the hoses of the liquid cooling system of the TEC to the water main, open the water supply and activate the cooling system;
- Raise and fix the upper cold heat exchanger in the upper position;
- Place the investigated HFS on the working surface of the lower cold heat exchanger;
- Connect the leads of the investigated HFS to the corresponding terminals on the switchboard;
- Install the lower protective screen;
- Place the hot heat exchanger with the annular protective heater on the HFS and on the upper edge of the protective screen;
- Install the upper protective screen;
- Lower the upper cold heat exchanger, so that its heat equalizing plate touches the upper protective screen, while the pressing force is adjusted using weights;
- On the thermostats of control unit 2, set the temperature of the lower cold heat exchanger.
- On the control unit 2, set the measurement switch to the "Heater voltage" position. Turn on the measuring instrument 3 and switch it to the "DC voltage" mode with automatic range selection. Using the formula

$$W = U^2 \cdot R$$

(where R is the resistance of the heater), determine the voltage that must be applied to the hot heat exchanger heater to achieve the required electrical power in the range from 10 mW to 1 W.

- While watching the "hot heat exchanger temperature" indicator on the corresponding channel of the thermostat operating in the temperature sensor mode, and waiting for this temperature to stabilize, set an identical temperature value on the upper cold heat exchanger. The temperature of the annular heater is automatically regulated;
- Set the switch on control unit 2 to the "HFS thermoEMF" position;
- After the temperatures on the stationary heat exchangers reach the specified values, measure the thermoEMF value of thermoelectric HFS;
- Switch the measurement switch to the "Hot Heat Exchanger Heater Voltage" and "Hot Heat Exchanger Heater Current" positions in sequence to accurately determine the corresponding electrical parameters.
- Calculate the heater power using the following formula:

$$W = U \cdot I. \tag{2}$$

- Calculate the volt-watt sensitivity of a thermoelectric HFS using this mathematical formula:

$$\nu = \frac{E}{W}. \tag{3}$$

3. Procedure for calibrating two thermoelectric heat flux sensors (HFS)

Paired calibration of two thermoelectric heat flux sensors (HFSs) is performed simultaneously only for identical samples. This process differs from the calibration of a single HFS in that the second HFS is placed on top of the hot heat exchanger. The leads of this second HFS are connected to the corresponding terminals on the measuring unit 1, and the measurement of the thermal EMF signal of the HFS is carried out using the corresponding position of the measurement switch on the control unit 2.

The same temperature is set on the upper cold heat exchanger as on the lower one using a thermostat. The electric power released on the hot heat exchanger is distributed equally between the two HFSs and dissipated through the two cold heat exchangers. Since the hot side temperatures of both HFSs are common, and the cold side temperatures are the same and controlled by a thermostat, the volt-watt sensitivities of each HFS can be calculated using the following formulae:

$$\nu_1 = \frac{2 \cdot E_1}{W}, \tag{4}$$

$$\nu_2 = \frac{2 \cdot E_2}{W}. \tag{5}$$

where E_1 and E_2 are thermoEMF values for the first and second investigated HFS, accordingly. The number "2" in the numerator of the formula arises because the total power dissipated in the hot heat exchanger is divided equally between the two HFSs, so half the power value is used for each of them. Thus, the volt-watt sensitivities of each of the HFSs can be calculated using the following expression:

$$W_1 = W_2 = \frac{W}{2}. \tag{6}$$

4. Results of measuring HFS parameters

As a result of modification of the geometric parameters of the half-elements in the thermoelectric microthermopiles, prototypes of primary converters of the HFS with dimensions of 22 × 22 × 4 mm were created. These prototypes are characterized by an improved design, providing increased sensitivity and accelerated response to changes (see Fig. 3). The metrological parameters of these converters, such as volt-watt sensitivity and time constant, were analyzed using a specially designed test bench for HFS calibration, according to the described methodology.

Visualization of the above HFS prototypes is presented in Fig. 3.

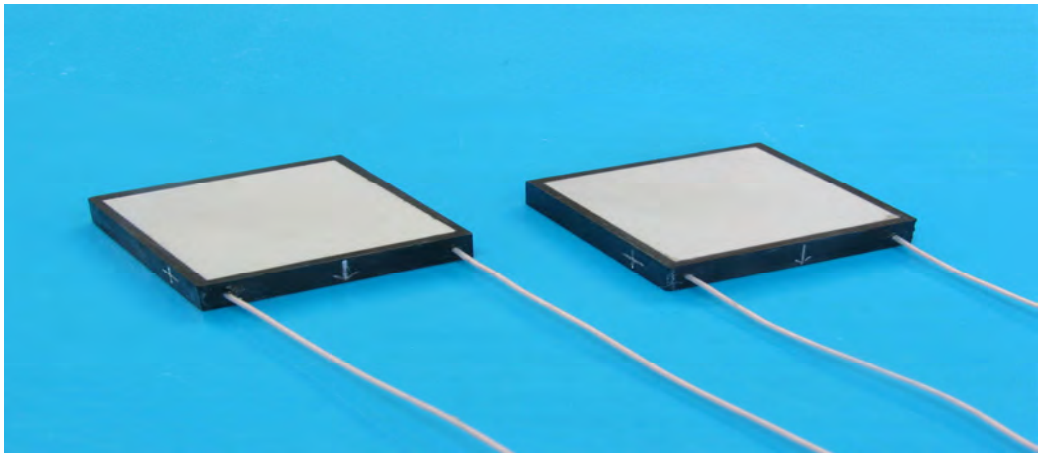

Fig. 3. Visualization of experimental models of HFS with dimensions of 22×22×4 mm.

Table 1 represents data obtained as a result of measuring characteristics of two prototypes of HFS with dimensions of 22 × 22 × 4 mm.

Table 1

Measured data of the characteristics of thermoelectric heat flux sensors with dimensions of 22 × 22 × 4 mm

№	Parameter name	HFS	
		№1	№2
1.	Heat flux range, W/m^2	$10^{-2} \div 10^3$	$10^{-2} \div 10^3$
2.	Sensitivity, V/W	1.48	1.51
3.	Time constant, s	12	12
4.	Working temperature range, ºC	– 30 ÷ + 130	– 30 ÷ + 130
5.	Overall dimensions of thermopile, mm	22 × 22 × 4	22 × 22 × 4

A new design of thermoelectric converters was created, allowing simultaneous recording of temperature and heat flux of the human body surface. Visualization of experimental prototypes of these HFSs with dimensions of 16×16×3 mm is presented in Fig. 4.

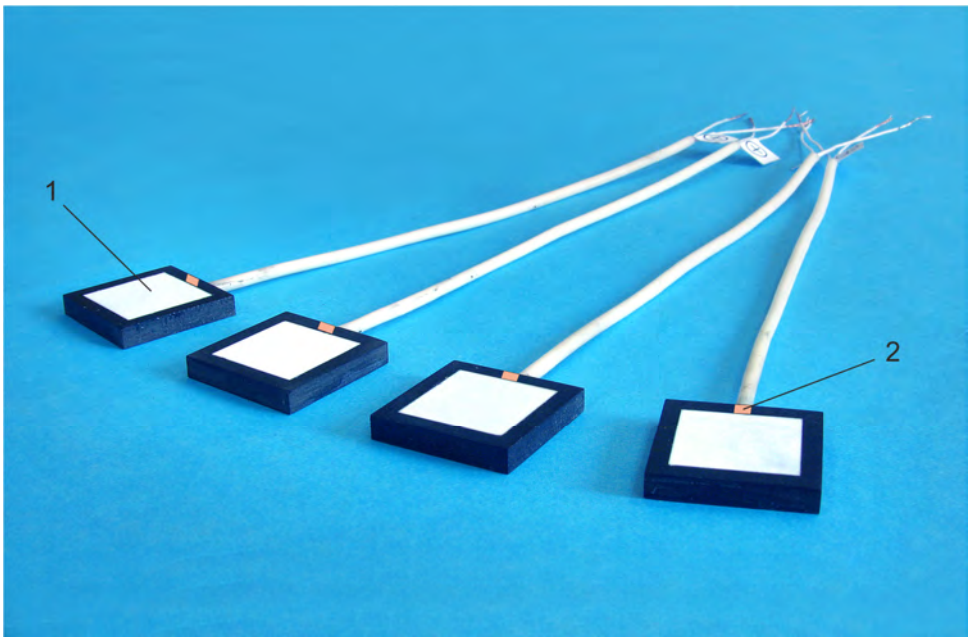

Fig. 4. Visualization of experimental models of HFS with dimensions of 16×16×3 mm: 1 – thermoelectric heat flux sensor, 2 – temperature sensor.

Table 2 presents the results of measuring the main characteristics of the four prototypes of HFS with dimensions of 16×16×3 mm.

Table 2

Measured data of the characteristics of thermoelectric heat flux sensors with dimensions of 16 × 16 × 3 mm

№	Parameter name	HFS			
		№ 1	№ 2	№ 3	№ 4
1.	Heat flux range, W/m^2	$10^{-2} \div 10^3$	$10^{-2} \div 10^3$	$10^{-2} \div 10^3$	$10^{-2} \div 10^3$
2.	Sensitivity, V/W	3.2	3.32	3.1	3.25
3.	Time constant, s	10	11	11	10
4.	Overall dimensions of thermopile, mm	16 × 16 × 3	16 × 16 × 3	16 × 16 × 3	16 × 16 × 3

Time parameters of the above thermoelectric HFS are presented in Fig. 5.

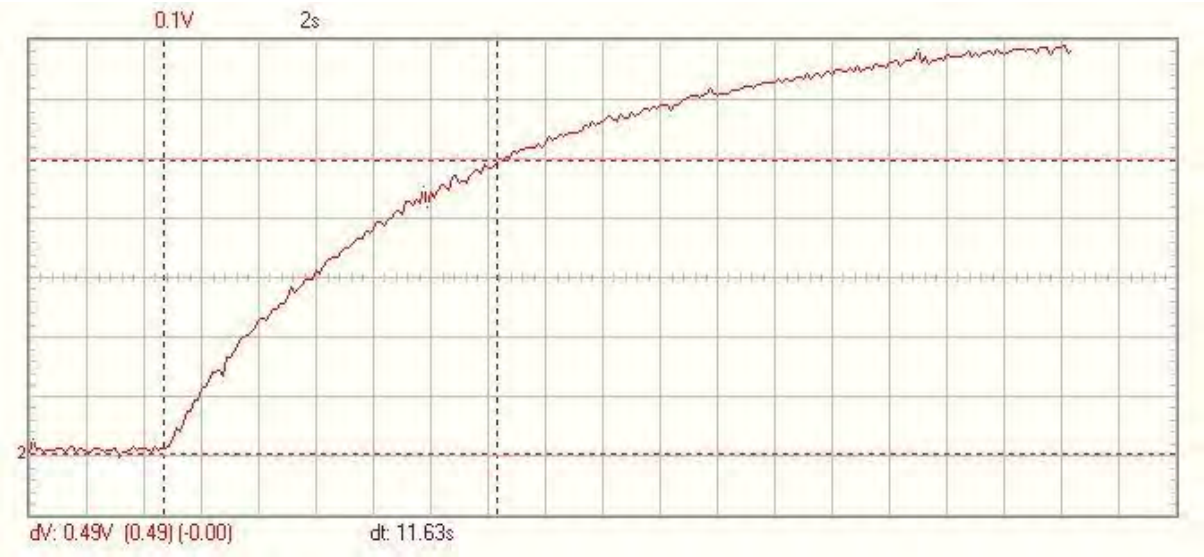

Fig. 5. Time characteristic graph of thermoelectric HFS with dimensions of 16×16×3 mm, equipped with ceramic receiving surface.

Therefore, a specialized bench for calibrating thermoelectric HFS provides the ability to analyze the characteristics of these converters and effectively transmit measurement data to a personal computer in real time. At the same time, the developed thermoelectric sensors, which simultaneously measure temperature and heat flux, allow for continuous monitoring of a person's temperature and thermal state, which is important for various applications in medicine and other industries.

Conclusions

1. A bench for calibrating thermoelectric heat flux sensors has been created and put into operation, which provides the ability to analyze their metrological parameters and transmit measurement data to a personal computer in real time. A methodology has been developed for calibrating both one and two converters simultaneously.

2. An innovative type of thermoelectric converters has been created that allows for simultaneous measurement of temperature and heat flux, which opens up opportunities for continuous monitoring of a person's temperature and thermal state in real time.
3. An improved method for calibrating thermoelectric sensors has been introduced using an additional highly sensitive heat flux converter, which helps to increase the accuracy of determining the volt-watt sensitivity of these devices.

References

1. Anatychuk L.I. (2003). *Thermoelectricity. Vol.2. Thermoelectric power converters*. Kyiv, Chernivtsi: Institute of Thermoelectricity.
2. Anatychuk L.I. (1998). *Thermoelectricity. Vol.1. Physics of thermoelectricity*. Kyiv, Chernivtsi: Institute of Thermoelectricity.
3. Anatychuk L.I. (2007). Current status and some prospects of thermoelectricity. *J. Thermoelectricity*, 2, 7 – 20.
4. Demchuk B.M., Kushneryk L.Ya., Rublenyk I.M. (2002). Thermoelectric sensors for orthopaedics. *J. Thermoelectricity*, 4, 80 – 85.
5. *Patent of Ukraine 53104 A* (2003). Sensor for preliminary diagnosis of inflammatory processes of the mammary glands. A.A. Ashcheulov, A.V. Klepikovskyi, L.Ya. Kushneryk, et al.
6. Ashcheulov A.A., Kushneryk L.Ya. (2004). Thermoelectric device for medico-biological express diagnostics. *Technology and Design in Electronic Equipment*, 4, 38 – 39.
7. *Patent of Ukraine 71619* (2012). L.I. Anatychuk, R.R. Kobylianskyi. Thermoelectric medical heat meter. Institute of Thermoelectricity (In Ukrainian).
8. *Patent of Ukraine 72032* (2012). L.I. Anatychuk, R.R. Kobylianskyi. Thermoelectric sensor for temperature and heat flux measurement. Institute of Thermoelectricity (In Ukrainian).
9. *Patent of Ukraine 73037* (2012). P.D. Mykytiuk, R.R. Kobylianskyi, T.V. Slepeniuk. Thermoelectric medical device. Institute of Thermoelectricity (In Ukrainian).
10. *Patent of Ukraine 78619* (2013). L.I. Anatychuk, R.R. Kobylianskyi. Method for determination of heat flux density. Institute of Thermoelectricity. (In Ukrainian).
11. *Patent of Ukraine 79929* (2013). L.I. Anatychuk. Thermoelectric converter of heat flux for gradient heat meters. Institute of Thermoelectricity (In Ukrainian).
12. Gischuk V.S. (2012). Electronic recorder of human heat flux sensor signals. *J. Thermoelectricity*, 4, 105 – 108.
13. Gischuk V.S. (2013). Electronic recorder with signal processing of thermoelectric heat flux sensor. *J. Thermoelectricity,* 1, 82 – 86.
14. Gischuk V.S. (2013). Modernized device for measuring human heat fluxes. *J. Thermoelectricity,* 2, 91 – 95.
15. Anatychuk L.I., Kobylianskyi R.R. (2012). Study of the influence of thermoelectric heat meter on determination of human heat release. *J. Thermoelectricity,* 4, 60 – 66.
16. Anatychuk L.I., Kobylianskyi R.R. (2012). 3D-model for determination of the influence of thermoelectric heat meter on the accuracy of measuring human heat release. *Scientific Herald of Chernivtsi University: Collected papers. Physics. Electronics. Vol. 2, Issue 1*. Chernivtsi: Chernivtsi National University, 15 – 20.
17. Anatychuk L.I., Kobylianskyi R.R. (2013). Computer simulation of thermoelectric heat meter readings in real-world operating conditions. *J. Thermoelectricity,* 1, 53 – 60.

18. Anatychuk L.I., Giba R.G., Kobylianskyi R.R. On some features of the use of medical heat meters in the study of local human heat release. *J. Thermoelectricity*,2, 67 – 73.
19. Anatychuk L.I., Kobylianskyi R.R., Konstantynovich I.A. (2013). On the influence of a thermoelectric power source on the accuracy of temperature and heat flux measurement. *J. Thermoelectricity*, 6, 53 – 61.
20. Ivashchuk O.I., Morar I.K., Kobylianskyi R.R., Nepelyak L.V., Deley V.D. (2013). The role of abdominal heat flow in monitoring acute destructive pancreatitis. *Abstracts of scientific and practical conference "Current issues in surgery"*, Chernivtsi, Ukraine, 254 – 259.
21. Kobylianskyi R.R. (2016). The influence of thermal insulation on the readings of thermoelectric medical sensor. *Scientific Herald of Chernivtsi University: Collected papers. Physics. Electronics. Vol. 5, Issue 1*. Chernivtsi: Chernivtsi National University, 45 – 49.
22. Kobylianskyi R.R. (2016). Computer simulation of readings of a medical thermoelectric sensor. *J. Thermoelectricity*, 4. 69 – 77.
23. Gischuk V.S., Kobylianskyi R.R., Cherkez R.G. (2014). Multichannel device for measuring the temperature and density of heat fluxes. *Scientific Herald of Chernivtsi University: Collected papers. Physics. Electronics. Vol. 3, Issue. 1*. Chernivtsi: Chernivtsi National University, 96 – 100.
24. Kobylianskyi R.R., Boychuk V.V. (2015). The use of thermoelectric heat meters in medical diagnostics. *Scientific Herald of Chernivtsi University: Collected papers. Physics. Electronics. Vol. 4, Issue 1*. Chernivtsi: Chernivtsi National University, 90 – 96.
25. Anatychuk L.I., Ivashchuk O.I., Kobylianskyi R.R., Postevka I.D., Bodiaka V.Yu., Gushul I.Ya. (2016). Thermoelectric device for measuring the temperature and density of heat flux "ALTEC-10008". *J. Thermoelectricity*. 1, 76 – 84.
26. Anatychuk L.I., Yuryk O.E., Kobylianskyi R.R., Roy I.V., Fishchenko Ya.V., Slobodianiuk N.P., Yuryk N.E., Duda B.S. (2017). Thermoelectric device for diagnosing inflammatory processes and neurological manifestations of osteochondrosis of the human spine. *J. Thermoelectricity*, 3, 54 – 67.
27. Yuryk O.E., Anatychuk L.I., Roy I.V., Kobylianskyi R.R., Fishchenko Ya.V., Slobodianuk N.P., Yuryk N.E., Duda B.S. (2017). Peculiarities of heat exchange in patients with neurological manifestations of osteochondrosis in the lumbosacral spine. *Trauma*, 18(6).
28. Anatychuk L.I., Luste O.J, Kobylianskyi R.R. (2017). Information and energy theory of thermoelectric temperature and heat flux sensors for medical purposes. *J. Thermoelectricity*, 4, 5 – 20.
29. Anatychuk L.I., Kobylianskyi R.R., Cherkez R.G., Konstantynovych I.A., Hoshovskyi V.I., Tiumentsev V.A. (2017). Thermoelectric device with electronic control unit for diagnostics of inflammatory processes in the human organism. *Tekhnologiya i Konstruirovanie v Elektronnoi Apparature – Technology and Design in Electronic Equipment*, 6, 44 – 48.
30. Anatychuk L.I., Ivashchuk O.I., Kobylianskyi R.R., Postevka I.D., Bodiaka V.Yu., Gushul I.Ya., Chuprovska Yu.Ya. (2018). On the influence of ambient temperature on the readings of thermoelectric medical sensors. *Sensor Electronics and Microsystem Technologies*, 15 (1), 17 – 29.
31. Anatychuk L.I., Pasyechnikova N.V., Naumenko V.O., Zadorozhnyi O.S., Havryliuk M.V., Kobylianskyi R.R. (2018). Thermoelectric device for determination of heat flux from the surface of eyes. *J. Thermoelectricity*, 5, 52 – 67.
32. Anatychuk L.I., Kobylianskyi R.R., Konstantynovich I.A. (2014). Calibration of thermoelectric heat flux sensors. *Proc. of XV International scientific and practical conference "Modern information and electronic technologies"* (Odesa, Ukraine, May 26-30, 2014.) Vol.2, 30 – 31.

33. Anatychuk L.I., Kobylianskyi R.R., Konstantynovich I.A., Lysko V.V., Pugantseva O.V., Rozver Yu.Yu., Tiumentsev V.A. (2016). Calibration bench for thermoelectric heat flux converters. *J. Thermoelectricity,* 5, 71 – 79.
34. Anatychuk L.I., Kobylianskyi R.R., Konstantynovich I.A., Kuz R.V., Manyk O.M., Nitsovich O.V., Cherkez R.G. (2016). Manufacturing technology of thermoelectric microthermopiles. *J. Thermoelectricity,* 6, 49 – 54.
35. Anatychuk L.I., Razinkov V.V., Bukharayeva N.R., Kobylianskyi R.R. (2017). Thermoelectric bracelet. *J. Thermoelectricity,* 2, 58 – 72.
36. Anatychuk L.I., Todurov B.M., Kobylianskyi R.R., Dzhal S.A. (2019). On the use of thermoelectric microgenerators to power pacemakers. *J. Thermoelectricity,* 5, 63 – 88.
37. Anatychuk L.I., Yuryk O.E., Strafun S.S., Stashkevich A.T., Kobylianskyi R.R., Cheviuk A.D., Yuryk N.E., Duda B.S. (2021). Thermometric indicators in patients with chronic low back pain. *J. Thermoelectricity,* 1, 52 – 66.
38. Chunzhi Wang, Hongzhe Jiao, Lukyan Anatychuk, Nataliya Pasyechnikova, Volodymyr Naumenko, Oleg Zadorozhnyy, Lyudmyla Vikhor, Roman Kobylianskyi, Roman Fedoriv, Orest Kochan (2022). Development of a temperature and heat flux measurement system based on microcontroller and its application in ophthalmology. *Measurement Science Review*, 22 (2), 73 – 79.
39. Kobylianskyi R.R., Prybyla A.V., Konstantynovich I.A., Boychuk V.V. (2022). Results of experimental investigations of thermoelectric medical heat flux sensors, *J. Thermoelectricity*, 3-4, 70 – 83.
40. Yuryk O., Anatychuk L., Kobylianskyi R., Yuryk N. (2023). *Measurement of heat flux density as a new method of diagnosing neurological diseases.* Kharkiv: PC Technology Center, 31 – 68.

Submitted 11.07.2023.

Анатичук Л.І., *акад. НАН України* [1,2]
Кобилянський Р.Р., *канд. фіз.-мат. наук* [1,2]
Лисько В.В., *канд. фіз.-мат. наук* [1,2]
Прибила А.В., *канд. фіз.-мат. наук* [1,2]
Константинович І.А., *канд. фіз.-мат. наук* [1,2]
Кобилянська А.К., *канд. фіз.-мат. наук* [1]
Гаврилюк М.В. [1,2]
Бойчук В.В. [2]

[1] Інститут термоелектрики НАН та МОН України,
вул. Науки, 1, Чернівці, 58029, Україна;
[2] Чернівецький національний університет імені Юрія Федьковича,
вул. Коцюбинського 2, Чернівці, 58012, Україна
e-mail: anatych@gmail.com

МЕТОДИКА КАЛІБРУВАННЯ ТЕРМОЕЛЕКТРИЧНИХ СЕНСОРІВ МЕДИЧНОГО ПРИЗНАЧЕННЯ

У даній роботі представлено результати створення експериментального стенду для калібрування термоелектричних датчиків теплового потоку та аналізу їхніх метрологічних властивостей. Розроблені процедури калібрування як для одного, так і для двох датчиків одночасно. Також було створено та випробувано новий тип термоелектричних датчиків, які здатні одночасно вимірювати температуру та тепловий потік на поверхні тіла людини.
Ключові слова: калібрувальний стенд, термоелектричний датчик, тепловий потік, вольт-ватна чутливість.

Література

1. Анатичук Л.І. Термоелектрика. Т.2. Термоелектричні перетворювачі енергії. Київ, Чернівці: Інститут термоелектрики, 2003. – 376 с.
2. Anatychuk L.I. (1998). *Thermoelectricity. Vol.1. Physics of thermoelectricity*. Kyiv, Chernivtsi: Institute of Thermoelectricity.
3. Анатичук Л.І. Сучасний стан і деякі перспективи термоелектрики // Термоелектрика. – 2007. – № 2. – С. 7 – 20.
4. Демчук Б.М., Кушнерик Л.Я., Рубленик І.М. Термоелектричні датчики для ортопедії.// Термоелектрика. – 2002. – №4. – С. 80 – 85.
5. Патент України 53104 А. Датчик для попередньої діагностики запальних процесів молочних залоз // А.А.Ашеулов, А.В.Клепіковський, Л.Я. Кушнерик та ін. – 2003.
6. Ащеулов А.А., Кушнерик Л.Я. Термоелектричний прилад для медико-біологічної експрес-діагностики // Технологія та конструювання в електронній апаратурі. – №4. – 2004. – С. 38 – 39.
7. Пат. 71619 Україна, МПК H01L 35/00. Термоелектричний медичний тепломір / Анатичук Л.І., Кобилянський Р.Р.; Інститут термоелектрики. – № u 2011 14007; заявл. 28.11.11; опубл. 25.07.12, Бюл. № 14.
8. Пат. 72032 Україна, МПК H01L 35/00. Термоелектричний сенсор для вимірювання температури і теплового потоку / Анатичук Л.І., Кобилянський Р.Р.; Інститут термоелектрики. – № u 2011 14005; заявл. 28.11.11; опубл. 10.08.12, Бюл. № 15.
9. Пат. 73037 Україна, МПК H01L 35/02. Термоелектричний медичний пристрій / Микитюк П.Д., Кобилянський Р.Р., Слепенюк Т.В.; Інститут термоелектрики. – № u 2012 01922; заявл. 20.02.12; опубл. 10.09.12, Бюл. № 17.
10. Пат. 78619 Україна, МПК H01L 35/00. Метод визначення густини теплового потоку / Анатичук Л.І., Кобилянський Р.Р.; Інститут термоелектрики. – № u 2012 11018; заявл. 21.09.12; опубл. 25.03.13, Бюл. № 6.
11. Пат. 79929 Україна, МПК H01L 35/00. Термоелектричний перетворювач теплового потоку для градієнтних тепломірів / Анатичук Л.І.; Інститут термоелектрики. – № u 2012 11857; заявл. 15.10.12; опубл. 13.05.13, Бюл. № 9.
12. Гищук В.С. Електронний регістратор сигналів сенсорів теплового потоку людини // Термоелектрика. − № 4. – 2012. – С. 105 – 108.
13. Гищук В.С. Електронний регістратор з обробкою сигналів термоелектричного сенсора теплового потоку // Термоелектрика. − № 1. – 2013. – С. 82 – 86.
14. Гищук В.С Модернізований прилад для вимірювання теплових потоків людини // Термоелектрика. – №2. – 2013. – С. 91 – 95.
15. Анатичук Л.І., Кобилянський Р.Р. Дослідження впливу термоелектричного тепломіра на визначення тепловиділення людини // Термоелектрика. − № 4. – 2012. – С. 60 – 66.

16. Анатичук Л.І., Кобилянський Р.Р. 3D-модель для визначення впливу термоелектричного тепломіра на точність вимірювання тепловиділення людини // Науковий вісник Чернівецького університету: збірник наук. праць. Фізика. Електроніка. – Т. 2, Вип. 1. – Чернівці: Чернівецький національний університет, 2012. – С. 15 – 20.
17. Анатичук Л.І., Кобилянський Р.Р. Комп'ютерне моделювання показів термоелектричного тепломіра в умовах реальної експлуатації // Термоелектрика. − № 1. – 2013. – С. 53 – 60.
18. Анатичук Л.І., Гіба Р.Г., Кобилянський Р.Р. Про деякі особливості використання медичних тепломірів при дослідженні локальних тепловиділень людини // Термоелектрика. − № 2. – 2013. – С. 67 – 73.
19. Анатичук Л.І., Кобилянський Р.Р., Константинович І.А. Про вплив термоелектричного джерела живлення на точність вимірювання температури і теплового потоку // Термоелектрика. − № 6. – 2013. – С. 53 – 61.
20. Іващук О.І., Морар І.К., Кобилянський Р.Р., Непеляк Л.В., Делей В.Д. Роль теплового потоку черевної порожнини в моніторингу гострого деструктивного панкреатиту // Збірник тез науково-практичної конференції "Актуальні питання хірургії", м. Чернівці, Україна. – 2013. – С. 254 – 259.
21. Кобилянський Р.Р. Про вплив теплової ізоляції на покази термоелектричного сенсора медичного призначення // Науковий вісник Чернівецького університету: збірник наук. праць. Фізика. Електроніка. – Т. 5, Вип. 1. – Чернівці: Чернівецький національний університет, 2016. – С. 45 – 49.
22. Кобилянський Р.Р. Комп'ютерне моделювання показів термоелектричного сенсора медичного призначення // Термоелектрика. − № 4. – 2016. – С. 69 – 77.
23. Гищук В.С., Кобилянський Р.Р., Черкез Р.Г. Багатоканальний прилад для вимірювання температури і густини теплових потоків // Науковий вісник Чернівецького університету: збірник наук. праць. Фізика. Електроніка. – Т. 3, Вип. 1. – Чернівці: Чернівецький національний університет, 2014. – С. 96 – 100.
24. Кобилянський Р.Р., Бойчук В.В. Використання термоелектричних тепломірів у медичній діагностиці // Науковий вісник Чернівецького університету: збірник наук. праць. Фізика. Електроніка. – Т. 4, Вип. 1. – Чернівці: Чернівецький національний університет, 2015. – С. 90 – 96.
25. Анатичук Л.І., Іващук О.І., Кобилянський Р.Р., Постевка І.Д., Бодяка В.Ю., Гушул І.Я. Термоелектричний прилад для вимірювання температури і густини теплового потоку "АЛТЕК-10008" // Термоелектрика. − № 1. – 2016. – С. 76 – 84.
26. Анатичук Л.І., Юрик О.Є., Кобилянський Р.Р., Рой І.В., Фіщенко Я.В., Слободянюк Н.П., Юрик Н.Є., Дуда Б.С. Термоелектричний прилад для діагностики запальних процесів та неврологічних проявів остеохондрозу хребта людини // Термоелектрика. − № 3. – 2017. – С. 54 – 67.
27. Юрик О.Є., Анатичук Л.І., Рой І.В., Кобилянський Р.Р., Фіщенко Я.В., Слободянюк Н.П., Юрик Н.Є., Дуда Б.С. Особливості теплового обміну у пацієнтів з неврологічними проявами остеохондрозу в попереково-крижовому відділі хребта // Травма. − Т.18. – № 6. – 2017.
28. Анатичук Л.І., Лусте О.Я., Кобилянський Р.Р. Інформаційно-енергетична теорія термоелектричних сенсорів температури і теплового потоку медичного призначення // Термоелектрика. − № 4. – 2017. – С. 5 – 20.
29. Anatychuk L.I., Kobylianskyi R.R., Cherkez R.G., Konstantynovych I.A., Hoshovskyi V.I., Tiumentsev V.A. (2017). Thermoelectric device with electronic control unit for diagnostics of

inflammatory processes in the human organism. *Tekhnologiya i Konstruirovanie v Elektronnoi Apparature – Technology and Design in Electronic Equipment*, 6, 44 – 48.

30. Анатичук Л.І., Іващук О.І., Кобилянський Р.Р., Постевка І.Д., Бодяка В.Ю., Гушул І.Я., Чупровська Ю.Я. Про вплив температури навколишнього середовища на покази термоелектричних сенсорів медичного призначення // Сенсорна електроніка і мікросистемні технології. − Т. 15. – № 1. – 2018. – С. 17 – 29.
31. Анатичук Л.І., Пасєчнікова Н.В., Науменко В.О., Задорожний О.С., Гаврилюк М.В., Кобилянський Р.Р. Термоелектричний прилад для визначення теплового потоку з поверхні очей // Термоелектрика. − № 5. – 2018. – С. 52 – 67.
32. Анатичук Л.І., Кобилянський Р.Р., Константинович І.А. Градуювання термоелектричних сенсорів теплового потоку // Труди XV Міжнародної науково-практичної конференції «Сучасні інформаційні та електронні технології» 26-30 травня 2014 року. – Т. 2. – Одеса, Україна. – 2014. – С. 30 – 31.
33. Анатичук Л.І., Кобилянський Р.Р., Константинович І.А., Лисько В.В., Пуганцева О.В., Розвер Ю.Ю., Тюменцев В.А. Стенд для градуювання термоелектричних перетворювачів теплового потоку // Термоелектрика. − № 5. – 2016. – С. 71 – 79.
34. Анатичук Л.І., Кобилянський Р.Р., Константинович І.А., Кузь Р.В., Маник О.М., Ніцович О.В., Черкез Р.Г. Технологія виготовлення термоелектричних мікробатарей // Термоелектрика. − № 6. – 2016. – С. 49 – 54.
35. Анатичук Л.І., Разіньков В.В., Бухараєва Н.Р., Кобилянський Р.Р. Термоелектричний браслет // Термоелектрика. − № 2. – 2017. – С. 58 – 72.
36. Анатичук Л.І., Тодуров Б.М., Кобилянський Р.Р., Джал С.А. Про використання термоелектричних мікрогенераторів для живлення електрокардіостимуляторів // Термоелектрика. − № 5. – 2019. – С. 63 – 88.
37. Анатичук Л.І., Юрик О.Є., Страфун С.С., Сташкевич А.Т., Кобилянський Р.Р., Чев'юк А.Д., Юрик Н.Є., Дуда Б.С. Теплометричні показники у пацієнтів з хронічним болем у попереку // Термоелектрика. − № 1. – 2021. – С. 52 – 66.
38. Chunzhi Wang, Hongzhe Jiao, Lukyan Anatychuk, Nataliya Pasyechnikova, Volodymyr Naumenko, Oleg Zadorozhnyy, Lyudmyla Vikhor, Roman Kobylianskyi, Roman Fedoriv, Orest Kochan (2022). Development of a temperature and heat flux measurement system based on microcontroller and its application in ophthalmology. *Measurement Science Review*, 22 (2), 73 – 79.
39. Кобилянський Р.Р., Прибила А.В., Константинович І.А., Бойчук В.В. Результати експериментальних досліджень термоелектричних медичних сенсорів теплового потоку // Термоелектрика. – №3-4. – 2022. – 70 – 83.
40. Yuryk O., Anatychuk L., Kobylianskyi R., Yuryk N. (2023). *Measurement of heat flux density as a new method of diagnosing neurological diseases.* Kharkiv: PC Technology Center, 31 – 68.

Надійшла до редакції: 11.07.2023.

Anatychuk L.I., *Acad. NAS Ukraine* [1,2]
Panasiuk O.L., [3]
Diachenko P.A., [3]
Zaremba A.V., [3]
Havryliuk M.V., [1]
Kobylianskyi R.R., *Cand. Sc (Phys &Math)* [1,2]
Lysko V.V., *Cand. Sc (Phys &Math)* [1,2]

[1] Institute of Thermoelectricity of the NAS and MES of Ukraine, 1 Nauky str., Chernivtsi, 58029, Ukraine;
[2] Yuriy Fedkovych Chernivtsi National University, 2 Kotsiubynskyi str., Chernivtsi, 58000, Ukraine;
[3] SI "L.V. Gromashevsky Institute of Epidemiology and Infectious Diseases of the NAMS of Ukraine", 5 M.Amosova str., Kyiv, 03038, Ukraine
e-mail: anatych@gmail.com

THERMOELECTRIC DEVICE FOR COLLECTING EXHALED AIR CONDENSATE

The article presents the results of the design development and a description of the manufactured experimental sample of a new highly efficient thermoelectric condenser of pulmonary air for the diagnosis of coronavirus and other diseases with an extended range of condensation temperatures below – 20 °C and close to – 70 °C. The method of using the developed device in medical diagnostics and the results of its experimental studies are described. Bibl. 5, Figs. 5.
Key words: diagnostics, coronavirus, condensate, exhaled air, thermoelectric cooling.

Introduction

Exhaled air condensate is a promising source of lung disease biomarkers. It can be considered either as a body fluid or as a condensate of exhaled gas. There are three main contributions to exhaled air condensate. First, these are particles or droplets of various sizes that are aerosolized from the liquid lining the respiratory tract – such particles probably reflect the liquid itself. Secondly, it is distilled water that condenses from the gas phase with almost water-saturated exhalation, significantly diluting the aerosolized liquid of the respiratory tract. Thirdly, these are water-soluble volatile substances that are exhaled and absorbed into the condensing breath. Of interest are both non-volatile components, mainly derived from particles of liquid lining the respiratory tract, and water-soluble volatile components, which are present in much higher concentrations and, therefore, easier to analyze than non-volatile compounds.

Diagnostic testing plays a crucial role in overcoming the pandemic of the coronavirus disease COVID-19, caused by the severe acute respiratory syndrome coronavirus SARS-CoV-2. Given that COVID-19 is transmitted through aerosols and droplets exhaled by humans, the detection of SARS-CoV-2 in lung condensate may serve as a promising non-invasive diagnostic method. This method is proposed in the works of scientists from Japan, the USA, Ireland and other countries as a more sensitive and reliable method of detecting COVID-19 [1 – 3]. Usually, special devices are used to collect condensate - condensers, in which vapors from the air exhaled by a person condense at a temperature

from 0 to – 70 °C and are collected in a container for further research by the RT-PCR method [4]. Lowering the condensation temperature makes it possible to speed up obtaining the amount of biological material required for research. At the same time, the operating temperatures of condensers that use ice at 0 °C or compressor cooling down to – 20 °C are insufficiently efficient and do not provide a high condensation rate. In addition, compressor condensers are complex, expensive, with insufficient regulation and maintenance of operating temperature, as well as the presence of dangerous refrigerants. The temperature of – 70 °C, which is achieved using dry ice (solid $CO2$), is excessive and extremely inconvenient for operation, which radically reduces the possibilities of using this method. The paper [5] gives the results of the computer design of a thermoelectric device for collecting exhaled air condensate with precisely regulated condensation temperatures lower than – 20 °C and close to – 70 °C without the use of dry ice.

The purpose of this work is to develop the design of the thermoelectric condenser of pulmonary air, its manufacture and experimental studies.

1. Description of the design of a thermoelectric condenser of pulmonary air

The general design of the developed device for collecting exhaled human condensate from the air is shown in Fig. 1. The device consists of two units – a cooling unit, in which a test tube for collecting condensate is placed, and a control unit for the device.

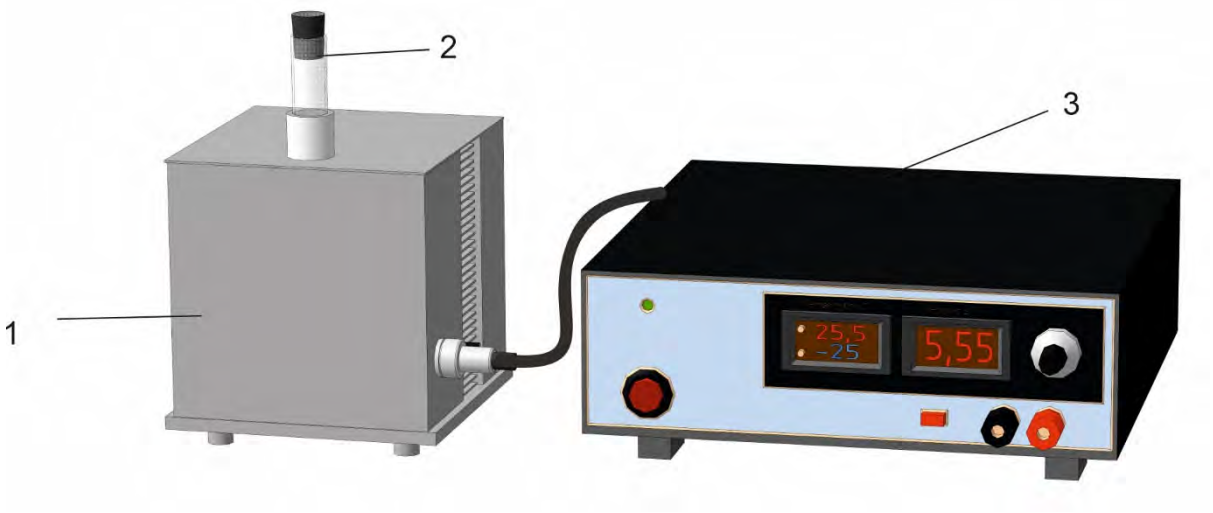

Fig. 1. General view of the design of a thermoelectric device for collecting condensate from the air exhaled by a person: 1 – cooling unit; 2 – tube for collecting condensate; 3 – device control unit.

Fig. 2 shows the expanded design of the cooling unit of the thermoelectric condenser of pulmonary air.

The cooling unit consists of a housing 1, a working cooling chamber 2, a thermoelectric module 3 of the Altec-2 type, and a system for removing heat from the thermoelectric module into the environment, containing an air heat exchanger 4 and a fan 5.

The device for collecting exhaled air condensate works as follows: when the control unit supplies electric current to the thermoelectric module, the latter ensures the set temperature in the working cooling chamber, where the tube for collecting condensate is placed. The air exhaled by the patient enters the test tube, where it cools. At the same time, exhaled air vapours are condensed and collected in a test tube for further research by the RT-PCR method or others.

The cooler control unit is designed to provide electrical power to the elements of the heat exchange unit and measure the temperature of the refrigerating chamber.

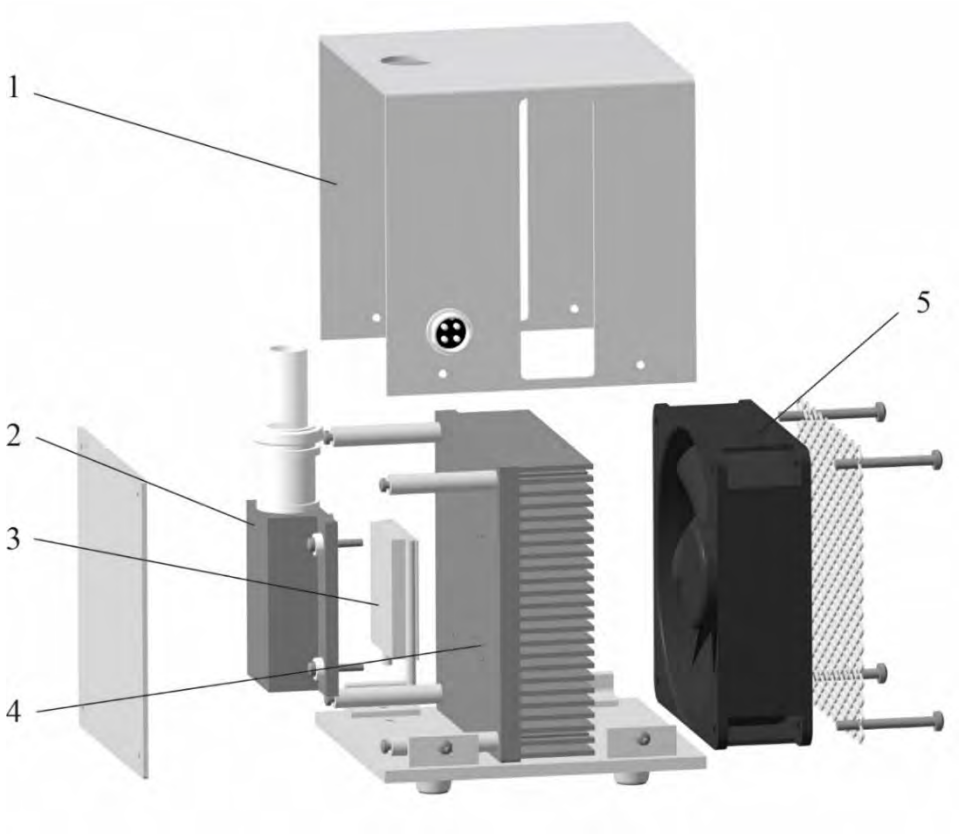

Fig. 2. Cooling unit of thermoelectric condenser of pulmonary air: 1 – housing; 2 – working cooling chamber; 3 – thermoelectric module of the type Altec-2; 4 – air heat exchanger; 5 – fan.

The control unit diagram is shown in Fig. 3. The unit consists of a standard pulse power supply unit – A1, with an output voltage of 12V DC, up to 20 A. Such power is due to the use of a high-power thermoelectric module in the cooling unit.

To fine-tune the speed of cooling by the thermoelectric module of the working chamber, it is necessary to select the voltage (current) of its power supply. For this purpose, the output voltage of the pulsed power supply unit is supplied through the step-down DC/DC voltage converter A3 with the possibility of its adjustment within wide limits. The control unit uses a panel DC voltmeter A2 to control the supply voltage of the module. The output voltage from the pulse power supply is also supplied to the cooling fan, in the circuit of which the rheostat R3 is connected - to regulate the rotation speed within small limits. The supply voltage for the thermoelectric module and the fan is supplied to the cooling unit via the power cable through the connector X2.

To limit the maximum cooling of the working chamber, the digital thermostat A4 is used in the control unit. To turn off the current through the thermoelectric module when setting the operating mode of the thermostat, an additional switch SW2 is used in the control unit circuit. The power key on the field-effect transistor Q1, connected to the output of the thermostat, switches the current through the thermoelectric module and also serves to increase the reliability of the control unit. Temperature control in the working chamber is carried out by the NTC sensor, which is located in the housing of the working chamber and is connected to the control unit by a separate cable X3.

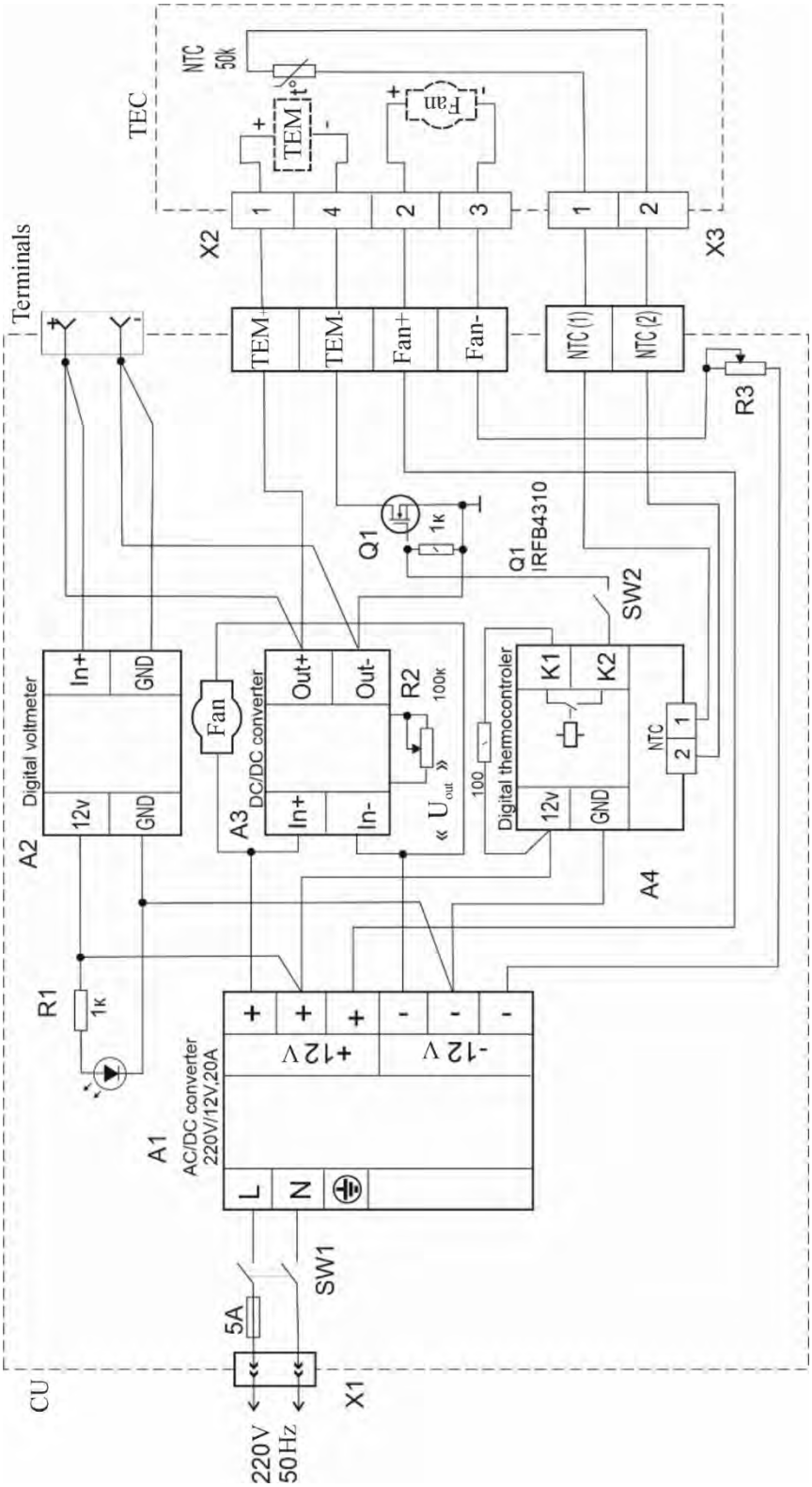

Fig. 3. Schematic diagram of the control unit of the thermoelectric condenser of pulmonary air.

The displays of the voltmeter A2 and the thermoregulator A4, the switches SW1 and SW2, the handle of the supply voltage regulator R2 and the control terminals are located on the front panel of the control unit housing. The handle of the fan regulator R3 and the power cables with connectors X1, X2, X3 and the fuse are on the rear panel of the control unit housing.

The appearance of the developed and manufactured pulmonary air condenser for the diagnosis of coronavirus and other diseases "ITE-ДПЛ " is shown in Fig. 4.

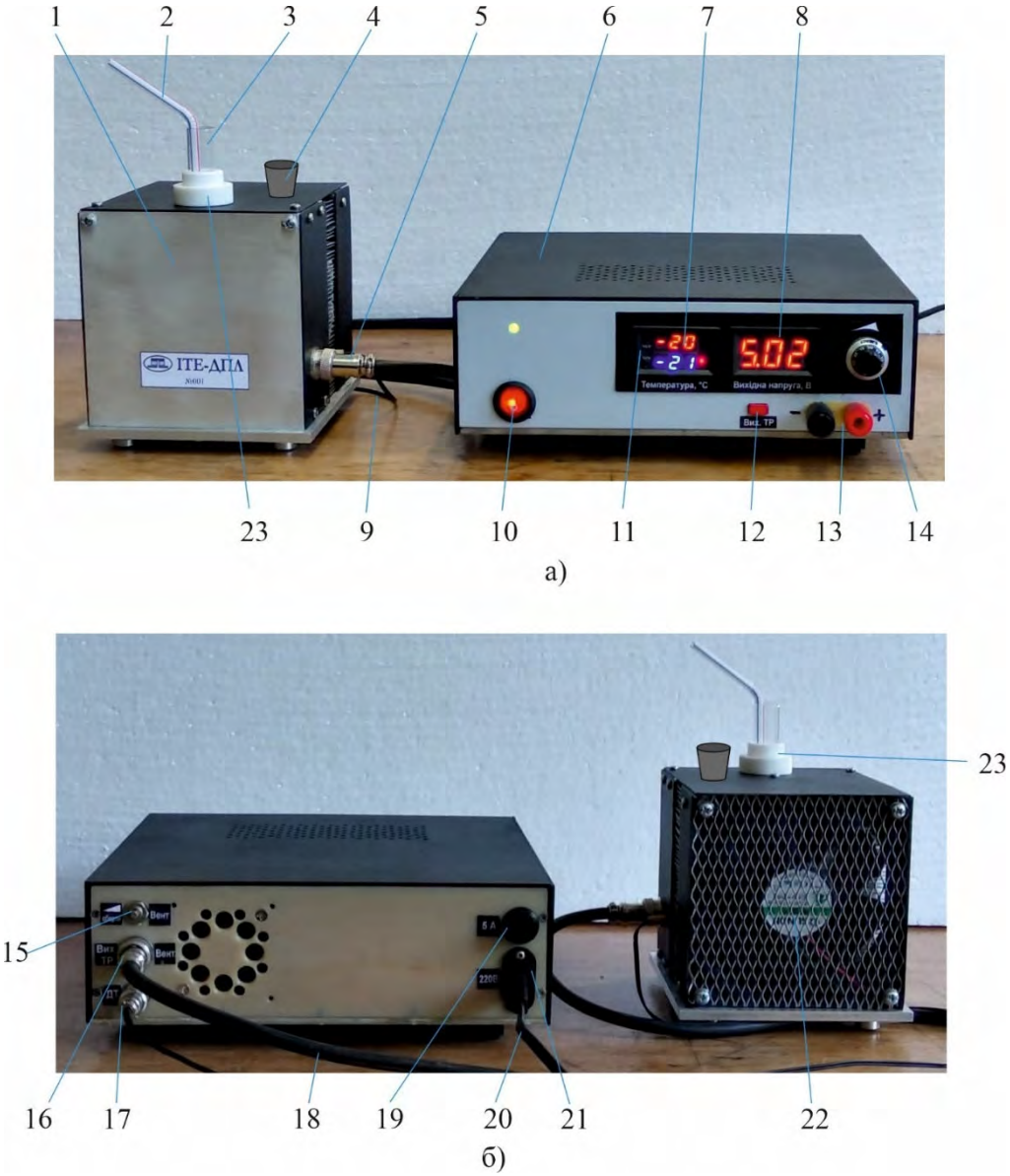

Fig. 4. Pulmonary air condenser for diagnostics of coronavirus and other diseases: a) – front view; b) – back view.

In Fig. 4: 1 – cooling unit; 2 – plastic tube; 3 – test tube; 4 – rubber stopper; 5 – connector for inter-unit cable; 6 – device control unit; 7 – thermal regulator panel; 8 – digital voltmeter of the cooler output supply voltage; 9 – temperature sensor cable 10 – button for turning on the device in the 220 V network; 11 – thermal regulator control buttons; 12 – "Thermal regulator output" button; 13 – additional direct source terminals of the power source; 14 – knob for regulating the output supply voltage of the heat exchanger module; 15 – cooling fan speed controller; 16 – connector for inter-unit cable; 17 – connector for connecting the temperature sensor; 18 – inter-unit cable; 19 – 220 V network fuse; 20 – 220 V network cable; 21 220 V network cable connector; 22 – cooling unit fan; 23 – fluoroplastic cylinder.

The ITE-DPL device kit includes: cooling unit 1 with cable 9; device control unit – 6; inter-unit

cable 18; network cable 20; test tube 3 (included – 10 pieces); plastic tube 2 (included – 20 pieces); rubber plug 4 (included – 2 pieces).

The device in the assembled state is shown in Fig. 3.1. The procedure for connecting the parts of the device is as follows:

- cooling unit 1 and device control unit 6 are installed on the work table. The distance between the units is approximately 20 – 40 cm;
- the following are connected to the units: inter-unit cable 18 with one end to connector 5 and the other end to connector 16 and temperature sensor cable 9 to connector 17;
- cable 20 is connected to connector 21, the other end of which is connected to the 220V network;
- 0.2 – 0.5 ml of a 50% x 50% alcohol aqueous solution is introduced into the hole of the fluoroplastic cylinder 23 using a plastic tube 2 to prevent the tube 3 from freezing into the cooling unit 1. After that, the plastic tube is removed outside the unit;
- a test tube 3 is inserted into the hole of the fluoroplastic cylinder 23. In this case, the alcohol solution is displaced by 3 – 10 cm in height into the space between the test tube and the hole to improve cooling of the test tube;
- a plastic tube 2 is inserted into the test tube. After that, the device is ready for work.

2. The method of using a thermoelectric condenser of pulmonary air and its experimental studies

To obtain a liquid condensate of a gas mixture exhaled from the lungs, the following must be done:

- with key 10, the device is connected to the 220V network. As a result, the thermal regulator panel 6 and the operating voltage indication panel start to light up, the fan 22 starts spinning in the control unit;
- regulator 15 regulates the intensity of the fan operation. At an ambient temperature of 20 – 30 °C, the fan operation mode is minimal, which is achieved by turning the regulator to the extreme counterclockwise position. At ambient temperatures above 30 °C, the fan is switched to the intensive operation mode by turning the regulator to the extreme clockwise position;
- the knob 14 regulates the supply voltage of the device cooler. When the knob is set to the extreme counter clockwise position, the voltage is minimal. When the knob is turned to the extreme clockwise position, the supply voltage is maximal. By regulating the voltage, it is possible to supply the cooler depending on the test tube cooling temperature. The voltage value is displayed by indicator 8;
- the required temperature in the test tube is set by buttons 11, which are located on the panel of the thermal regulator 7. At the same time, its indicators provide information about the set temperature – the lower indicator, and the actual temperature – the upper indicator. To set/change the set cooling temperature, briefly (up to 2 s) press the upper button "SET", and when the lower blue indicator of the thermostat panel starts flashing, release the upper button. Then decrease the value of the set temperature with the lower button "°C/F" or increase the value of the set temperature to the desired value with the same upper button "SET". Release the buttons and after a 2-3 second pause, the set value of the set temperature will be fixed;
- press the "Thermal regulator output" button 12 on the front panel of the control unit. The test tube cooling process will begin;
- after setting the required temperatures (approximately 10 – 15 minutes), an air mixture from the

lungs is introduced into the test tube through a plastic tube 2 by exhaling it through the mouth. The condensed liquid collects at the bottom of the test tube in approximately 3 minutes in a volume of about 0.5 ml and increases proportionally with an increase in the exhalation time;

- after receiving the required volume of liquid, the test tube is taken outside the device to conduct the appropriate analysis of the condensate;
- the opening of the fluoroplastic cylinder 23 is closed with a rubber plug 4.

The latter is important, since the entry of various foreign particles into the hole for the test tube can lead to jamming of the test tube and its destruction.

If it is necessary to take a number of samples of condensed liquid, the established temperature modes can be used. Thus, one sample for analysis can be taken in 5 – 10 minutes, i.e. approximately 8 – 10 samples can be obtained in one hour.

If necessary, condensate can be obtained in the form of ice. For this purpose, it is recommended to collect samples at maximum supply voltages of unit 1 and lower cooling temperatures (– 20 °C and below). To prevent freezing of plastic tube 2, it should be gradually raised so that its lower end is above the condensed ice. Such control is easily achieved by touching the plastic tube to the formed ice surface.

To turn off the device, press the "Thermal Regulator Output" button 12 on the front panel of the control unit, and then use key 10 to disconnect the device from the 220 V network.

The set values of the supply voltage and the set cooling temperature are saved after the device is switched off and do not need to be re-entered when switched on again, unless there is a need to specifically change the modes to others.

Such a device allows collecting the condensate of air exhaled by the patient with precisely regulated temperatures lower than – 20 °C and close to – 70 °C without the use of dry ice.

Fig. 5. Experimental studies of the developed thermoelectric condenser of pulmonary air.

The developed device can also be used for patients on artificial ventilation of the lungs. For this purpose, the respiratory circuit is connected via a special adapter for the exhalation circuit hoses of the artificial ventilation of the lungs. This allows for diagnostics of patients for whom traditional nasopharyngeal swab sampling is impossible, to study the body's response to a specific type of treatment and, thus, to monitor the effectiveness of therapy. The device is applicable for both adults and children of any age.

Experimental studies of the developed thermoelectric condenser of pulmonary air for the diagnosis of coronavirus and other diseases were conducted at the Center for Infectious Lesions of the Nervous System of the State Institution “L.V. Gromashevsky Institute of Epidemiology and Infectious Diseases of the National Academy of Medical Sciences of Ukraine” (Fig. 5).

Based on the research results, recommendations have been formulated for further improvement of the thermoelectric condenser of pulmonary air, aimed primarily at increasing the convenience of its use. The following studies of its effectiveness are also planned, including for the detection of other respiratory pathogens (viruses, rickettsia, mycoplasma, chlamydia, etc.), including by means of a chain polymerase reaction.

Conclusions

1. The design of a new highly efficient thermoelectric condenser of pulmonary air for the diagnosis of coronaviruses and other diseases with an extended range of condensation temperatures, lower than – 20 °C and close to – 70 °C, without the use of dry ice, has been developed.
2. An experimental sample of a thermoelectric condenser of pulmonary air for the diagnosis of coronavirus and other diseases was manufactured and tested. A method of using a thermoelectric condenser of pulmonary air in medical diagnostics has been developed.
3. The developed device was tested at the State Institution " L.V. Gromashevsky Institute of Epidemiology and Infectious Diseases of the National Academy of Medical Sciences of Ukraine". Based on the research results, recommendations were formed for further improvement of the thermoelectric pulmonary air condenser, aimed primarily at increasing the convenience of its use.

References

1. Hunt John (2007). Exhaled breath condensate – an overview. *Immunol Allergy Clin North Am*., 27 (4), 587 – 596.
2. Hunt J. (2002). Exhaled breath condensate: An evolving tool for noninvasive evaluation of lung disease. *J Allergy Clin Immunol*, 110 (1), 28 – 34.
3. Horvath I., Hunt J. and Barnes P.J. (2005). Exhaled breath condensate: methodological recommendations and unresolved questions. *Eur Respir J*., 26, 523 – 548.
4. Konstantinidi Efstathia M., Lappas Andreas S., Tzortzi Anna S., and Behrakis Panagiotis K. (2015). Exhaled breath condensate: technical and diagnostic aspects. *Scientific World Journal*, 2015, Article ID 435160, 25 pages.
5. Anatychuk L.I., Kobylianskyi R.R., Lysko V.V. (2022). Computer design of a thermoelectric condenser of pulmonary air for the diagnosis of coronavirus and other diseases. *J. Thermoelectricity*, 1, 65 – 72.

Submitted: 19.07.2023.

Анатичук Л.І., *акад. НАН України* [1,2]
Панасюк О.Л., [3]
Дьяченко П.А., [3]
Заремба А.В., [3]
Гаврилюк М.В., [1]
Кобилянський Р.Р., *канд. фіз.-мат. наук* [1,2]
Лисько В.В., *канд. фіз.-мат. наук* [1,2]

[1] Інститут термоелектрики НАН та МОН України,
вул. Науки, 1, Чернівці, 58029, Україна;
[2] Чернівецький національний університет імені Юрія Федьковича,
вул. Коцюбинського 2, Чернівці, 58012, Україна;
[3] ДУ "Інститут епідеміології та інфекційних хвороб ім. Л.В. Громашевського" НАМН України,
вул. М. Амосова, 5, Київ, 03038, Україна
e-mail: anatych@gmail.com

ТЕРМОЕЛЕКТРИЧНИЙ ПРИЛАД ДЛЯ ЗБИРАННЯ КОНДЕНСАТУ ВИДИХУВАНОГО ПОВІТРЯ

Наведено результати розробки конструкції та опис виготовленого експериментального зразка нового високоефективного термоелектричного конденсатора легеневого повітря для діагностики коронавірусних та інших захворювань з розширеним діапазоном температур конденсації, нижчими від – 20 °С та близькими до – 70 °С. Описано методику використання розробленого приладу у медичній діагностиці та результати його експериментальних досліджень. Бібл. 5, рис. 5.

Ключові слова: діагностика, коронавірус, конденсат, видихуване повітря, термоелектричне охолодження.

Література

1. Hunt John (2007). Exhaled breath condensate – an overview. *Immunol Allergy Clin North Am*., 27 (4), 587 – 596.
2. Hunt J. (2002). Exhaled breath condensate: An evolving tool for noninvasive evaluation of lung disease. *J Allergy Clin Immunol*, 110 (1), 28 – 34.
3. Horvath I., Hunt J. and Barnes P.J. (2005). Exhaled breath condensate: methodological recommendations and unresolved questions. *Eur Respir J*., 26, 523 – 548.
4. Konstantinidi Efstathia M., Lappas Andreas S., Tzortzi Anna S., and Behrakis Panagiotis K. (2015). Exhaled breath condensate: technical and diagnostic aspects. *Scientific World Journal*, 2015, Article ID 435160, 25 pages.
5. Анатичук Л.І., Кобилянський Р.Р., Лисько В.В. Комп’ютерне проєктування термоелектричного конденсатора легеневого повітря для діагностики коронавірусних та інших захворювань // Термоелектрика. – 2022, № 1. – С. 65 – 72.

Надійшла до редакції: 19.07.2023.

R.R. Kobylianskyi, *Cand.Sc.(Phys-Math)* [1,2]
Yu.Yu. Rozver, *Researcher* [1,2]
A.V. Prybyla, *Cand. Sc (Phys &Math)* [1,2]
A.K. Kobylianska, *Cand. Sc (Phys &Math)* [1]
M.M. Ivanochko, *Cand. Sc (Phys &Math)* [2]

[1] Institute of Thermoelectricity of the NAS and MES of Ukraine,
1 Nauky str., Chernivtsi, 58029, Ukraine;
[2] Yuriy Fedkovych Chernivtsi National University, 2 Kotsiubynskyi str.,
Chernivtsi, 58000, Ukraine
e-mail: anatych@gmail.com

ON MEDICAL RESTRICTIONS TO COOLING MODES OF THERMOELECTRIC AIR CONDITIONERS

The paper provides a detailed description of the temperature restrictions imposed on the conditioned environment. The considered medical aspects of the impact of sharp temperature changes on the human body make it possible to create and operate air conditioners that will meet the necessary conditions for their safe use. The main advantages and disadvantages of using thermoelectric air conditioners in comparison with compression air conditioners from the standpoint of medical restrictions are identified.
Key words: thermoelectric air conditioner, medical restrictions, temperature difference, compression air conditioner.

Introduction

General characterization of the problem. Using an air conditioner is today the most common method of reducing the temperature in an office, apartment or vehicle. This is mainly due to the fact that air conditioners allow people to survive the summer heat more easily. This is especially important for those who suffer from cardiovascular diseases and are at risk of suffering from a hypertensive crisis or heart attack due to the heat and the excessive load it causes on the heart and blood vessels.

Despite their obvious benefits in providing comfortable conditions, air conditioners have a number of significant drawbacks. For example, the accumulation of carbon dioxide, viral and infectious microorganisms in the absence of any ventilation, which quickly evaporate with normal ventilation. Also, cooled, overdried air, which is harmful to the skin and mucous membranes of the respiratory tract. But the main and most common disadvantage is associated with a sharp change in temperature between the ambient and conditioned environment, which causes a number of negative consequences for human health. This problem is increasingly becoming the subject of various studies, but, unfortunately, only as a component of a broader problem, which consists in the general study of human thermal comfort.

To create an effective air conditioner, it is necessary to take into account and, if possible, minimize all its negative effects on the human body. To do this, it is necessary to study the available information in this area and draw the necessary conclusions on the medical restrictions of air conditioners in cooling mode. At the same time, special interest will be focused on thermoelectric air conditioners, and their

comparison with compression air conditioners from the standpoint of medical restrictions will allow us to determine rational ways of their safe and effective use.

The purpose of this work is to determine the necessary medical restrictions on the cooling modes of thermoelectric air conditioners and compare them with compression air conditioners.

Temperature requirements for air conditioning of premises and vehicles

Requirements for air conditioning of premises.

According to GOST 30494-2011 "Residential and public buildings. Microclimate parameters in premises", the following optimal and permissible temperature norms for residential, public, and administrative premises are determined [1].

Table 1

Optimal and permissible microclimate parameters

Time of year	Air temperature, °C		General temperature, °C		Relative humidity, %		Air speed, m/s	
	Optimal	Permissible	Optimal	Permissible	Optimal	Permissible	Optimal	Permissible
Warm	22-25	20-28	22-24	18-27	30-60	65	0.2	0.3

In general, the optimal air conditioning temperature for cooling air is 22 – 25 °C (Table 1). The acceptable comfort standard is considered to be the range from 20 °C to 28 °C. But this is provided that the temperature difference between the air-conditioned room and the outdoor environment is no more than ~ 7 °C [1]. Otherwise, when the environment changes, the additional load on the human body will increase dramatically. For some, such a difference is equal to a slight feeling of discomfort, and for others – the threat of getting sick. The negative consequences of a sharp temperature drop were studied in the most detail in [2]. The aforementioned work states that when the air temperature changes by more than 5 °C, negative consequences for the respiratory system are already possible and for the human body there is a serious risk of exacerbation of symptoms of respiratory disease (asthma and chronic obstructive pulmonary disease). This is because the respiratory tract is lined with a thin layer of fluid. Cool air causes this fluid to evaporate more quickly, which in turn causes it to dry out [3, 4]. But even in people without serious respiratory diseases, cool air causes changes in the respiratory tract. The action of cooled air increases the number of granulocytes and macrophages (their role is to phagocytosis (envelopment and digestion) of cell debris and pathogens, both stationary and mobile cells, as well as to stimulate lymphocytes and other immune cells to respond to pathogen penetration) in the lower respiratory tract [5]. Nasal breathing of cooled air causes submucosal venous sinus dilation [6], leading to coughing, congestion, and sneezing in both healthy subjects and patients with rhinitis [7]. However, these effects are greater in subjects with rhinitis than in healthy volunteers [8] and greater in subjects with asthma and rhinitis than in subjects with rhinitis alone [9]. In the short term, cold air causes

bronchial constriction in asthmatics [10], especially in children and young adults. Long-term responses to temperature changes include airway changes, and some are anatomical, including increased bronchoalveolar lavage fluid granulocytes in healthy subjects [5], loss of ciliated epithelium, increased inflammatory cell counts, hypersensitivity, and airway obstruction [11]. But it should be noted that all of the above mainly applies to a sharp temperature drop of more than 5 °C. With a gradual decrease in temperature with a certain step, the recommended range may be higher than 5 °C.

Thus, according to [12], in order to prevent possible diseases, the temperature difference can be higher than 5 °C, depending on the ambient temperature and reach 13 °C (Table 2).

Table 2

The value of the temperature difference depending on the ambient temperature

Ambient air temperature (°C)	Temperature difference (°C)
< 32	5
34	7
36	9
38	11
40	13

A room cooling system installed to ensure comfort can cause various ailments. Respiratory illness from air conditioning that cools the air is a common phenomenon of our time. A sharp temperature drop, for example from 32 °C to 18 °C, becomes a stress for the body A condition occurs that resembles a cold in the autumn-winter period. In the first days, the malaise is accompanied by muscle aches, headache, general weakness, a slight increase in body temperature, sneezing. If treatment is not started, the situation is complicated by sore throat and cough. In a neglected state, the disease leads to chronic diseases of the respiratory system [13].

Requirements for vehicle air conditioning.

Air conditioning equipment does not have a strictly set temperature for cooled air. Conclusions about cooling efficiency should be drawn not from the air temperature, but from the difference between the ambient and cooled air. It is accepted that the air conditioner works effectively if it manages to provide a difference with the outside temperature of 15 – 20 °C. That is, the temperature of the air stream coming out of the interior deflector should be approximately 20 °C lower than the outside air temperature.

Car engineers are researching air conditioning modes to create systems that provide maximum comfort for the driver and passengers. It has been found that the optimum temperature for a car interior is 22 °C. Depending on their own preferences, drivers can adjust it within 2 °C. Studies have shown that it is this microclimate that allows maximum concentration on the road [14]. When the temperature drops to 18 °C, there is a risk of colds. If the temperature is higher than 24 °C, this significantly affects the driver's fatigue, making him fall asleep, which is especially dangerous when driving at night.

If the air conditioner is turned on in a garage where the thermometer shows + 25 °C, the air temperature coming out of the deflector should be no lower than + 5 °C. At an outside temperature of (+ 30 ÷ + 32) °C, cooling the air to (+ 12 ÷ + 14) °C is considered a completely normal indicator. At the same time, it is not recommended to make the temperature in the cabin too low, the optimal value is 5 °C lower than outside. That is, at an outside air temperature of + 30 °C, the cabin should be about + 25 °C in order not to provoke a cold, sore throat or pneumonia [2]. But according to [15], a difference of 5 °C mainly applies to short-term trips. That is, when the driver or passengers often leave the car.

During long trips (or simply a long stay in a car), it is recommended to gradually lower the temperature. According to [16], the temperature difference can reach 10 – 12 °C. However, the step of transition to a larger difference should not exceed 5 °C. That is, if you need to cool the car interior by 10 °C, for example from 35 °C to 25 °C, then this must be done in at least two steps: first to 30 °C, and after a while to 25 °C. Also, when using the air conditioner in a vehicle, it is necessary to direct the flow of cold air up, to the side or down. Thanks to this, you can also significantly reduce the likelihood of various diseases.

A significant disadvantage of compression air conditioners is the need to use freon. Freon is a refrigerant used in most modern air conditioners. Freon is heavier than air, so if it leaks, it can displace air from the room. Some types of freon release dangerous toxins when decomposed and can cause poisoning.

Medical aspects of the impact of high temperature drops on the human body

When air temperature drops rapidly without any gradual adaptation, even with small changes of up to 2 – 3 °C, but especially with changes of more than 5 °C, negative consequences for the human body are possible. For example, such changes can cause the risk of serious exacerbation of symptoms of obstructive respiratory diseases (asthma and chronic obstructive pulmonary disease) [2].

The main negative impact of this temperature difference concerns the respiratory system. According to [17], the respiratory tract is lined with ciliated epithelium and secretory cells. The cilia interact with a thin layer of fluid that covers the outer surface of the epithelium in contact with the air, the airway surface layer (ASL). The ASL includes a low-viscosity periciliary layer (PCL), which lubricates airway surfaces and facilitates ciliary function, and an additional layer of mucus above it. The volume, pH, ion and nutrient content of the ASL are important for regulating antimicrobial activity and mucociliary transport. Antimicrobial factors found in the ASL participate in innate and adaptive defense mechanisms that protect the airways from internal pathogens [18].

In other words, airway surface layer (ASL) is a thin layer of fluid that covers the luminal surface for normal airway physiology. Inhaling chilled air can cause ASL to evaporate faster than it is replenished, leading to ASL drying out and a number of serious negative health consequences.

Medical research confirms that the human body needs time to acclimatize from heat to cold or from cold to high temperature [19]. Blood vessels accumulate heat in winter, and vice versa in summer. A sharp change in temperature affects their functioning and, as a result, the work of the heart. Whenever there is a change in air temperature, immunity weakens and the body becomes more susceptible to viral infections. A sudden change in temperature can cause severe discomfort in people with respiratory diseases. Patients with asthma, respiratory ailments, and heart problems can experience acute stress.

Optimal temperature conditions of a thermoelectric air conditioner in cooling mode

The use of thermoelectric air conditioners allows for precise and smooth temperature control in residential premises and vehicles. Unlike compression air conditioners, thermoelectric air conditioners do not require the presence of liquid coolants (for example, freon), which eliminates the possibility of air poisoning when hydraulic units are depressurized. In addition, thermoelectric air conditioners have a number of advantages: lower weight and dimensions, high reliability, ease of maintenance, independence from spatial orientation, the possibility of spatial dispersion according to operating conditions, and simple switching from cooling mode to heating mode [20 – 23]. It should also be noted that, unlike compression air conditioners, the efficiency of thermoelectric air conditioners increases with decreasing power,

increasing air temperature, and decreasing the temperature difference between outside and inside the conditioned environment, which also creates additional advantages for them (Fig. 1).

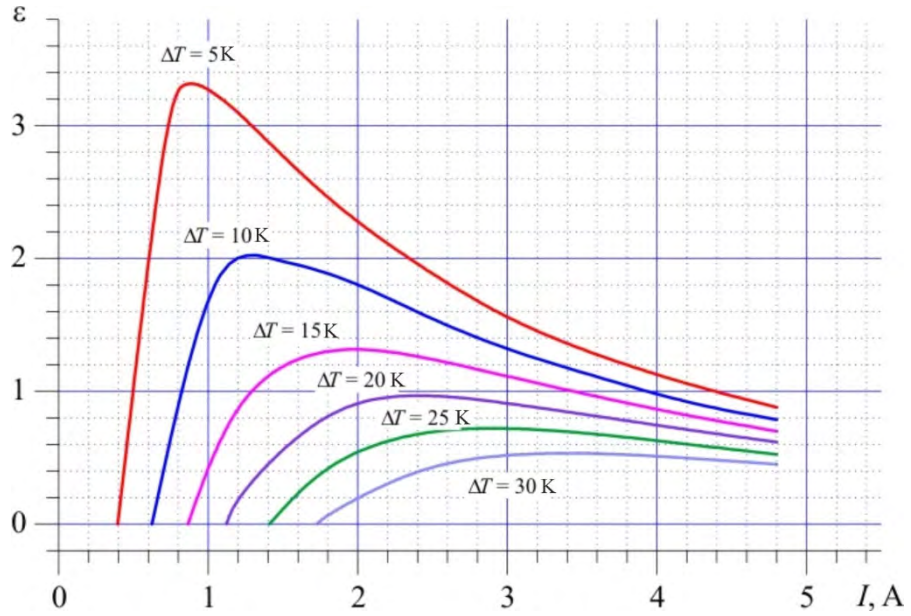

Fig. 1. Typical dependence of the coefficient of performance of a thermoelectric air conditioner on the supply current for different values of the temperature difference between its hot and cold sides.

As can be seen from Fig. 1, the efficiency of a thermoelectric air conditioner is maximum at temperature differences of about 5 °C, which is recommended by medical opinions and competes with compression air conditioners in many climatic zones (Fig. 2).

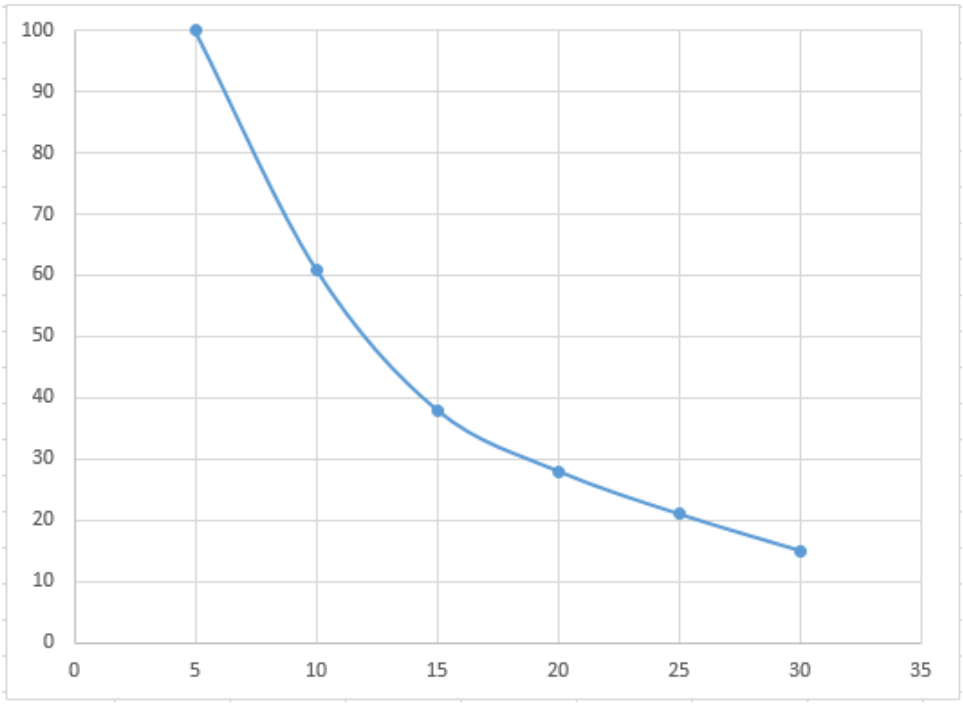

Fig. 2. Dependence of the efficiency of a thermoelectric air conditioner on the temperature difference.

As can be seen from Fig. 2, the efficiency of a thermoelectric air conditioner decreases with increasing temperature difference, while the electrical power consumption increases.

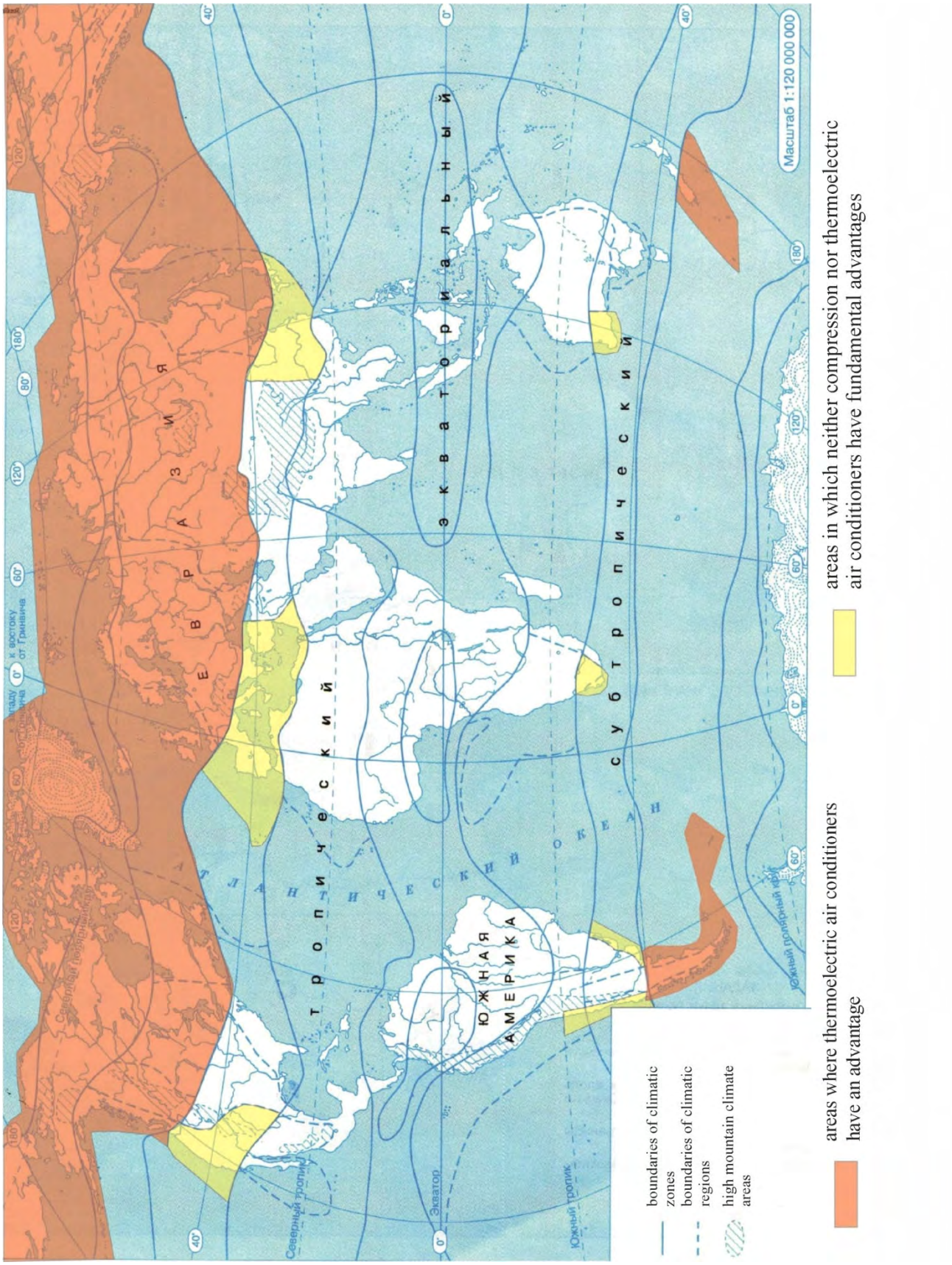

Fig. 3 Climatic zones for rational use of thermoelectric air conditioning.

The average statistical values of winter and summer air temperatures in areas of appropriate use of thermoelectric air conditioners are given in Table 3.

Table 3

Seasonal air temperature in the zones of thermoelectric air conditioning advantages

Name of the climate zone	Summer temperature, °C	Winter temperature, °C
Moderate maritime climate	14 ± 6	8 ± 3
Moderate continental climate	20 ± 5	– 5 ± 3
Moderate monsoon climate	23 ± 4	– 20 ± 6
Subarctic climate	8 ± 2	– 23 ± 4
Arctic climate	10 ± 6	– 40 ± 3

As can be seen from Table 3, the temperature range for the operation of a thermoelectric air conditioner covers extreme values from 10 °C to 27 °C in summer and from – 43 °C to 11 °C in winter.

Conclusions

1. The medical aspects of the impact of low temperatures on the human body when using air conditioners have been studied. It has been established that sharp temperature drops can cause diseases of the respiratory system and exacerbation of chronic lung diseases.
2. The optimal temperature difference between the ambient and conditioned environments was determined, which is $\Delta T \leq 5$ °C.
3. The advantages of the thermoelectric method of conditioning over the compression method are analyzed.
4. Temperature ranges for operation of thermoelectric air conditioning systems have been established for climatic zones in which the use of such systems is energy efficient.

References

1. GOST 30494-2011.
2. D'Amato Maria, Molino Antonio, Calabrese Giovanna, Cecchi Lorenzo, Annesi-Maesano Isabella and D'Amato Gennaro (2018). The impact of cold on the respiratory tract and its consequences to respiratory health. *Clinical and Translational Allergy*.
3. Daviskas E, Gonda I, Anderson S.D. (1990). Mathematical modeling of heat and water transport in human respiratory tract. *J Appl Physiol*., 69, 362 – 372.
4. Freed A.N, Davis M.S. (1999). Hyperventilation with dry air increases airway surface fluid osmolality in canine peripheral airways. *Am J Respir Crit Care Med*.159, 1101 – 1107.
5. [http://health-ua.com/article/67252-mukotcilarnij-klrens-zdorovya-dihalnih-shlyahv].
6. Cole P, Forsyth R, Haight J.S. (1983). Effects of cold air and exercise on nasal T patency. *Ann Otol Rhinollaryngol*. 92, 96 – 98.

7. Millqvist E, Bengtsson U, Bake B. (1987). Occurrence of breathing problems induced by cold climate in asthmatics – a questionnaire survey. *Eur Respir J*. 71, 444 – 449.
8. Driessen J.M, van derPalen J, van Aalderen W.W, de Jongh F.H, Thio R.J. (2012). Inspiratory airflow limitation after exercise challenge in cold air in asthmatic children. *Respir Med*. 106 (10), 1362 – 1368.
9. Hyrkas H, Jaakkola M.S., Ikaheimo T.M, Hugg T.T, Jaakkola J.J.K. (2014). Asthma and allergic rhinitis increase respiratory symptoms in cold weather among young adults. *Res Med*. 108, 63 – 70.
10. Bousquet J, van Cauwenberge P, Khaltaev N, (2001). Aria Workshop Group, World Health Organization. Allergic rhinitis and its impact on asthma. *J Allergy Clin Immunol*. 108, 147 – 334.
11. Larsson K, Tornling G, Gavhed D, Mиller-Suur C, Palmberg L. (1998). Inhalation of cold air increases the number of inflammatory cells in the lungs in healthy subjects. *Eur Respir J*. 12, 825 – 830.
12. https://zakon.rada.gov.ua/laws/show/v1182400-74.#Text.
13. https://strojdvor.ru/kondicionirovanie/obslujivanie/mozhno-li-zabolet-ot-konditsionera-v-pomeshchenii-i-kak-etogo-izbezhat/
14. https://WWWdrivenn.ru/journal/novosti/kakuyu-temperaturu-optimalnee-vsego-derzhat-v-salone-avtomobilya-id30137
15. https://economics.segodny.ua/economics/avto/kak-ne-prostuditsya-i-ne-zabolet-v-zharu-ot-konditsionera-v-avtomobile-728083.html
16. https://car.ru/news/autogramota/76638-kak-ne-prostuditsya-i-ne-zabolet-v-zharu-ot-konditsionera-v-mashine/
17. http://health-ua.com/article/67252-mukotcilarnij-klrens-zdorovya-dihalnih-shlyahv
18. https://www.ncbi.nlm.nih.gov/pmc/articles/PMC2233658/
19. https://timesofindia.indiatimes.com/life-stile/health-fitness/health-news/alert-sudden-change-from-hot-to-cold-can-be-harmful-to-your-health/articleshow/69354918.cms
20. Anatychuk L.I., Prybyla A.V. (2016). Comparative analysis of thermoelectric and compression heat pumps for individual air conditioners. *J. Thermoelectricity*, 2, 33 – 42.
21. Anatychuk L.I., Prybyla A.V., Korop M.M. (2016). Comparative analysis of thermoelectric and compression heat pumps for individual air conditioners at elevated ambient temperatures. *J. Thermoelectricity*, 5, 95 – 98.
22. Anatychuk L.I., Vykhor L.M, Kotsur M.P., Kobylianskyi R.R., Kadeniuk T.Ya. (2016). Optimal control of time dependence of cooling temperature in thermoelectric devices. *J. Thermoelectricity*, 5, 5 – 11.
23. Anatychuk L.I., Kobylianskyi R.R., Kadeniuk T.Ya. (2017). Computer simulation of local thermal effect on human skin. *J. Thermoelectricity*, 1, 69 – 79.

Submitted: 25.07.2023.

Кобилянський Р.Р., *канд. фіз.-мат. наук* [1,2]
Розвер Ю.Ю., *науковий співробітник* [1,2]
Прибила А.В., *канд. фіз.-мат. наук* [1,2]
Кобилянська А.К., *канд. фіз.-мат. наук* [1]
Іваночко М.М., *канд. фіз.-мат. наук* [2]

[1] Інститут термоелектрики НАН та МОН України,
вул. Науки, 1, Чернівці, 58029, Україна;
[2] Чернівецький національний університет імені Юрія Федьковича,
вул. Коцюбинського 2, Чернівці, 58012, Україна
e-mail: anatych@gmail.com

ПРО МЕДИЧНІ ОБМЕЖЕННЯ ДО РЕЖИМІВ ОХОЛОДЖЕННЯ ТЕРМОЕЛЕКТРИЧНИХ КОНДИЦІОНЕРІВ

У роботі проведено детальний опис температурних обмежень, що накладаються на кондиційоване середовище. Розглянуті медичні аспекти впливу різких перепадів температури на організм людини дають можливість створювати та експлуатувати кондиціонери, що будуть відповідати необхідним умовам їх безпечного використання. Визначено основні переваги та недоліки використання термоелектричних кондиціонерів у порівнянні із компресійними кондиціонерами з позиції медичних обмежень.

Ключові слова: термоелектричний кондиціонер, медичні обмеження, перепад температури, компресійний кондиціонер.

Література

1. GOST 30494-2011.
2. D'Amato Maria, Molino Antonio, Calabrese Giovanna, Cecchi Lorenzo, Annesi-Maesano Isabella and D'Amato Gennaro (2018). The impact of cold on the respiratory tract and its consequences to respiratory health. *Clinical and Translational Allergy*.
3. Daviskas E, Gonda I, Anderson S.D. (1990). Mathematical modeling of heat and water transport in human respiratory tract. *J Appl Physiol*., 69, 362 – 372.
4. Freed A.N, Davis M.S. (1999). Hyperventilation with dry air increases airway surface fluid osmolality in canine peripheral airways. *Am J Respir Crit Care Med*.159, 1101 – 1107.
5. [http://health-ua.com/article/67252-mukotcilarnij-klrens-zdorovya-dihalnih-shlyahv].
6. Cole P, Forsyth R, Haight J.S. (1983). Effects of cold air and exercise on nasal T patency. *Ann Otol Rhinollaryngol*. 92, 96 – 98.
7. Millqvist E, Bengtsson U, Bake B. (1987). Occurrence of breathing problems induced by cold climate in asthmatics – a questionnaire survey. *Eur Respir J*. 71, 444 – 449.
8. Driessen J.M, van derPalen J, van Aalderen W.W, de Jongh F.H, Thio R.J. (2012). Inspiratory airflow limitation after exercise challenge in cold air in asthmatic children. *Respir Med*. 106 (10), 1362 – 1368.
9. Hyrkas H, Jaakkola M.S., Ikaheimo T.M, Hugg T.T, Jaakkola J.J.K. (2014). Asthma and allergic rhinitis increase respiratory symptoms in cold weather among young adults. *Res Med*. 108, 63 – 70.
10. Bousquet J, van Cauwenberge P, Khaltaev N, (2001). Aria Workshop Group, World Health Organization. Allergic rhinitis and its impact on asthma. *J Allergy Clin Immunol*. 108, 147 – 334.
11. Larsson K, Tornling G, Gavhed D, Миller-Suur C, Palmberg L. (1998). Inhalation of cold air increases the number of inflammatory cells in the lungs in healthy subjects. *Eur Respir J*. 12, 825 – 830.
12. https://zakon.rada.gov.ua/laws/show/v1182400-74.#Text.

13. https://strojdvor.ru/kondicionirovanie/obslujivanie/mozhno-li-zabolet-ot-konditsionera-v-pomeshchenii-i-kak-etogo-izbezhat/
14. https://WWWdrivenn.ru/journal/novosti/kakuyu-temperaturu-optimalnee-vsego-derzhat-v-salone-avtomobilya-id30137
15. https://economics.segodny.ua/economics/avto/kak-ne-prostuditsya-i-ne-zabolet-v-zharu-ot-konditsionera-v-avtomobile-728083.html
16. https://car.ru/news/autogramota/76638-kak-ne-prostuditsya-i-ne-zabolet-v-zharu-ot-konditsionera-v-mashine/
17. http://health-ua.com/article/67252-mukotcilarnij-klrens-zdorovya-dihalnih-shlyahv
18. https://www.ncbi.nlm.nih.gov/pmc/articles/PMC2233658/
19. https://timesofindia.indiatimes.com/life-stile/health-fitness/health-news/alert-sudden-change-from-hot-to-cold-can-be-harmful-to-your-health/articleshow/69354918.cms
20. Anatychuk L.I., Prybyla A.V. (2016). Comparative analysis of thermoelectric and compression heat pumps for individual air conditioners. *J. Thermoelectricity*, 2, 33 – 42.
21. Anatychuk L.I., Prybyla A.V., Korop M.M. (2016). Comparative analysis of thermoelectric and compression heat pumps for individual air conditioners at elevated ambient temperatures. *J. Thermoelectricity*, 5, 95 – 98.
22. Anatychuk L.I., Vykhor L.M, Kotsur M.P., Kobylianskyi R.R., Kadeniuk T.Ya. (2016). Optimal control of time dependence of cooling temperature in thermoelectric devices. *J. Thermoelectricity*, 5, 5 – 11.
23. Anatychuk L.I., Kobylianskyi R.R., Kadeniuk T.Ya. (2017). Computer simulation of local thermal effect on human skin. *J. Thermoelectricity*, 1, 69 – 79.

Надійшла до редакції: 25.07.2023.

ARTICLE SUBMISSION GUIDELINES

For publication in a specialized journal, scientific works are accepted that have never been printed before. The article should be written on an actual topic, contain the results of an in-depth scientific study, the novelty and justification of scientific conclusions for the purpose of the article (the task in view).

The materials published in the journal are subject to internal and external review which is carried out by members of the editorial board and international editorial board of the journal or experts of the relevant field. Reviewing is done on the basis of confidentiality. In the event of a negative review or substantial remarks, the article may be rejected or returned to the author(s) for revision. In the case when the author(s) disagrees with the opinion of the reviewer, an additional independent review may be done by the editorial board. After the author makes changes in accordance with the comments of the reviewer, the article is signed to print.

The editorial board has the right to refuse to publish manuscripts containing previously published data, as well as materials that do not fit the profile of the journal or materials of research pursued in violation of ethical norms (for instance, conflicts between authors or between authors and organization, plagiarism, etc.). The editorial board of the journal reserves the right to edit and reduce the manuscripts without violating the author's content. Rejected manuscripts are not returned to the authors.

Submission of manuscript to the journal

The manuscript is submitted to the editorial office of the journal in paper form in duplicate and in electronic form on an electronic medium (disc, memory stick). The electronic version of the article shall fully correspond to the paper version. The manuscript must be signed by all co-authors or a responsible representative.

In some cases it is allowed to send an article by e-mail instead of an electronic medium (disc, memory stick).

English-speaking authors submit their manuscripts in English. Russian-speaking and Ukrainian-speaking authors submit their manuscripts in English and in Russian or Ukrainian, respectively. Page format is A4. The number of pages shall not exceed 15 (together with References and extended abstracts). By agreement with the editorial board, the number of pages can be increased.

To the manuscript is added:

1. Official recommendation letter, signed by the head of the institution where the work was carried out.

2. License agreement on the transfer of copyright (the form of the agreement can be obtained from the editorial office of the journal or downloaded from the journal website – Dohovir.pdf). The license agreement comes into force after the acceptance of the article for publication. Signing of the license agreement by the author(s) means that they are acquainted and agree with the terms of the agreement.

3. Information about each of the authors – full name, position, place of work, academic title, academic degree, contact information (phone number, e-mail address), ORCID code (if available). Information about the authors is submitted as follows:

authors from Ukraine - in three languages, namely Ukrainian, Russian and English;
authors from the CIS countries - in two languages, namely Russian and English;
authors from foreign countries – in English.

4. Medium with the text of the article, figures, tables, information about the authors in electronic form.

5. Colored photo of the author(s). Black-and-white photos are not accepted by the editorial staff. With the number of authors more than two, their photos are not shown.

Requirements for article design

The article should be structured according to the following sections:

- *Introduction*. Contains the problem statement, relevance of the chosen topic, analysis of recent research and publications, purpose and objectives.
- *Presentation of the main research material* and the results obtained.
- *Conclusions* summing up the work and the prospects for further research in this direction.
- *References*.

The first page of the article contains information:

1) in the upper left corner – UDC identifier (for authors from Ukraine and the CIS countries);

2) surname(s) and initials, academic degree and scientific title of the author(s);

3) the name of the institution where the author(s) work, the postal address, telephone number, e-mail address of the author(s);

4) article title;

5) abstract to the article – not more than 1 800 characters. The abstract should reflect the consistent logic of describing the results and describe the main objectives of the study, summarize the most significant results;

6) key words – not more than 8 words.

The text of the article is printed in Times New Roman, font size 11 pt, line spacing 1.2 on A4 size paper, justified alignment. There should be no hyphenation in the article.

Page setup: "mirror margins" – top margin – 2.5 cm, bottom margin – 2.0 cm, inside – 2.0 cm, outside – 3.0 cm, from the edge to page header and page footer – 1.27 cm.

Graphic materials, pictures shall be submitted in color or, as an exception, black and white, in .opj or .cdr formats, .jpg or .tif formats being also permissible. According to author's choice, the tables and partially the text can be also in color.

Figures are printed on separate pages. The text in the figures must be in the font size 10 pt. On the charts, the units of measure are separated by commas. Figures are numbered in the order of their arrangement in the text, parts of the figures are numbered with letters – a, b, .. On the back of the figure, the title of the article, the author (authors) and the figure number are written in pencil. Scanned images and graphs are not allowed to be inserted.

Tables are provided on separate pages and must be executed using the MSWord table editor. Using pseudo-graph characters to design tables is inadmissible.

Formulae shall be typed in Equation or MatType formula editors. Articles with formulae written by hand are not accepted for printing. It is necessary to give definitions of quantities that are first used in the text, and then use the appropriate term.

Captions to figures and tables are printed in the manuscript after the references.

Reference list shall appear at the end of the article. References are numbered consecutively in the order in which they are quoted in the text of the article. References to unpublished and unfinished works are inadmissible.

Attention! In connection with the inclusion of the journal in the international bibliographic abstract database, the reference list should consist of two blocks: CITED LITERATURE and REFERENCES (this requirement also applies to English articles):

CITED LITERATURE – sources in the original language, executed in accordance with the

Ukrainian standard of bibliographic description DSTU 8302:2015. With the aid of VAK.in.ua (http://vak.in.ua) you can automatically, quickly and easily execute your "Cited literature" list in conformity with the requirements of State Certification Commission of Ukraine and prepare references to scientific sources in Ukraine in understandable and unified manner. This portal facilitates the processing of scientific sources when writing your publications, dissertations and other scientific papers.

REFERENCES – the same cited literature list transliterated in Roman alphabet (recommendations according to international bibliographic standard APA-2010, guidelines for drawing up a transliterated reference list "References" are on the site http//www.dse.org.ua, section for authors).

To speed up the publication of the article, please adhere to the following rules:

- in the upper left corner of the first page of the article – the UDC identifier;
- family name and initials of the author(s);
- academic degree, scientific title;

begin a new line, Times New Roman font, size 12 pt, line spacing 1.2, center alignment;

- name of organization, address (street, city, zip code, country), e-mail of the author(s);

begin a new line 1 cm below the name and initials of the author(s), Times New Roman font, size 11 pt, line spacing 1.2, center alignment;

- the title of the article is arranged 1 cm below the name of organization, in capital letters, semi-bold, font Times New Roman, size 12 pt, line spacing 1.2, center alignment. The title of the article shall be concrete and possibly concise;
- the abstract is arranged 1 cm below the title of the article, font Times New Roman, size 10 pt, in italics, line spacing 1.2, justified alignment in Ukrainian or Russian (for Ukrainian-speaking and Russian-speaking authors, respectively);
- key words are arranged below the abstract, font Times New Roman, size 10 pt, line spacing 1.2, justified alignment. The language of the key words corresponds to that of the abstract. Heading "Key words" - font Times New Roman, size 10 pt, semi-bold;
- the main text of the article is arranged 1 cm below the abstract, indent 1 cm, font Times New Roman, size 11 pt, line space spacing 1.2, justified alignment;
- formulae are typed in formula editor, fonts Symbol, Times New Roman. Font size is "normal" – 12 pt, "large index" – 7 pt, "small index" – 5 pt, "large symbol" – 18 pt, "small symbol" – 12 pt. The formula is arranged in the text, center aligned and shall not occupy more than 5/6 of the line width, formulae are numbered in parentheses on the right;
- dimensions of all quantities used in the article are represented in the International System of Units (SI) with the explication of the symbols employed;
- figures are arranged in the text. The figures and pictures shall be clear and contrast; the plot axes – parallel to sheet edges, thus eliminating possible displacement of angles in scaling; figures are submitted in color, black-and-white figures are not accepted by the editorial staff of the journal;
- tables are arranged in the text. The width of the table shall be 1 cm less than the line width. Above the table its ordinary number is indicated, right alignment. Continuous table numbering throughout the text. The title of the table is arranged below its number, center alignment;

• references should appear at the end of the article. References within the text should be enclosed in square brackets behind the text. References should be numbered in order of first appearance in the text. Examples of various reference types are given below.

Examples of LITERATURE CITED

Journal articles

Anatychuk L.I., Mykhailovsky V.Ya., Maksymuk M.V., Andrusiak I.S. Experimental research on thermoelectric automobile starting pre-heater operated with diesel fuel. *J.Thermoelectricity*. 2016. №4. P.84–94.

Books

Anatychuk L.I. *Thermoelements and thermoelectric devices. Handbook.* Kyiv, Naukova dumka, 1979. 768 p.

Patents

Patent of Ukraine № 85293. Anatychuk L.I., Luste O.J., Nitsovych O.V. Thermoelement.

Conference proceedings

Lysko V.V. *State of the art and expected progress in metrology of thermoelectric materials.* Proceedings of the XVII International Forum on Thermoelectricity (May 14-18, 2017, Belfast). Chernivtsi, 2017. 64 p.

Authors' abstracts

Kobylianskyi R.R. *Thermoelectric devices for treatment of skin diseases*: extended abstract of candidate's thesis. Chernivtsi, 2011. 20 p.

Examples of REFERENCES

Journal articles

Gorskiy P.V. (2015). Ob usloviakh vysokoi dobrotnosti i metodikakh poiska perspektivnykh sverhreshetochnykh termoelektricheskikh materialov [On the conditions of high figure of merit and methods of search for promising superlattice thermoelectric materials]. *Termoelektrichestvo - J.Thermoelectricity*, 3, 5 – 14 [in Russian].

Books

Anatychuk L.I. (2003). *Thermoelectricity. Vol.2. Thermoelectric power converters*. Kyiv, Chernivtsi: Institute of Thermoelectricity.

Patents

Patent of Ukraine № 85293. Anatychuk L. I., Luste O.Ya., Nitsovych O.V. Thermoelements [In Ukrainian].

Conference proceedings

Rifert V.G. Intensification of heat exchange at condensation and evaporation of liquid in 5 flowing-down films. In: *Proc. of the 9th International Conference Heat Transfer.* May 20-25, 1990, Israel.

Authors'abstracts

Mashukov A.O. *Efficiency hospital state of rehabilitation of patients with color carcer.* PhD (Med.) Odesa, 2011 [In Ukrainian].